Journal of the
OPTICAL SOCIETY *of* AMERICA

VOLUME 32 MAY, 1942 NUMBER 5

Visual Sensitivities to Color Differences in Daylight*

DAVID L. MACADAM
Research Laboratories, Eastman Kodak Company, Rochester, New York
(Received January 7, 1942)

An apparatus is described which facilitates the presentation of pairs of variable colors without variation of luminance. With this instrument, various criteria of visual sensitivity to color difference have been investigated. The standard deviation of color matching was finally adopted as the most reproducible criterion. The test field was two degrees in diameter, divided by a vertical biprism edge, and was viewed centrally with a surrounding field of forty-two degrees diameter uniformly illuminated so as to have a chromaticity similar to that of the I.C.I. Standard Illuminant *C* (average daylight). The luminance of the test field was maintained constant at 15 millilamberts, and the surrounding field was 7.5 millilamberts. These fields were viewed monocularly through an artificial pupil, 2.6 mm in diameter. Over twenty-five thousand trials at color matching have been recorded for a single observer, and the readings are analyzed in detail and compared with previously available data. The standard deviations of the trials are represented in terms of distance in the standard 1931 I.C.I. chromaticity diagram. These increments of distance are represented as functions of position along straight lines in the chromaticity diagram, and also as functions of direction of departure from points representing certain standard chromaticities. Such representations are simpler than the traditional representations of wave-length thresholds and purity thresholds as functions of wave-length, and the accuracy of the representations is improved by this simplicity. Chromaticity discrimination for non-spectral colors is represented simultaneously and on the same basis as for spectral colors. Small, equally noticeable chromaticity differences are represented for all chromaticities and for all kinds of variations by the lengths of the radii of a family of ellipses drawn on the standard chromaticity diagram. These ellipses cannot be transformed into equal-sized circles by any projective transformation of the standard chromaticity diagram. The consistency of these data with the results of other investigators is exhibited in terms of the noticeabilities of wave-length differences in the spectrum and of the noticeabilities of purity differences from a neutral stimulus, as functions of dominant wave-length.

THE measurement and specification of color is a well-established technique. Familiarity with the fundamentals of this subject will be assumed throughout this report.[1] Color specifications reveal whether or not two sources radiating different spectral distributions appear to have the same color, for the average human observer. Similarly, the colors of reflecting materials are specified in a manner which indicates immediately whether or not several samples having different spectral reflectance characteristics appear alike under certain conditions of illumination. These specifications give precise meaning to color standards. The specifications of color standards can be recorded, and can be communicated, in the form of quantitative values which are reproducible at will in all adequately equipped laboratories. Color standards need no longer be dependent upon the preservation of material samples of questionable permanence.

* Communication No. 840 from the Kodak Research Laboratories.

[1] A. C. Hardy and collaborators, *Handbook of Colorimetry* (Technology Press, Cambridge, Massachusetts, 1936).

BOSTON UNIVERSITY
COLLEGE OF LIBERAL ARTS
LIBRARY

The standard specifications of color also provide a useful system for the classification of colors. The luminance[2] of a source of radiant energy, or of an object reflecting radiant energy, is the most familiar of the quantities in terms of which colors may be specified and classified. Alternatively, luminous reflectance may be used to specify the ratio between the luminance of an object and the luminance of a perfect diffuse reflector similarly illuminated. This ratio is characteristic of the reflecting surface, and consequently luminous reflectance is a convenient specification when the color of an object is to be discussed without reference to the illuminance[2] incident upon it.

The chromaticity, or quality of a color may be specified and classified in terms of dominant wave-length and purity.[1] Alternatively, the chromaticity of a color may be specified by a point in a plane diagram. This diagram represents the relative chromaticities of all colors in much the same manner as a plane map represents the relative locations of various places on the earth. An example of the representation of chromaticities by points on the chromaticity diagram is given in Fig. 1. As in the case of a plane map of an imperfectly spherical world, the relations exhibited between locations in this diagram are limited in significance. In a certain limited sense, differences of specifications correspond in order of magnitude to the apparent differences of colors. For example, if two adjacent objects having the same dominant wave-length and luminance differ in purity, the object having the greater purity will appear more saturated. An estimate of the ratio of the apparent saturations may not confirm the ratio of the measured purities, but equality, or the fact of greater or less purity will be confirmed subjectively. Similarly, two adjacent objects having the same luminance and purity but differing in dominant wave-length will differ in the subjectively appreciated quality called hue, in the same sense as they differ in dominant wave-length. A third object sharing the common values of luminance and purity but having a dominant wave-length greater or less than both of the original colors will exhibit a hue more nearly resembling that of the object from which it differs less with respect to dominant wave-length. The visually estimated ratio of differences in hue will not, in general, equal the ratio of the corresponding differences of dominant wave-length, but an object having a dominant wave-length intermediate between the dominant wave-lengths of two other objects will appear intermediate in hue also. In the presence of differences of luminance or purity, or both, equality of dominant wave-length does not necessarily assure equality of hue. Similarly, in the presence of differences in luminance or dominant wave-length, equality of purity rarely corresponds to equality of saturation. Finally, most of the difficulties peculiar to heterochromatic photometry arise from the fact that in the presence of differences in dominant wave-length or purity, or both, comparisons of brightness are difficult and unsatisfactory.

Many investigations of the noticeability of color differences[3–5] have been undertaken for the purpose of interpreting measured differences

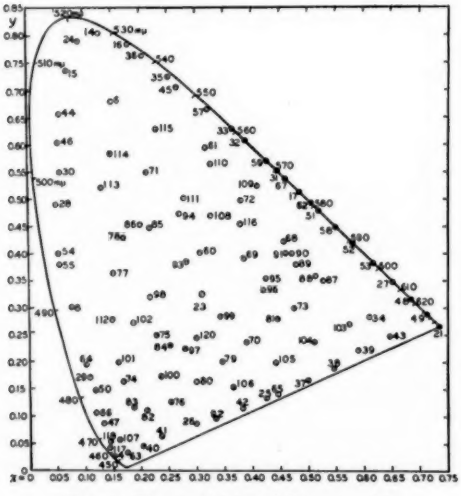

FIG. 1. Chromaticities of filters used in discrimination apparatus.

[2] L. A. Jones, "Colorimetry: Preliminary draft of a report on nomenclature and definitions," J. Opt. Soc. Am. **27**, 207–213 (1937).

[3] D. B. Judd, "A Maxwell triangle yielding uniform chromaticity scales," J. Opt. Soc. Am. **25**, 24–35 (1935).

[4] I. G. Priest and F. G. Brickwedde, "Minimum perceptible colorimetric purity as a function of dominant wave-length," J. Opt. Soc. Am. **28**, 133–139 (1938).

[5] W. D. Wright, "The sensitivity of the eye to small colour differences," Proc. Phys. Soc. **53**, 93–112 (1941).

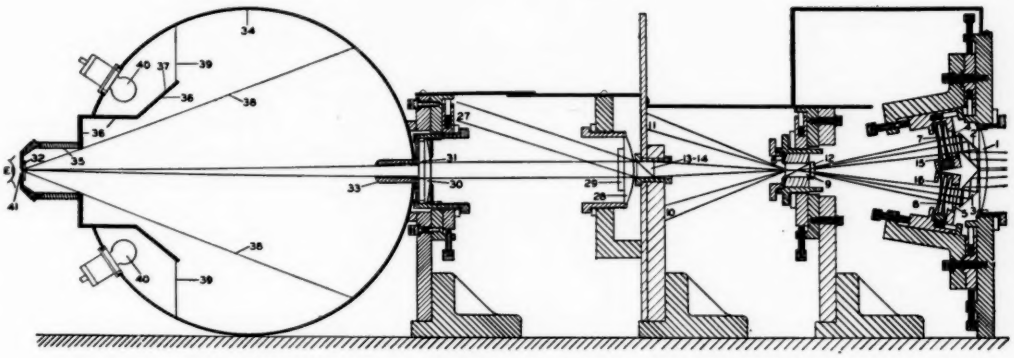

FIG. 2. Vertical cross section of chromaticity discrimination apparatus.

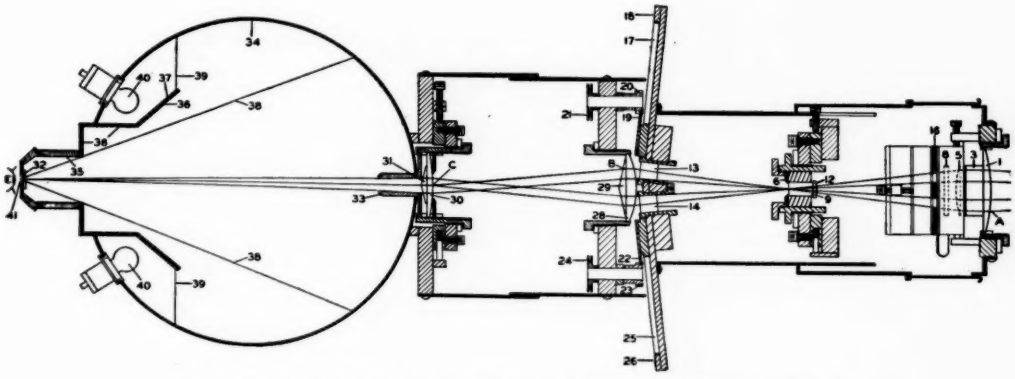

FIG. 3. Horizontal cross section of chromaticity discrimination apparatus.

in terms comparable with subjective estimates. In the present report, the results of such an investigation will be reported in terms of the standard 1931 I.C.I. specifications of the colors. No modification of this standard system of specifying colors will be recommended. Any modification of the chromaticity diagram adequately representing these data on noticeabilities of color differences would be so complicated as to be useless in practice. Such a sacrifice of the simplicity of the standard system is unnecessary, in view of the ease with which the supplementary data concerning noticeability can be applied to color specifications expressed in the standard system.

A. APPARATUS

The apparatus employed in this investigation was designed to provide the following features:

1. A two-degree comparison field, divided semicircularly.

2. A surrounding field of twenty-one degrees radius, of uniform color, which may be changed or extinguished, to provide any reasonable conditions of adaptation.

3. The observer is called upon to manipulate only a single control in order to produce the desired variations of color in each half of the comparison field.

4. Any selected kind of variation of chromaticity from any initial chromaticity can be produced in either half of the field, with (a) automatically constant luminance, if desired, or (b) the luminance can be made to vary proportionately in any desired ratio with any selected kind of chromaticity variation, or (c) the luminance alone of any selected chromaticity can be varied.

5. All visual stimuli are produced by additive mixtures of filtered beams from a single calibrated light source. The resultant heterogeneous stimuli are more nearly similar to ordinary visual stimuli than are the mixtures of homogeneous spectral stimuli frequently used for visual research. The results therefore correspond more closely than usual to the most practically important circumstances of vision. The stimuli produced in this apparatus are specified accurately by standard colorimetric analyses of the filters employed, and errors which frequently arise from unsuspected impurities of spectral components are avoided.

6. When the two halves of the comparison field are matched visually, their energy distributions are identical, so that individual differences of color-mixture characteristics have a minimum effect on the data for chromaticity sensibility. Errors of calibration of the color filters result in only unimportant second-order errors in the color differences calculated from those calibrations.

These features will be made evident by the description of the construction and functioning of the apparatus and by the discussion of its calibration and the method of investigation.

A vertical cross section of the apparatus is shown in Fig. 2. A horizontal cross section is shown in Fig. 3. The vertical cross section follows the axial rays of one of the two pairs of light paths, such as the ray indicated by *A-B-C-E* in Fig. 3. The light source, which is situated to the right of the instrument as represented in the drawings, is not shown on the drawings. It consists of a ground-glass plate illuminated by the light from a 6-volt projection lamp (Mazda C-8, vertical coil filament, clear bulb, T-10, medium prefocus base). This lamp is operated at the current which has been found by previous calibration to be necessary to maintain the desired 2848°K color temperature of the light entering the instrument from the illuminated ground glass. A ribbon filament lamp could be used in place of the coil filament and ground-glass combination if much higher field illuminance were desired. The ground-glass source has been used exclusively in the experiments which are now being reported. All observations were made with 15 millilamberts field luminance.

The light from each point of the extended source is collimated by the lens *1*. The light passing through the upper half of this lens is reflected vertically upwards and then downwards at an angle of ten degrees from the horizontal by two total internal reflections in the prism *2*. The other half of the collimated beam is reflected downwards and then upwards at an angle of ten degrees from the horizontal by two total internal reflections in prism *3*. The light in these two separated, but converging beams is then focused by lenses *4* and *5* to produce two coincident images of the light source in the plane of the diaphragm *6*. Light filters can be placed in the separated beams at *7* and *8*. Each of the two beams which intersect within the Wollaston double-image polarizing prism *9* is split into two beams, each diverging ten degrees in the vertical plane from the direction of the incident beam. Thus, the beam from the upper filter *7* is split into two beams, one of which proceeds along the horizontal axis of the instrument, and the other of which is deflected downwards at an angle of twenty degrees from the horizontal, being ultimately intercepted and absorbed by the blackened plate at *10*. The portion of the light from the upper incident beam which is directed along the axis by the Wollaston prism is polarized in the vertical plane. The beam from the lower filter *8* is also split by the Wollaston prism into two beams, one of which proceeds along the horizontal axis, together with part of the light from the upper incident beam. The other of the two beams into which the lower incident beam is split is deflected upwards at an angle of twenty degrees to the axis of the instrument and is intercepted and absorbed by the blackened plate at *11*. The portion of the light from the lower incident beam which is directed along the axis by the Wollaston prism is polarized in the horizontal plane. Coincident images of the light filters at *7* and *8* are focused by the lens *12* onto the pair of Rochon prisms at *13* and *14*.

The diaphragm *15* intercepts the light from all portions of the upper filter *7* except two areas which are focused by lens *12* onto the Rochon prisms *13* and *14*. Similarly, the diaphragm *16* intercepts the light from all portions of the lower filter *8* except two areas which are focused by lens *12* onto the Rochon prisms *13* and *14*.

Each of the Rochon prisms is mounted so that it can be rotated at will within a range of 90 degrees. Prism *13* is rigidly connected to the pointer *17* which indicates the azimuth of the prism on the scale *18* which is graduated in degrees. A vernier on the pointer *17* makes possible the recording of tenths of degrees. Prism *13* is rotated by the attached toothed segment *19* which meshes with the gear *20*. This gear *20* is activated by the chain drive *21* which is geared to a control knob which may be manipulated by the observer. Prism *14* is rotated by the gears *22* and *23* and chain *24*, coupling to a second control knob. The azimuth of prism *14* is indicated by a vernier on the pointer *25* read against the divided scale *26*.

The proportions of the beams from the filters *7* and *8* which are transmitted undeviated by each Rochon prism depend upon the azimuth of the prism. The portions of the beams which are deviated by the Rochon prisms are intercepted and absorbed by the blackened plate, as indicated at *27*. The scale readings are 0 degrees when the Rochon prisms transmit, without deviation, light polarized in a vertical plane, and 90 degrees when the undeviated beams are polarized in a horizontal plane. Consequently, if U represents the energy distribution of the light from the upper filter *7* incident on one of the Rochon prisms, and if V represents the energy distribution of the light from the lower filter *8* incident upon the same prism, then the energy distribution of the light transmitted undeviated by the prism is

$$W = T(U \sin^2 \theta + V \cos^2 \theta), \qquad (1)$$

where θ is the azimuth of the prism, as indicated by the scale reading, and T is the transmittance of the Rochon prism for light of such polarization that it is transmitted without deviation. If the values of any additive functions of the distributions U and V are equal, then the value of the same function of the transmitted distribution is constant, independently of all variations of θ and consequently of the proportions in which U and V are combined. In particular, if the filters at *7* and *8* have equal luminous transmittances for the I.C.I. Illuminant *A* (2848°K), which is the quality of the light incident upon them, then the luminous flux transmitted without deviation by each of the Rochon prisms will be constant, independently of θ and consequently of the proportions in which the colors from the two filters *7* and *8* are combined after transmission by the Rochon prisms. This property of the apparatus is responsible for the feature (4*a*) of automatically constant field luminance for the additive mixtures in all proportions of different colors, such as the colors of U and V. Similarly, if the luminous transmittances of the filters at *7* and *8* are unequal, the variation of field luminance will be proportional to the variation of chromaticity resulting from the variation of the proportions of the two beams transmitted undeviated by the Rochon prisms. In this manner the experimental condition (4*b*) can be secured. Finally, of course, the condition (4*c*) can be realized by substituting an opaque plate for the filter at *8* thus converting the instrument into one type of polarization photometer.

The beams transmitted without deviation by the Rochon prisms are collimated by the lens *28*. The biprism *29* refracts these beams and causes their axial rays to intersect on the dihedral edge of the field biprism *31*. The field lens *30* focuses coincident images of the light source on the pupil of the observer's eye *E*. The dihedral edge of the biprism *31* is at the focal point of the eye lens *32* so that the eye lens of the normal observer is completely relaxed. Other eye lenses can be substituted for this lens *32* to compensate for variations from normal refraction in the eyes of various observers. The boundary of the test field is defined by the end of the cylindrical field stop *33*. The inner bore of this cylinder is sufficiently conical so that none of the inner surface can be seen by the observer at *E*. The circular edge of this conical hole, nearest the eye, serves as the field stop. The hidden interior surface of this tube is coated with a dull black finish to absorb most of the light refracted from the axial beams by the field biprism. This useless light is kept at a minimum by the diaphragms *15* and *16* which are of such shape as to intercept all except those portions of the filtered beams which are necessary to illuminate the test field. The length of the tube *33* is sufficient to shield the biprism *31* from all parts of the whitened interior of the sphere *34*. The surfaces of the bi-

prism *31* and the field lens *30* are coated with a "non-reflecting" layer which further reduces the possibility of reflected stray light in the test field. This treatment of the surfaces of the biprisms *29* and *31* and of the lenses *28* and *30* also reduces to negligible magnitudes the variation of reflection losses at these surfaces, resulting from the oblique incidence of the polarized beams from the rotatable prisms *13* and *14*. The interiors of the eye tube *35* and of the lamp shield *36* are finished dull black, to minimize the reflection of light from the convex surface of the field lens *30*. The biprism *31* is cemented to the plane surface of the field lens *30* to eliminate the reflection of light from these plane surfaces. Similarly, the biprism *29* is cemented to the plane surface of the lens *28*. The external surfaces of the field stop *33*, the entire inner surface of the sphere *34*, and the outer surface *37* of the lamp shield are painted white. An opaque layer of smoke from burning magnesium ribbon was deposited simultaneously on the cylindrical field stop *33* and on the hemisphere visible from *E*, in order to obliterate completely all joints and irregularities. The illumination of the interior of the sphere is so uniform and diffused that the outlines of the cylindrical field stop *33* can be distinguished only with effort. The radius of the illuminated surrounding field is limited by the length of the eye tube *35*. The limiting rays are shown by *38*. The angular extent of the illuminated surrounding field could be increased somewhat by shortening the eye tube *35* or by increasing its diameter, but the advantage would appear to be negligible in comparison with the increased difficulties of construction, and discomfort of the observer, who would be required to place his head very close to the sphere lamps and their connections. An annular ring *39* of filter film can be placed between the lamp shield and the sphere, to introduce whatever chromaticity may be desired in the surrounding field. The intensity of the surrounding field can be changed by altering the number or size of the lamps *40* employed, or by varying the current passing through them. The chromaticity and the luminance of the surrounding field are calibrated by establishing a color match between the surrounding field and the test field. The colorimetric specifications of the surrounding field are then equal to those calculated for the test field from the azimuth of the Rochon prisms and the colorimetric specifications of the filters, placed at *7* and *8*. The various adjusting and clamping devices which are provided for the focusing and centering of the optical elements are indicated in Figs. 2 and 3. The appropriate procedure for placing such an instrument in adjustment can be devised by any person familiar with the maintenance of precision optical instruments. An artificial pupil may be placed over the eye lens at *41*. Such an artificial pupil, with a diameter of 2.6 millimeters, was used to fix the level of retinal illumination in the experiments described in this paper.

This instrument is designed for monocular observation but it could conceivably be converted into a binocular instrument. Equal transmissions for both eyes, and constant transmission for all planes of polarization are essential requirements of any binocular viewing device employed with this instrument. The Maxwellian field, and the large illuminated surrounding field impose further requirements which eliminate practically all known binocular eyepieces. Color-mixture data, luminosity data, and sensibilities to color differences are occasionally, although not commonly, distinctly different for the right and left eye of a single observer. Such differences are not confined to observers who exhibit definitely anomalous color discrimination, but have also been detected in the case of observers classed as "normal" by all of the usual tests. Such differences would result in erratic results of binocular observations. The results of binocular observations would not be expected to average consistently the different characteristics of the two eyes. Rather, one eye would be expected to dominate and govern the results of the majority of the observations, with the subordinate eye gaining dominance occasionally and contributing erratic observations, as the result of either conscious or unconscious binocular rivalry.

A movable eye shield which permits the use of either eye has been employed throughout the monocular observations which are the subject of this report. This shield protects the idle eye from all light, permitting the idle eye to remain open and relaxed.

TABLE I. Filters for chromaticity instrument (in Illuminant *A*).

Filter number	Constituents Chromatic	Neutral	*X*	*Y*	*Z*	*m*	*x*	*y*
4	34,38	0.07	0.01640	0.00280	0.08855	0.10775	0.152	0.026
6	65,8	1.25	0.00059	0.00265	0.00066	0.00390	0.150	0.680
8	75	0.42	0.00071	0.00280	0.00575	0.00911	0.077	0.302
14	*X*1	0.24	0.00044	0.00276	0.00023	0.00343	0.128	0.805
15	3(63)		0.00027	0.00280	0.00076	0.00383	0.070	0.736
16	3(74)	0.10	0.00062	0.00270	0.00011	0.00353	0.180	0.785
17	2(73)	0.50	0.00256	0.00272	0.00000	0.00528	0.485	0.514
21	70	0.50	0.00769	0.00280	0.00000	0.01049	0.737	0.263
23	78	1.17	0.00278	0.00294	0.00339	0.00911	0.305	0.323
24	*X*2	0.10	0.00035	0.00297	0.00043	0.00375	0.092	0.790
25	35	0.51	0.00943	0.00295	0.00980	0.02218	0.425	0.133
26	*X*3	0.65	0.01153	0.00311	0.02400	0.03864	0.299	0.086
27	72	0.78	0.00549	0.00293	0.00000	0.00842	0.651	0.348
28	4(65*A*)		0.00029	0.00286	0.00268	0.00583	0.050	0.490
29	45*A*	0.55	0.00188	0.00298	0.01247	0.01733	0.108	0.172
30	3(65)	0.08	0.00029	0.00278	0.00199	0.00506	0.057	0.550
31	21,53	1.21	0.00216	0.00268	0.00000	0.00484	0.446	0.553
32	16,53	1.45	0.00181	0.00283	0.00002	0.00466	0.388	0.608
33	2(16),2(53)	0.48	0.00151	0.00260	0.00002	0.00413	0.365	0.630
34	31,86*C*	1.84	0.00583	0.00270	0.00102	0.00955	0.610	0.283
35	2(61),15	1.00	0.00097	0.00280	0.00009	0.00386	0.251	0.725
36	2(61),12	1.12	0.00075	0.00280	0.00011	0.00366	0.205	0.764
37	35,86*C*	0.68	0.00919	0.00305	0.00611	0.01835	0.500	0.166
38	35,86*B*	0.66	0.00879	0.00302	0.00427	0.01608	0.546	0.188
39	35,86*A*	0.70	0.00784	0.00294	0.00252	0.01330	0.590	0.221
40	34,78*A*	0.30	0.01293	0.00275	0.04780	0.06348	0.203	0.045
41	34,78*B*	0.45	0.01075	0.00285	0.03180	0.04540	0.237	0.063
42	35,78*B*	0.40	0.00987	0.00297	0.01304	0.02588	0.382	0.115
43	35,86*A*	0.60	0.00756	0.00290	0.00125	0.01171	0.646	0.248
44	63,2(65)		0.00028	0.00284	0.00132	0.00444	0.057	0.656
45	61,12	1.67	0.00105	0.00280	0.00011	0.00396	0.266	0.706
46	3(65),2(4)		0.00025	0.00278	0.00161	0.00464	0.054	0.603
47	49*A*	0.47	0.00603	0.00301	0.03600	0.04504	0.133	0.067
48	25	2.00	0.00605	0.00280	0.00000	0.00885	0.684	0.316
49	29	1.71	0.00695	0.00280	0.00000	0.00975	0.712	0.288
50	46	0.95	0.00225	0.00283	0.01405	0.01913	0.118	0.148
51	15	2.60	0.00355	0.00290	0.00001	0.00646	0.550	0.449
52	21	2.45	0.00382	0.00278	0.00000	0.00660	0.580	0.420
53	22	2.35	0.00453	0.00280	0.00000	0.00733	0.617	0.382
54	75,65*A*,2(4)		0.00038	0.00290	0.00396	0.00724	0.053	0.400
55	75,65*A*,*A*		0.00040	0.00275	0.00408	0.00723	0.055	0.380
57	61,2(15)	1.46	0.00136	0.00280	0.00005	0.00421	0.322	0.666
58	2(16)	2.50	0.00378	0.00285	0.00001	0.00664	0.570	0.429
59	21,53	0.90	0.00209	0.00280	0.00001	0.00490	0.427	0.571
60	38,78*B*	1.92	0.00206	0.00270	0.00195	0.00671	0.307	0.402
61	59	2.15	0.00149	0.00280	0.00040	0.00470	0.318	0.595
62	53,22	0.93	0.00287	0.00280	0.00000	0.00567	0.506	0.494
63	34,78*AA*		0.01450	0.00275	0.06550	0.08275	0.175	0.033
64	75,45	0.56	0.00177	0.00310	0.01296	0.01783	0.102	0.195
65	35,2	0.49	0.00850	0.00270	0.00783	0.01903	0.446	0.1415
66	2(46)	0.36	0.00320	0.00285	0.02083	0.02688	0.119	0.106
67	2(21),53	1.00	0.00230	0.00269	0.00000	0.00499	0.460	0.539
68		2.60	0.00296	0.00274	0.00078	0.00648	0.457	0.423
69	78*A*	2.13	0.00257	0.00262	0.00149	0.00668	0.385	0.392
70	78,30	0.85	0.00478	0.00290	0.00457	0.01225	0.390	0.237
71	69	1.87	0.00110	0.00285	0.00123	0.00518	0.212	0.550
72	66	2.37	0.00217	0.00285	0.00070	0.00572	0.380	0.498
73	78*AA*,30	1.34	0.00460	0.00290	0.00217	0.00967	0.475	0.300
74	78,78*AA*	0.65	0.00265	0.00259	0.01052	0.01576	0.168	0.164
75	78,78*B*	1.15	0.00251	0.00275	0.00574	0.01100	0.228	0.250
76	78,78*AA*,30	0.25	0.00522	0.00260	0.01280	0.02052	0.253	0.126
77	44*A*	1.62	0.00110	0.00280	0.00354	0.00729	0.151	0.364
78	44	1.70	0.00111	0.00250	0.00261	0.00652	0.170	0.430
79	78,78*B*,30	0.60	0.00503	0.00290	0.00656	0.01449	0.347	0.200
80	78,78*A*,30	0.45	0.00570	0.00310	0.01020	0.01900	0.300	0.163
81	78*AA*,78*C*,30	1.23	0.00421	0.00265	0.00260	0.00946	0.445	0.280
82	78,78*AA*,*X*4	0.37	0.00550	0.00288	0.01780	0.02618	0.210	0.110
83	78,78*AA*,*X*5	0.45	0.00438	0.00272	0.01633	0.02343	0.187	0.116
84	78,78*AA*,*X*6	0.60	0.00307	0.00280	0.00630	0.01217	0.252	0.230
85	67	1.70	0.00149	0.00308	0.00231	0.00688	0.217	0.448
86	67,78*C*	1.60	0.00132	0.00300	0.00229	0.00661	0.200	0.454
87	30	2.20	0.00445	0.00295	0.00104	0.00844	0.527	0.350
88	*X*4	2.30	0.00416	0.00290	0.00105	0.00811	0.513	0.358
89	*X*7	2.44	0.00387	0.00307	0.00115	0.00809	0.478	0.380
90	*X*8	2.44	0.00330	0.00280	0.00099	0.00700	0.471	0.400
91	*X*6	2.48	0.00327	0.00285	0.00099	0.00711	0.460	0.401
92	*X*9,34	0.70	0.01055	0.00300	0.01803	0.03158	0.334	0.095
93	38,78*B*	1.85	0.00194	0.00265	0.00229	0.00688	0.282	0.385
94	51,38*A*	1.77	0.00175	0.00306	0.00166	0.00647	0.270	0.473
95	*X*7,78*A*	1.77	0.00361	0.00300	0.00188	0.00849	0.425	0.354
96	*X*5,78*A*	1.74	0.00378	0.00300	0.00223	0.00901	0.420	0.333
97	*X*7,78	1.74	0.00387	0.00312	0.00687	0.01386	0.279	0.225
98	38*A*,78*B*	1.50	0.00190	0.00280	0.00405	0.00875	0.217	0.320
99	*X*7,78*AA*	1.45	0.00380	0.00315	0.00413	0.01108	0.343	0.284
100	*X*7,78,78*A*	0.84	0.00385	0.00281	0.00957	0.01623	0.237	0.173
101	38*A*,78	0.80	0.00224	0.00280	0.00895	0.01399	0.160	0.200
102	78*A*,38*A*	1.20	0.00195	0.00285	0.00564	0.01044	0.187	0.273
103	31	1.87	0.00627	0.00295	0.00171	0.01093	0.574	0.270
104	31,78*B*	1.50	0.00669	0.00310	0.00830	0.01309	0.511	0.237
105	31,78*A*	1.16	0.00622	0.00280	0.00505	0.01407	0.442	0.199
106	31,78*AA*	0.73	0.00694	0.00290	0.00912	0.01896	0.366	0.153
107	*X*5,2(78)	0.10	0.00763	0.00270	0.03700	0.04733	0.161	0.057
108	66,78*A*	1.70	0.00201	0.00290	0.00126	0.00617	0.326	0.470
109	59*A*	1.28	0.00242	0.00310	0.00038	0.00590	0.410	0.525
110	59*A*,38	0.95	0.00182	0.00315	0.00060	0.00557	0.327	0.565
111	59*A*,78	1.13	0.00175	0.00315	0.00138	0.00628	0.279	0.502
112	3(38*A*)	1.13	0.00141	0.00265	0.00542	0.00948	0.149	0.279
113	65	1.28	0.00065	0.00260	0.00174	0.00499	0.131	0.521
114	65,86	0.88	0.00069	0.00270	0.00125	0.00464	0.148	0.583
115	60	1.84	0.00103	0.00280	0.00063	0.00446	0.230	0.629
116	2(51),78*A*	1.75	0.00213	0.00255	0.00092	0.00560	0.380	0.455
117	48*A*	0.32	0.00944	0.00280	0.05312	0.06536	0.144	0.042
118	48*A*,2(2*A*)	0.24	0.00766	0.00285	0.04235	0.05276	0.145	0.054
119	34,30	0.72	0.00928	0.00290	0.00976	0.02194	0.423	0.132
120	*X*7,78*AA*,78*B*	1.20	0.00369	0.00300	0.00561	0.01230	0.300	0.244

B. CALIBRATED COLOR FILTERS

A set of about 100 color filters has been prepared for use with this instrument. The luminous transmittances of these filters are all within 10 percent of their average, 0.00285. The luminous transmittances of these filters, and their chromaticities, have been calculated from their spectral transmittances and for the standard I.C.I. observer and Illuminant *A*. The filters consist of one or more pieces of gelatin filter film cemented between microscope slide glasses. Most of the filter components were selected from the commercial Wratten filters. A few special filter films were required in order to secure chromaticities unobtainable with combinations of the standard filters. These special filter films were designed and made by Mr. Albert Smith, of these Laboratories, whose interest and assistance is here gratefully acknowledged.

Table I indicates the constituents and colorimetric specifications of the assembled filters. The chromaticities of these filters are represented in Fig. 1. The serial numbers with which these filters are designated in Fig. 1 and column 1 of Table I bear no relation to the Wratten filter numbers of the components. The serial numbers correspond approximately to the order in which the filters were assembled. The Wratten filter numbers of the constituents of each filter are listed in the second column. Special filter components are numbered serially, with the letter *X* preceding each of these numbers to avoid confusion with the Wratten filter numbers. In many cases, two or more pieces of one type of

filter film were used. Such cases are indicated by parentheses around the Wratten filter number preceded by a numeral indicating the number of pieces used. In the fourth column is given the density of the Wratten neutral filter film em-

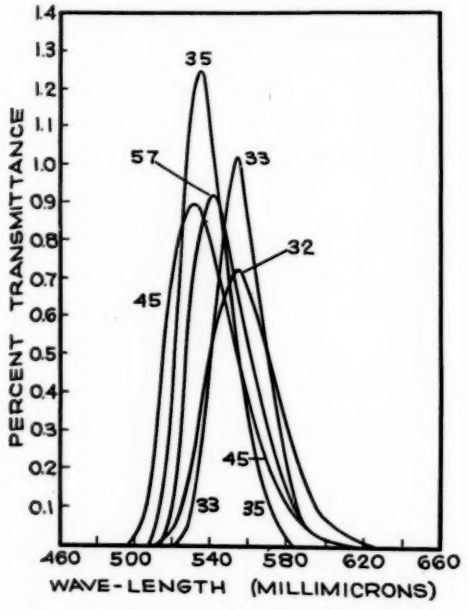

FIG. 4. Spectrophotometric curves of five filters.

ployed to adjust the various filters to the desired value of luminous transmittance. The I.C.I. tristimulus values, X, Y, and Z are given in the fifth, sixth, and seventh columns. The value of Y is the luminous transmittance of each filter. The sum m of the three tristimulus values is given in the eighth column. This value is the weight which may be assigned to the color transmitted by each filter in computations of the chromaticities of mixtures according to the center of gravity principle.[6,7] The coordinates, x, y, of the points representing each filter in the chromaticity diagram, Fig. 1, are given in columns 9 and 10 of Table I.

These filters have such low luminous transmittances that in most cases sufficiently accurate spectrophotometric data could not be secured by direct measurements of the finished filters. The spectrophotometric data, such as those represented by the curves shown in Figs. 4 and 5, have been determined in various ways, but mostly by spectrophotometric measurement of the separate components of each filter, followed by computation of the transmittance of the cemented combinations. The effects of cementing on total absorption and in the reduction of reflection losses were carefully investigated and taken into account in these computations. As a final check, the relative luminous transmittances of filters of similar chromaticities were compared visually. The instrument represented in Figs. 2 and 3 was used for these comparisons. This apparatus functioned as a polarization photometer, when an opaque plate was placed at position *8*. The two filters being compared were placed at *7*, each filter covering one of the openings in the diaphragm *15*. Filters represented by neighboring points in Fig. 1 have sufficiently similar chromaticities so that these heterochromatic comparisons of luminous transmittances could be made quite satisfactorily. The relative luminous transmittances of filters compared in this manner are inversely proportional to the ratio of the squares of the sines of the azimuths of the corresponding Rochon prisms. This use of the sine square law is very favorable for the comparison of nearly equal transmittances, such as are involved in the comparisons of the set of filters employed here. Systematic variations from the computed values of the luminous transmittances were observed and correlated with the positions of the points representing the filters in the chromaticity diagram. These systematic variations were confirmed by repetitions of the comparisons by the same observer on different days, but were different for different observers. Although these variations and correlations require further study in relation to the actual luminosity curves for the observers involved, before any positive conclusions can be stated, these variations are tentatively attributed to variations of the luminosity curves of the observers from the standard I.C.I. data used in the computations. In particular, all observers seemed to have higher than standard luminosity values for the extreme red end of the spectrum,

[6] D. L. MacAdam, "The theory of the maximum visual efficiency of colored materials," J. Opt. Soc. Am. **25**, 249–252 (1935).

[7] D. L. MacAdam, "Projective transformations of I.C.I. color specifications," J. Opt. Soc. Am. **27**, 294–299 (1937).

and somewhat lower than standard luminosity values for the extreme violet end of the spectrum. Such an effect might be expected and attributed to the differences in the conditions of observation from those employed by Gibson and Tyndall.[8,9] In particular, the large illuminated surrounding field, and the maintenance of a fairly high constant retinal illuminance (200 photons, or 8 lux) for all comparisons, including the extreme red, violet, and purples, may have contributed appreciably to this effect. Although the high, central portions of the standard curve, which are usually most important in practice, were determined at normal levels of retinal illuminance,[8] the relative luminosities of wave-lengths in the extreme red and violet regions of the spectrum were determined with considerably lower retinal illuminances. Consequently, near the ends of the visible spectrum the rates of change of the standard curve with wave-length may be more nearly representative of the scotopic curve than of the photopic curve. Such an effect would not cause appreciable errors in most practical problems, but would be expected to give rise to noticeable discrepancies for filters whose luminous transmittances occur largely at either or both of the extremes of the visible spectrum. No attempt was made to compensate for the systematic discrepancies between the observed and computed luminous transmittances. Very few discrepancies, other than the systematic variations, were detected between the observed and computed values. The few isolated errors were traced to spectrophotometric or computational errors. Such errors were corrected and eliminated before Table I and Figs. 1, 4, and 5 were completed.

All of the filters were stored so as to minimize changes in any of the components which may be unstable. The use of unstable components was avoided as far as possible, and those filters which contained constituents suspected of instability were checked periodically, both spectrophotometrically and visually.

[8] K. S. Gibson and E. P. T. Tyndall, "Visibility of radiant energy," Sci. Papers Nat. Bur. Standards **19**, 131–191 (1924); Trans. Illum. Eng. Soc. **19**, 176–196 (1924).

[9] *Proceedings of the Sixth Session, International Commission on Illumination* (Geneva, 1924), pp. 67 and 232.

C. COLORIMETRIC CALIBRATION OF APPARATUS

Colorimetric specifications of the mixtures obtained in the test field of the instrument represented in Figs. 2 and 3 can be computed by use of the tristimulus values of the filters in equations similar to Eq. (1). Let the symbols X_u, Y_u, Z_u represent the tristimulus values of the field when $\theta = 90$ degrees, that is, when the color of the field is produced by the filter at position 7, alone. Let the symbols X_v, Y_v, Z_v represent the tristimulus values of the field when $\theta = 0$ degrees, that is, when the color of the field is produced by the filter at position 8, alone. Then, for any scale reading θ the tristimulus values X, Y, Z of the mixture are given by the equations:

$$X = X_u \sin^2\theta + X_v \cos^2\theta, \tag{2}$$

$$Y = Y_u \sin^2\theta + Y_v \cos^2\theta, \tag{3}$$

$$Z = Z_u \sin^2\theta + Z_v \cos^2\theta. \tag{4}$$

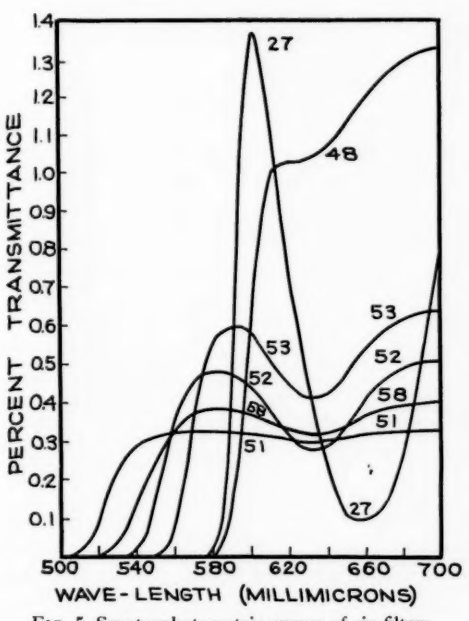

FIG. 5. Spectrophotometric curves of six filters.

Since the value of Y is the luminance of the field, the luminance of any mixture is given by Eq. (3). If the luminous transmittances of the filters at 7 and 8 are equal for the quality of light which is incident upon them (Illuminant A), then the

luminance Y of the field is constant for all values of θ.

The coordinates of the point representing the mixture in the chromaticity diagram can be calculated from the values X, Y, Z given by Eqs. (2), (3), and (4). The center of gravity principle provides a much more convenient method of locating the point. Let the symbol m_u represent the "mass" $X_u+Y_u+Z_u$, assigned in Table I to the filter at position 7, which produces the color of the field when $\theta=90$ degrees. Let the symbol m_v represent the "mass" $X_v+Y_v+Z_v$ assigned in Table I to the filter at position 8. Then the point representing the mixture for the scale reading θ divides the straight line joining the points representing the filters in the ratio $m_u \sin^2\theta$ to $m_v \cos^2\theta$. Let the chromaticity of the field when $\theta=90$ degrees be represented by the point U. Let the chromaticity of the field when $\theta=0$ degrees be represented by the point V. Let the chromaticity of the field for the scale reading θ be represented by the point W. If the ratio of the distances VW/VU is represented by the fraction f then

$$f=1/(r\cot^2\theta+1), \tag{5}$$

where $r=m_v/m_u$.

The fractional distance of W from V toward U may be estimated for any values of r and θ from the curves shown in Fig. 6. A special slide rule was designed and used for all of the computations of f involved in this investigation. This slide rule, illustrated in Fig. 7, avoids the difficulties and errors of interpolation encountered in the use of Fig. 6. The bottom scale A on the frame of the rule represents values of the ratio r from 0.01 to 100.0. The distances in inches to the right from the center index to the divisions are given by the equation:

$$D=5\log_{10} r. \tag{6}$$

The lower scale B on the slide represents reciprocals of the ratio r from $1/r=0.004$ to $1/r=40.0$. Scale B is divided in exactly the same manner as is scale A, except that the index is displaced two inches to the right of the center of the slide. The upper scale T on the slide represents values of the angle θ from 9 degrees to 86.5 degrees. The distances in inches to the right from the index to the divisions of this scale are given by the equation:

$$D=10\log_{10}\cot\theta. \tag{7}$$

The 45-degree index is at exactly the same position on the slide as the unit index on scale B, that is, two inches to the right of the center of the slide. Finally, the top scale F on the frame, represents values of the fraction f from 0.01 to 0.99. The distances in inches from the center index to the divisions of this scale are given by the equation:

$$D=5\log_{10}(1-f)/f. \tag{8}$$

In all of the scales, positive values of D are measured to the right of the index and negative values to the left. When the 45-degree index of the slide is aligned with the value of r on the A scale, the value of f can be found on the F scale opposite the value of θ on the T scale. Alternatively, the value of the reciprocal of the ratio $1/r$ on the B scale can be aligned with the center index of the frame. Since Eq. (5) reduces to $f=\sin^2\theta$, when $r=1.0$, the values of $\sin^2\theta$ required in Eq. (3) for the calculation of luminance can be determined by setting the 45-degree index of the slide at $r=1.0$ and reading the values of $\sin^2\theta$ from the F scale. The values of $\cos^2\theta$ which are also required in Eq. (3) are easily determined by subtracting the values of $\sin^2\theta$ from 1.0.

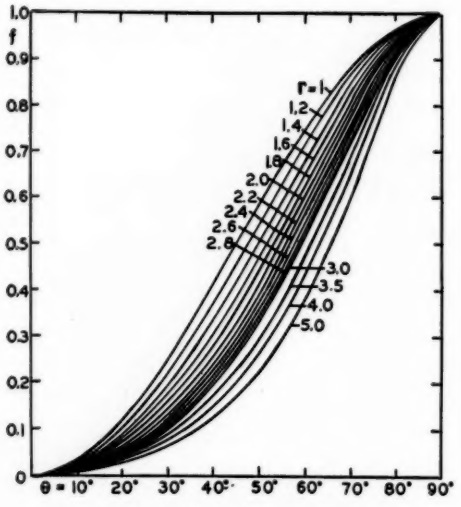

FIG. 6. Calibration curves of chromaticity discrimination apparatus.

FIG. 7. Slide rule for calculation of chromaticities synthesized in discrimination apparatus.

The distance VW of the point representing the mixture from the point representing the chromaticity of the field when $\theta=0$ degrees is equal to the value f multiplied by the distance UV between the points representing the chromaticities of the field when $\theta=0$ degrees and $\theta=90$ degrees. When the distance UV is measured in the same units as the coordinate scales of the chromaticity diagram, it is represented by the symbol S.

$$S=[(x_u-x_v)^2+(y_u-y_v)^2]^{\frac{1}{2}}, \tag{9}$$

where $x_u=X_u/m_u$, $y_u=Y_u/m_u$,
$x_v=X_v/m_v$, $y_v=Y_v/m_v$.

The distance VW measured in the same units as the coordinate scales is represented by the symbol s. The distances S and s may be measured with reasonable accuracy by use of a pair of dividers with a chromaticity diagram drawn accurately to a fairly large scale. The multiplication,

$$s=fS, \tag{10}$$

can be carried out with comparable accuracy by using in the customary manner the A and B scales of the slide rule represented in Fig. 7.

Differences of the chromaticities corresponding to small changes, $\Delta\theta$, of the position of either Rochon prism *13* or *14* in Fig. 3, can be determined with great accuracy by calculating the product

$$\Delta s=\Delta\theta(ds/d\theta). \tag{11}$$

A sufficiently accurate value of the derivative can be found by subtracting the values of f indicated by the slide rule for neighboring values of θ, dividing this difference by the difference of the values of θ, and multiplying this ratio by the value of S. Small differences of chromaticity computed from Eq. (11) are considerably more accurate than the chromaticities of the filters used to synthesize the colors.

D. STANDARD DEVIATIONS OF COLOR MATCHING

Several criteria were investigated for the measurement of the noticeability of color differences. The just noticeable difference was used extensively with results consistent with those which are given in this paper, but intercomparisons of data for different series of colors were unsatisfactory because of rather great fluctuations to which this criterion appeared to be subject. A consistent system of data, including representative kinds of color difference throughout the entire gamut of colors attainable with the instrument, could not be determined satisfactorily with a criterion subject to such fluctuations. Adjustments of the data to compensate for such fluctuations were considered inadmissible, since they might be influenced by preconceptions concerning the probable trend of the data and accumulated errors of such adjustments might introduce spurious characteristics and obscure essential features of the results.

Attempts were made to adjust color differences to equal certain standard color differences, several times greater than just noticeable. Observations of the standard color differences were alternated with the adjustments of the test differences. This criterion provided more consistent results than the criterion of just noticeability, but was exceedingly tedious and required extensive training of the observer. Such training cannot be given to subjects who are available for only a short examination during which an adequate determination of color discrimination must be completed. These examinations are one of the most important immediate applications of the instrument employed in the present investigation, and a criterion was sought which would be applicable in both routine testing and research. Such a criterion must be more reliable than the just noticeable difference and require less training and experience than either that or the judgment of equally noticeable color differences.

König and Dieterici[10] employed the mean error

[10] A. König and C. Dieterici, "Über die Empfindlichkeit des normalen Auges für Wellenlangenunterschiede des Lichtes," Wied. Ann. d. Physik und Chemie **22**, 579–589 (1884); Graefes Archiv. **30** (2), 158 (1884); *Gesammelte Abhandlungen zur Physiologischen Optik* (Leipzig, 1903), p. 23.

TABLE II. Standard deviations of color matching.

0° Filter number	90° Filter number	θ° Average setting	Δθ° Standard deviation	Average chromaticity x	Average chromaticity y	Distance from 0° point =s	Δs Standard deviation	Δy/Δx
4	23	83.8	0.239	0.286	0.286	0.294	0.00271	1.94
4	23	79.1	0.256	0.259	0.233	0.232	0.00370	1.94
4	23	79.1	0.230	0.259	0.233	0.232	0.00332	1.94
4	23	74.1	0.247	0.230	0.177	0.171	0.00290	1.94
4	23	69.0	0.382	0.208	0.135	0.122	0.00312	1.94
4	23	68.5	0.304	0.206	0.131	0.117	0.00242	1.94
4	23	58.4	0.335	0.180	0.081	0.062	0.00150	1.94
4	23	42.1	0.477	0.162	0.045	0.022	0.00067	1.94
4	23	25.1	0.563	0.155	0.031	0.006	0.00028	1.94
100	23	43.7	0.823	0.259	0.254	0.056	0.00213	2.21
66	23	73.9	0.284	0.268	0.280	0.229	0.00163	1.16
66	23	60.9	0.314	0.216	0.219	0.139	0.00184	1.16
66	23	52.0	0.334	0.185	0.183	0.102	0.00156	1.16
66	23	47.2	0.430	0.169	0.165	0.080	0.00176	1.16
66	23	45.1	0.423	0.166	0.161	0.072	0.00154	1.16
66	23	32.8	0.507	0.142	0.133	0.035	0.00116	1.16
66	23	16.7	0.642	0.125	0.113	0.008	0.00064	1.16
64	23	73.0	0.400	0.274	0.303	0.203	0.00157	0.63
64	23	58.7	0.302	0.220	0.269	0.139	0.00139	0.63
64	23	44.3	0.372	0.169	0.237	0.078	0.00139	0.63
64	23	30.2	0.652	0.132	0.214	0.035	0.00156	0.63
64	23	15.9	0.988	0.110	0.200	0.009	0.00122	0.63
8	23	74.1	0.531	0.288	0.322	0.213	0.00113	0.09
8	23	59.6	0.376	0.247	0.318	0.172	0.00147	0.09
8	23	45.2	0.504	0.192	0.313	0.116	0.00206	0.09
8	23	30.9	0.591	0.137	0.308	0.061	0.00215	0.09
23	55	21.7	0.469	0.277	0.329	0.029	0.00119	−0.23
23	55	30.7	0.322	0.251	0.335	0.056	0.00112	−0.23
23	55	31.1	0.326	0.249	0.336	0.057	0.00117	−0.23
23	55	45.3	0.296	0.193	0.349	0.116	0.00131	−0.23
23	55	46.0	0.430	0.191	0.349	0.118	0.00170	−0.23
23	55	46.2	0.436	0.190	0.349	0.119	0.00172	−0.23
23	55	60.6	0.614	0.126	0.364	0.185	0.00265	−0.23
23	55	61.2	0.587	0.124	0.364	0.187	0.00245	−0.23
23	55	75.6	1.080	0.074	0.376	0.238	0.00278	−0.23
23	55	77.4	0.953	0.070	0.377	0.243	0.00211	−0.23
23	28	21.4	0.432	0.282	0.338	0.027	0.00111	−0.66
23	28	30.7	0.430	0.258	0.354	0.057	0.00142	−0.66
23	28	45.2	0.332	0.205	0.389	0.120	0.00173	−0.66
23	28	45.7	0.391	0.203	0.390	0.123	0.00203	−0.66
23	28	59.6	0.490	0.139	0.432	0.200	0.00275	−0.66
23	28	74.0	0.778	0.079	0.471	0.271	0.00310	−0.66
23	46	20.2	0.370	0.289	0.341	0.024	0.00094	−1.12
23	46	20.8	0.515	0.288	0.342	0.026	0.00125	−1.12
23	46	30.1	0.425	0.269	0.364	0.055	0.00162	−1.12
23	46	30.4	0.298	0.278	0.365	0.056	0.00113	−1.12
23	46	30.8	0.327	0.267	0.366	0.058	0.00123	−1.12
23	46	44.6	0.461	0.222	0.416	0.126	0.00232	−1.12
23	46	45.8	0.441	0.218	0.420	0.132	0.00259	−1.12
23	46	45.5	0.410	0.219	0.419	0.130	0.00241	−1.12
23	46	58.4	0.423	0.162	0.483	0.218	0.00308	−1.12
23	46	59.4	0.437	0.157	0.489	0.225	0.00320	−1.12
23	46	59.9	0.536	0.153	0.491	0.228	0.00393	−1.12
23	46	60.9	0.510	0.149	0.497	0.235	0.00374	−1.12
23	46	59.8	0.428	0.154	0.491	0.228	0.00311	−1.12
23	46	70.8	0.690	0.102	0.549	0.305	0.00498	−1.12
23	46	74.1	0.928	0.088	0.564	0.327	0.00527	−1.12
23	46	77.5	1.027	0.076	0.578	0.346	0.00507	−1.12
38	23	31.8	0.572	0.503	0.212	0.050	0.00182	−0.56
38	23	46.0	0.376	0.456	0.248	0.104	0.00171	−0.56
38	23	60.6	0.267	0.391	0.275	0.179	0.00141	−0.56
38	23	75.8	0.232	0.329	0.309	0.250	0.00090	−0.56
65	23	30.7	0.392	0.426	0.168	0.033	0.00089	−1.29
65	23	31.1	0.408	0.426	0.168	0.033	0.00093	−1.29
65	23	45.3	0.250	0.400	0.201	0.075	0.00089	−1.29
65	23	75.4	0.172	0.323	0.300	0.201	0.00059	−1.29
65	23	75.4	0.187	0.323	0.300	0.201	0.00065	−1.29
25	23	31.9	0.460	0.408	0.159	0.031	0.00093	−1.58
25	23	45.4	0.363	0.390	0.189	0.066	0.00119	−1.58
25	23	60.9	0.234	0.357	0.240	0.127	0.00107	−1.58
25	23	76.2	0.187	0.320	0.298	0.196	0.00071	−1.58
42	23	15.2	0.865	0.380	0.120	0.006	0.00065	−2.70
42	23	21.3	0.584	0.378	0.126	0.011	0.00065	−2.70
42	23	31.1	0.372	0.373	0.138	0.025	0.00065	−2.70
42	23	44.5	0.250	0.362	0.168	0.059	0.00077	−2.70
42	23	60.4	0.221	0.342	0.223	0.116	0.00102	−2.70
42	23	74.4	0.241	0.319	0.285	0.182	0.00099	−2.70
79	23	28.9	0.614	0.340	0.220	0.021	0.00087	−2.92
79	23	44.0	0.408	0.332	0.245	0.048	0.00084	−2.92
79	23	73.9	0.603	0.310	0.309	0.115	0.00106	−2.92
41	23	30.2	0.477	0.241	0.080	0.017	0.00059	3.82
41	23	44.9	0.427	0.248	0.106	0.045	0.00113	3.82
41	23	45.1	0.421	0.249	0.107	0.046	0.00111	3.82
41	23	60.3	0.296	0.263	0.163	0.103	0.00151	3.82
76	23	29.6	0.706	0.260	0.142	0.026	0.00127	3.80
76	23	33.5	0.729	0.262	0.158	0.033	0.00155	3.80
76	23	44.4	0.637	0.268	0.163	0.061	0.00178	3.80
76	23	60.8	0.563	0.288	0.241	0.121	0.00231	3.80
76	23	74.9	0.555	0.298	0.295	0.176	0.00176	3.80
40	23	30.1	0.662	0.208	0.058	0.014	0.00069	2.73
40	23	45.1	0.531	0.216	0.080	0.038	0.00122	2.73
40	23	60.0	0.388	0.234	0.128	0.090	0.00193	2.73
40	23	74.7	0.293	0.270	0.228	0.195	0.00274	2.73
63	23	15.2	1.503	0.176	0.035	0.003	0.00058	2.23
63	23	28.7	1.090	0.179	0.043	0.010	0.00078	2.23
63	23	33.6	1.345	0.181	0.046	0.013	0.00127	2.23
63	23	40.0	1.010	0.184	0.054	0.021	0.00133	2.23
63	23	41.6	1.082	0.185	0.056	0.026	0.00173	2.23
63	23	45.2	0.810	0.188	0.062	0.029	0.00153	2.23
63	23	50.0	0.920	0.193	0.082	0.039	0.00226	2.23
63	23	59.4	0.759	0.206	0.103	0.076	0.00384	2.23
63	23	59.6	0.800	0.207	0.103	0.078	0.00405	2.23
63	23	69.3	0.443	0.232	0.160	0.140	0.00370	2.23
63	23	70.1	0.443	0.234	0.166	0.148	0.00370	2.23
63	23	74.7	0.354	0.252	0.205	0.190	0.00373	2.23
63	23	79.0	0.296	0.272	0.250	0.238	0.00350	2.23
23	24	21.9	0.422	0.292	0.352	0.032	0.00130	−2.19
23	24	31.2	0.458	0.277	0.384	0.068	0.00214	−2.19
23	24	44.3	0.508	0.245	0.454	0.145	0.00378	−2.19
23	24	59.4	0.551	0.190	0.576	0.280	0.00575	−2.19
23	24	73.1	0.880	0.131	0.704	0.422	0.00857	−2.19
23	36	30.0	0.539	0.293	0.375	0.054	0.00206	−4.41
23	36	44.5	0.470	0.277	0.445	0.126	0.00307	−4.41
23	36	58.2	0.526	0.254	0.549	0.233	0.00470	−4.41
23	36	72.3	0.794	0.225	0.675	0.363	0.00697	−4.41
23	36	72.9	0.777	0.224	0.680	0.369	0.00679	−4.41
23	33	28.6	1.043	0.312	0.360	0.038	0.00284	5.03
23	33	44.2	0.777	0.323	0.415	0.094	0.00350	5.03
23	33	59.1	0.812	0.338	0.494	0.176	0.00496	5.03
23	33	74.4	1.385	0.356	0.585	0.268	0.00729	5.03
23	59	15.2	1.585	0.310	0.332	0.011	0.00219	2.04
23	59	18.7	1.438	0.312	0.338	0.016	0.00293	2.04
23	59	25.8	1.000	0.319	0.351	0.031	0.00246	2.04
23	59	41.6	0.689	0.341	0.397	0.084	0.00286	2.04
23	59	42.5	0.681	0.341	0.400	0.088	0.00286	2.04
23	59	58.0	0.774	0.376	0.466	0.162	0.00418	2.04
23	59	69.6	1.037	0.402	0.520	0.223	0.00563	2.04
23	17	22.8	0.866	0.322	0.341	0.024	0.00185	1.06
23	17	44.7	0.510	0.370	0.392	0.096	0.00215	1.06
23	17	59.9	0.608	0.419	0.444	0.168	0.00299	1.06
23	17	75.9	1.028	0.468	0.496	0.239	0.00368	1.06
23	51	17.4	0.557	0.321	0.331	0.018	0.00116	0.51
23	51	29.1	0.360	0.349	0.346	0.051	0.00122	0.51
23	51	43.8	0.397	0.402	0.373	0.110	0.00190	0.51
23	51	43.8	0.378	0.402	0.373	0.110	0.00181	0.51
23	51	59.1	0.437	0.468	0.407	0.186	0.00219	0.51
23	51	72.4	0.835	0.520	0.434	0.244	0.00302	0.51
23	53	13.3	0.415	0.318	0.326	0.014	0.00087	0.19
23	53	28.9	0.246	0.365	0.334	0.062	0.00102	0.19
23	53	43.8	0.334	0.437	0.348	0.136	0.00179	0.19
23	53	58.4	0.452	0.518	0.363	0.218	0.00243	0.19
23	53	71.3	0.668	0.578	0.375	0.280	0.00268	0.19
34	23	75.6	0.271	0.325	0.320	0.291	0.00073	−0.13
34	23	60.5	0.218	0.381	0.313	0.233	0.00104	−0.13
34	23	46.5	0.267	0.453	0.304	0.160	0.00147	−0.13
34	23	41.5	0.289	0.479	0.300	0.134	0.00154	−0.13
34	23	32.1	0.390	0.527	0.294	0.085	0.00187	−0.13
34	23	23.3	0.462	0.564	0.289	0.046	0.00176	−0.13
21	23	75.5	0.166	0.336	0.319	0.405	0.00070	−0.14
21	23	60.4	0.210	0.422	0.307	0.318	0.00150	−0.14
21	34	35.2	1.342	0.698	0.269	0.039	0.00262	−0.16

TABLE II.—Continued.

0° Filter number	90° Filter number	θ° Average setting	Δθ° Standard deviation	Average chromaticity x	Average chromaticity y	Distance from 0° point =s	Δs Standard deviation	Δy/Δx
4	40	10.2	0.663	0.153	0.026	0.001	0.000135	0.37
4	40	20.3	0.379	0.156	0.027	0.004	0.000156	0.37
4	40	30.1	0.296	0.160	0.029	0.009	0.000179	0.37
4	40	39.8	0.266	0.167	0.032	0.016	0.000218	0.37
4	40	45.2	0.254	0.171	0.033	0.020	0.000224	0.37
4	40	50.1	0.274	0.175	0.035	0.025	0.000268	0.37
4	40	60.0	0.360	0.185	0.038	0.035	0.000372	0.37
4	40	69.7	0.532	0.194	0.042	0.044	0.000483	0.37
4	40	70.2	0.509	0.194	0.042	0.045	0.000463	0.37
4	66	21.0	1.733	0.151	0.031	0.003	0.00068	−2.43
4	66	29.5	1.185	0.150	0.032	0.006	0.00057	−2.43
4	66	29.9	1.297	0.150	0.032	0.006	0.00062	−2.43
4	66	45.1	1.100	0.145	0.042	0.017	0.00104	−2.43
4	66	68.5	0.860	0.132	0.075	0.053	0.00178	−2.43
4	66	69.0	1.060	0.131	0.077	0.054	0.00219	−2.43
66	55	34.2	1.280	0.112	0.136	0.031	0.00274	−4.28
66	55	44.1	0.715	0.106	0.161	0.057	0.00222	−4.28
66	55	60.1	0.470	0.090	0.229	0.127	0.00265	−4.28
66	55	60.2	0.536	0.090	0.230	0.127	0.00302	−4.28
66	55	70.1	0.422	0.076	0.291	0.190	0.00286	−4.28
66	55	70.2	0.400	0.076	0.292	0.190	0.00271	−4.28
66	55	74.1	0.560	0.070	0.317	0.217	0.00363	−4.28
66	55	80.1	0.770	0.062	0.352	0.253	0.00393	−4.28
66	55	81.6	1.000	0.060	0.360	0.261	0.00450	−4.28
55	15	29.3	1.053	0.057	0.431	0.052	0.00385	16.18
55	15	43.8	0.747	0.060	0.499	0.118	0.00419	16.18
55	15	59.3	0.595	0.064	0.594	0.215	0.00409	16.18
55	15	59.4	0.790	0.064	0.595	0.216	0.00542	16.18
55	15	59.5	0.806	0.064	0.595	0.217	0.00554	16.18
55	15	73.7	0.985	0.068	0.687	0.308	0.00530	16.18
55	15	74.3	1.046	0.068	0.690	0.312	0.00563	16.18
55	15	74.4	1.012	0.068	0.691	0.312	0.00545	16.18
15	16	27.5	1.264	0.092	0.746	0.024	0.00205	0.45
15	16	28.1	1.441	0.093	0.746	0.025	0.00234	0.45
15	16	42.9	1.092	0.118	0.758	0.054	0.00225	0.45
15	16	59.3	1.009	0.150	0.772	0.088	0.00196	0.45
15	16	60.3	1.237	0.151	0.772	0.090	0.00240	0.45
17	16	20.9	0.445	0.465	0.532	0.036	0.00156	−0.89
17	16	30.2	0.339	0.436	0.558	0.076	0.00170	−0.89
17	16	30.4	0.370	0.436	0.558	0.078	0.00185	−0.89
17	16	30.6	0.397	0.435	0.559	0.078	0.00198	−0.89
17	16	30.8	0.419	0.434	0.560	0.079	0.00210	−0.89
17	16	30.7	0.327	0.435	0.559	0.079	0.00164	−0.89
17	16	40.4	0.353	0.392	0.596	0.135	0.00222	−0.89
17	16	45.0	0.308	0.370	0.616	0.165	0.00214	−0.89
17	16	45.4	0.348	0.368	0.618	0.167	0.00237	−0.89
17	16	45.6	0.327	0.367	0.619	0.169	0.00222	−0.89
17	16	50.1	0.357	0.343	0.641	0.201	0.00258	−0.89
17	16	59.2	0.352	0.291	0.687	0.268	0.00261	−0.89
17	16	59.7	0.418	0.283	0.694	0.272	0.00309	−0.89
17	16	60.1	0.486	0.281	0.696	0.275	0.00360	−0.89
17	16	60.5	0.456	0.278	0.698	0.278	0.00338	−0.89
17	16	73.1	0.815	0.217	0.752	0.360	0.00418	−0.89
17	16	74.9	0.738	0.210	0.758	0.370	0.00378	−0.89
17	16	75.3	0.890	0.208	0.760	0.372	0.00455	−0.89
21	33	21.6	0.397	0.723	0.276	0.019	0.00074	−0.99
21	33	31.2	0.358	0.706	0.293	0.043	0.00114	−0.99
21	33	46.2	0.216	0.659	0.340	0.109	0.00127	−0.99
21	33	50.7	0.188	0.638	0.360	0.138	0.00137	−0.99
21	33	60.5	0.136	0.576	0.422	0.225	0.00141	−0.99
21	33	70.4	0.112	0.492	0.505	0.343	0.00143	−0.99
21	33	75.3	0.143	0.447	0.549	0.406	0.00179	−0.99
48	33	21.6	0.521	0.661	0.338	0.032	0.00154	−0.98
48	33	45.6	0.161	0.576	0.422	0.153	0.00115	−0.98
48	33	60.5	0.178	0.491	0.506	0.272	0.00155	−0.98
48	33	70.3	0.179	0.430	0.566	0.358	0.00147	−0.98
40	21	29.3	0.354	0.229	0.056	0.028	0.00078	+0.41
40	21	39.4	0.282	0.256	0.067	0.058	0.00107	0.41
40	21	40.2	0.299	0.260	0.068	0.061	0.00114	0.41
40	21	49.9	0.369	0.304	0.086	0.109	0.00240	0.41
40	21	50.2	0.326	0.306	0.087	0.111	0.00212	0.41
40	21	60.1	0.366	0.381	0.118	0.192	0.00379	0.41
40	21	69.9	0.287	0.499	0.166	0.320	0.00447	0.41
40	21	74.5	0.268	0.566	0.193	0.392	0.00456	0.41
40	21	75.0	0.268	0.575	0.197	0.402	0.00456	0.41
40	21	79.6	0.308	0.646	0.226	0.478	0.00499	0.41
40	21	79.8	0.324	0.648	0.227	0.479	0.00524	0.41
40	21	84.6	0.498	0.705	0.240	0.545	0.00502	0.41
40	21	84.7	0.514	0.710	0.241	0.548	0.00518	0.41

of adjustment in their investigation of the noticeability of wave-length differences in the spectrum. This method has been mentioned as a possibility by several other investigators, but it has not been used to any considerable extent. In a very significant recent report[5] of an investigation similar to the present, Wright discussed his reasons for adopting a criterion of definitely noticeable color differences. He concludes this discussion with the following paragraph:

"It is, of course, quite true that some variations in judgment are inevitable. No doubt the ideal method would be to make a large number of matches at each point in the colour chart and then to analyse the spread of the observations, but in practice this would be an impossibly lengthy process."

The program which Wright describes as ideal becomes practical with the apparatus used in the present investigation, in which any one desired variable can be investigated independently of all other variations. In an oral report[11] of the present investigation, the results were presented in terms of the probable errors of color matching. In the discussion of that report, the suggestion was made that the results be published in terms of the standard deviation, the root mean square of the individual deviations from the average setting. The significance of the concept of probable error is questionable when the distribution of errors does not fit the "normal" distribution curve very accurately. In order to avoid implications not justified by the observations, the results will be reported here in terms of standard deviation rather than in terms of probable error. This change in the data reported previously[11] involved only the omission of a constant factor, 0.6745.

The apparatus employed in this investigation is particularly suitable for the matching method

[11] D. L. MacAdam, "Noticeability of color differences in daylight," J. Opt. Soc. Am. **30**, 657A (1940).

TABLE III. Standard deviations of color matching.

0° Filter number	90° Filter number	$\theta°$ Average setting	$\Delta\theta°$ Standard deviation	Average chromaticity x	Average chromaticity y	$\Delta y/\Delta x$	Δs Standard deviation
80	16	63.1	0.281	0.258	0.450	−5.18	0.00388
84	35	57.1	0.445	0.258	0.450	−500	0.00424
23	14	44.1	0.586	0.258	0.450	−2.72	0.00413
64	33	65.0	0.292	0.258	0.450	1.66	0.00323
90	28	48.8	0.241	0.258	0.450	−0.47	0.00188
90	28	49.1	0.240	0.258	0.450	−0.47	0.00186
74	57	66.5	0.320	0.258	0.450	3.26	0.00398
23	14	43.8	0.563	0.258	0.450	−2.72	0.00397
60	44	32.4	0.548	0.258	0.450	−1.02	0.00237
54	17	48.0	0.304	0.258	0.450	0.26	0.00234
54	17	48.1	0.317	0.258	0.450	0.26	0.00244
80	36	64.0	0.315	0.258	0.450	−6.33	0.00430
106	104	52.7	0.874	0.441	0.198	0.58	0.00270
119	73	50.7	0.400	0.441	0.198	3.24	0.00123
25	81	51.0	0.452	0.441	0.198	7.35	0.00108
79	38	39.7	0.352	0.441	0.198	−0.06	0.00137
79	38	40.0	0.306	0.441	0.198	−0.06	0.00119
79	38	39.6	0.387	0.441	0.198	−0.06	0.00150
80	43	44.4	0.300	0.441	0.198	0.25	0.00190
42	52	53.5	0.350	0.441	0.198	1.54	0.00176
92	53	52.8	0.338	0.441	0.198	1.02	0.00241
65	70	50.0	0.401	0.441	0.198	−1.70	0.00095
37	120	44.5	0.278	0.441	0.198	−0.39	0.00114
77	69	48.0	0.330	0.280	0.385	0.12	0.00138
70	44	50.0	0.218	0.280	0.385	−1.26	0.00185
50	59	64.8	0.265	0.280	0.385	1.37	0.00320
75	33	50.2	0.596	0.280	0.385	2.77	0.00391
84	61	53.5	0.560	0.280	0.385	5.54	0.00375
84	61	53.6	0.566	0.280	0.385	5.54	0.00379
80	35	60.5	0.296	0.280	0.385	−11.47	0.00326

0° Filter number	90° Filter number	$\theta°$ Average setting	$\Delta\theta°$ Standard deviation	Average chromaticity x	Average chromaticity y	$\Delta y/\Delta x$	Δs Standard deviation
72	46	50.9	0.430	0.212	0.550	−0.32	0.00266
30	31	38.8	0.341	0.212	0.550	0.01	0.00230
69	44	53.9	0.441	0.212	0.550	−0.80	0.00339
54	57	55.3	0.408	0.212	0.550	0.97	0.00283
28	61	51.8	0.440	0.212	0.550	0.39	0.00212
28	61	51.0	0.453	0.212	0.550	0.39	0.00218
75	16	64.1	0.480	0.212	0.550	−11.15	0.00555
23	6	60.7	0.631	0.212	0.550	−2.30	0.00491
23	6	61.9	0.554	0.212	0.550	−2.30	0.00431
77	35	55.9	0.603	0.212	0.550	3.61	0.00448
78	45	48.3	0.601	0.212	0.550	2.87	0.00308
78	45	47.2	0.610	0.212	0.550	2.87	0.00313
34	23	41.7	0.304	0.475	0.300	−0.16	0.00152
37	72	41.0	0.235	0.475	0.300	−2.76	0.00102
84	27	54.5	0.330	0.475	0.300	0.30	0.00246
70	53	43.5	0.593	0.475	0.300	0.64	0.00276
106	88	67.3	0.373	0.475	0.300	1.39	0.00190
86	14	59.3	1.481	0.150	0.680	−4.88	0.00918
86	14	59.2	1.481	0.150	0.680	−4.88	0.00918
85	24	57.9	1.233	0.150	0.680	−2.74	0.00757
30	36	61.0	0.626	0.150	0.680	1.45	0.00313
71	24	55.0	1.462	0.150	0.680	−2.00	0.00719
71	24	50.0	1.507	0.150	0.680	−2.00	0.00741
78	14	61.6	1.012	0.150	0.680	−8.93	0.00720
78	14	63.8	0.948	0.150	0.680	−8.93	0.00674
44	45	43.6	0.501	0.150	0.680	0.24	0.00200
44	45	44.9	0.505	0.150	0.680	0.24	0.00202
72	15	65.5	0.551	0.150	0.680	−0.77	0.00359
72	15	64.9	0.539	0.150	0.680	−0.77	0.00351
54	16	67.8	0.593	0.150	0.680	3.03	0.00489
46	35	52.6	0.587	0.150	0.680	0.62	0.00250

of determining the noticeability of color differences. Since the equality of luminance is automatically maintained by the instrument, only one adjustment need be made by the observer in order to establish the match. The analysis of the results of observations is simple and unambiguous, since variations of only one quantity need be considered. Fifty adjustments of the instrument for color match were customarily made at one sitting. The average of the observed angles was taken as the correct reading for the color match. This practice compensated automatically for any otherwise undetectable instrumental errors. The difference between the average and the angle to which the other prism was set throughout the series was an indication of the perfection with which the instrument had been prepared for the observations. In cases of appreciable discrepancies, the observations were repeated after the instrumental arrangements had been improved. Such imperfect arrangements of the instrument arose principally from slight nonuniformities in the filters. The experimenter customarily made a short series of observations of his own, and usually detected any serious disagreement between the angles of the two prisms at color match, and corrected the cause of such discrepancy before the regular observer commenced his observations.

Each of the angles observed was then subtracted from the average for the series, and these deviations were squared. The sum of the squares of the deviations was divided by the number of observations less one. The square root of this quantity is the standard deviation for a single observation of the angle for color match. This deviation of prism angle can be converted to standard deviation of distance in the chromaticity diagram by the use of Eq. (11). This standard deviation of chromaticity match can be assigned to the chromaticity corresponding to the average observed angle.

The criterion of color match is so familiar, and with the present instrument the adjustments required to establish a color match are so easy that the method has been found to be most useful in the investigation of the noticeability of color differences. This method has proved practical in extensive tests of all kinds of color differences for a few observers, and in tests for a few important kinds of color differences, using a large group of untrained and previously unexperienced observers. Extensive tests have indicated that the just noticeable differences of

TABLE III.—Continued.

0° Filter number	90° Filter number	$\theta°$ Average setting	$\Delta\theta°$ Standard deviation	Average chromaticity x	Average chromaticity y	$\Delta y/\Delta x$	Δs Standard deviation
106	34	59.0	0.464	0.510	0.236	0.53	0.00234
39	70	44.0	0.453	0.510	0.236	−0.08	0.00173
25	53	52.9	0.400	0.510	0.236	1.30	0.00202
37	91	45.1	0.356	0.510	0.236	−5.87	0.00114
38	81	50.9	0.452	0.510	0.236	−0.91	0.00120
65	52	49.7	0.428	0.510	0.236	2.08	0.00185
65	52	49.6	0.327	0.510	0.236	2.08	0.00141
65	52	49.4	0.405	0.510	0.236	2.08	0.00173
69	33	48.8	0.643	0.380	0.498	−11.90	0.00264
95	57	51.7	0.329	0.380	0.498	−3.02	0.00191
23	59	62.1	0.760	0.380	0.498	2.03	0.00373
23	59	60.8	0.939	0.380	0.498	2.03	0.00462
99	32	63.1	0.560	0.380	0.498	7.19	0.00353
68	110	54.9	0.388	0.380	0.498	−1.09	0.00132
68	110	51.9	0.444	0.380	0.498	−1.09	0.00150
108	31	40.4	0.655	0.380	0.498	0.52	0.00163
108	31	41.8	0.833	0.380	0.498	0.52	0.00208
60	109	62.8	0.848	0.380	0.498	1.19	0.00219
60	109	62.4	0.894	0.380	0.498	1.19	0.00224
64	79	30.4	0.277	0.160	0.200	0.02	0.00099
29	75	45.7	0.390	0.160	0.200	0.65	0.00095
82	8	55.2	0.376	0.160	0.200	−1.44	0.00160
47	85	62.2	0.227	0.160	0.200	4.53	0.00168
66	102	62.6	0.353	0.160	0.200	2.46	0.00128
74	112	41.6	1.127	0.160	0.200	−6.06	0.00203
84	104	47.5	0.270	0.390	0.237	0.03	0.00126
80	87	48.6	0.459	0.390	0.237	0.82	0.00240
80	87	48.4	0.452	0.390	0.237	0.82	0.00236
25	93	44.7	0.248	0.390	0.237	−1.76	0.00098
42	69	60.5	0.225	0.390	0.237	92.3	0.00123
92	91	63.4	0.258	0.390	0.237	2.42	0.00178
26	89	66.8	0.258	0.390	0.237	1.64	0.00216
37	98	50.9	0.176	0.390	0.237	−0.54	0.00107
65	99	63.2	0.286	0.390	0.237	−1.38	0.00105
100	27	48.2	0.274	0.390	0.237	0.42	0.00197
100	27	46.9	0.237	0.390	0.237	0.42	0.00170
70	72	65.1	0.471	0.385	0.393	−26.10	0.00242
79	109	66.8	0.440	0.385	0.393	5.15	0.00306
97	67	58.1	0.511	0.385	0.393	1.74	0.00361
97	67	59.0	0.506	0.385	0.393	1.74	0.00357
99	31	48.1	0.771	0.385	0.393	2.61	0.00375
103	94	59.3	0.204	0.385	0.393	−0.67	0.00160
98	51	44.9	0.277	0.385	0.393	0.39	0.00210
23	62	44.5	0.552	0.385	0.393	0.85	0.00247
70	23	52.0	0.412	0.344	0.284	−1.01	0.00089
102	73	47.3	0.197	0.344	0.284	0.09	0.00102
84	96	48.0	0.409	0.344	0.284	0.61	0.00142
97	95	45.7	0.557	0.344	0.284	0.88	0.00190
80	69	59.9	0.393	0.344	0.284	2.70	0.00198
80	69	60.4	0.437	0.344	0.284	2.70	0.00222
79	108	45.1	0.394	0.344	0.284	−12.85	0.00163
76	93	63.9	0.310	0.270	0.275	8.94	0.00178
74	116	47.8	0.427	0.228	0.250	1.38	0.00228
76	98	63.0	0.336	0.228	0.250	−5.38	0.00142
83	93	61.5	0.507	0.228	0.250	2.84	0.00296
82	94	58.0	0.378	0.228	0.250	6.05	0.00272
79	8	47.2	0.158	0.228	0.250	−0.38	0.00080
50	23	60.1	0.316	0.228	0.250	0.94	0.00160
100	30	60.2	0.397	0.152	0.365	−2.09	0.00347
83	113	70.0	0.353	0.152	0.365	−7.23	0.00360
84	28	56.0	0.514	0.152	0.365	−1.29	0.00324
64	71	58.5	0.373	0.152	0.365	3.23	0.00265
8	94	45.4	0.416	0.152	0.365	0.89	0.00175
23	55	54.2	0.526	0.152	0.365	−0.23	0.00232
66	76	47.5	0.221	0.187	0.118	0.15	0.00054
107	75	56.5	0.652	0.187	0.118	2.88	0.00207
107	75	56.0	0.608	0.187	0.118	2.88	0.00193
107	75	52.9	0.700	0.187	0.118	2.88	0.00222
63	98	65.3	0.373	0.187	0.118	6.82	0.00197
63	98	64.5	0.324	0.187	0.118	6.82	0.00172
82	50	35.6	0.393	0.187	0.118	−0.41	0.00057
47	100	59.6	0.310	0.187	0.118	1.02	0.00092
40	101	63.3	0.236	0.187	0.118	−3.61	0.00082
26	8	45.5	0.160	0.253	0.125	−0.97	0.00057
26	101	52.2	0.158	0.253	0.125	−0.82	0.00047
107	80	66.2	0.390	0.253	0.125	0.76	0.00153
82	106	37.6	0.277	0.253	0.125	0.28	0.00067
63	96	64.6	0.292	0.253	0.125	1.22	0.00227
41	97	57.7	0.392	0.253	0.125	3.84	0.00121
40	99	62.1	0.437	0.253	0.125	1.71	0.00221
117	100	43.8	0.502	0.160	0.057	1.41	0.00084
117	100	45.3	0.458	0.160	0.057	1.41	0.00079
118	106	30.3	0.265	0.160	0.057	0.44	0.00047
4	83	56.4	0.493	0.160	0.057	2.56	0.00081
40	47	62.3	0.278	0.160	0.057	−0.32	0.00036
40	47	58.5	0.276	0.160	0.057	−0.32	0.00036
63	66	50.9	0.287	0.160	0.057	−1.30	0.00040
26	87	53.7	0.564	0.365	0.153	1.16	0.00294
26	87	52.4	0.610	0.365	0.153	1.16	0.00318
26	87	53.0	0.577	0.365	0.153	1.16	0.00302
92	81	49.3	0.576	0.365	0.153	1.67	0.00189
25	80	52.5	0.462	0.365	0.153	−0.24	0.00122
42	79	52.6	0.474	0.365	0.153	−2.43	0.00078
76	38	41.5	0.332	0.365	0.153	0.21	0.00175
119	70	51.5	0.590	0.365	0.153	−3.18	0.00132
41	105	67.6	0.607	0.365	0.153	0.66	0.00336
92	81	51.0	0.554	0.365	0.153	1.67	0.00182
41	105	67.3	0.666	0.365	0.153	0.66	0.00369
38	67	56.3	0.185	0.527	0.350	−4.08	0.00128
106	52	70.1	0.284	0.527	0.350	1.25	0.00201
48	60	44.0	0.293	0.527	0.350	−0.23	0.00189
23	27	54.9	0.332	0.527	0.350	0.07	0.00194
120	53	62.8	0.416	0.527	0.350	0.44	0.00252
79	71	54.5	0.185	0.305	0.323	−2.59	0.00101
75	17	43.4	0.361	0.305	0.323	1.03	0.00203
74	67	56.8	0.247	0.305	0.323	1.28	0.00228
84	116	49.9	0.471	0.305	0.323	1.76	0.00213
112	95	50.9	0.191	0.305	0.323	0.27	0.00095
99	78	34.1	0.272	0.305	0.323	−0.84	0.00085
84	72	45.7	0.475	0.305	0.323	2.09	0.00215
79	48	47.1	0.389	0.596	0.283	0.34	0.00241
39	51	38.9	0.434	0.596	0.283	−5.70	0.00132
37	27	59.8	0.376	0.596	0.283	1.20	0.00152
43	69	35.9	0.324	0.596	0.283	−0.55	0.00138
21	73	50.2	0.440	0.596	0.283	−0.14	0.00203
81	49	51.0	0.503	0.596	0.283	0.03	0.00236
28	61	37.5	0.377	0.131	0.521	0.39	0.00212
94	30	55.3	0.560	0.131	0.521	−0.36	0.00222
8	36	55.7	0.366	0.131	0.521	3.60	0.00326
77	24	48.8	0.512	0.131	0.521	−7.21	0.00358
77	24	47.3	0.591	0.131	0.521	−7.21	0.00415
78	44	43.0	0.956	0.131	0.521	−2.00	0.00418
98	44	57.8	0.643	0.131	0.521	−2.04	0.00474
23	46	64.6	0.546	0.131	0.521	−1.12	0.00389
23	46	65.0	0.587	0.131	0.521	−1.12	0.00416
76	23	57.4	0.342	0.278	0.223	3.80	0.00137
76	23	57.5	0.360	0.278	0.223	3.80	0.00145
100	99	49.2	0.494	0.278	0.223	1.05	0.00129
100	99	49.1	0.518	0.278	0.223	1.05	0.00136
82	69	56.7	0.367	0.278	0.223	1.61	0.00224
79	75	51.8	0.258	0.278	0.223	−0.42	0.00046
106	75	62.3	0.197	0.278	0.223	−0.70	0.00059
82	69	55.1	0.411	0.278	0.223	1.61	0.00252
80	86	41.8	0.241	0.278	0.223	−2.91	0.00089
74	120	68.4	0.407	0.278	0.223	0.60	0.00103
74	120	69.0	0.407	0.278	0.223	0.60	0.00103
80	98	47.2	0.263	0.278	0.223	−1.89	0.00068
76	79	52.7	0.798	0.300	0.163	0.79	0.00181
26	120	60.6	0.237	0.300	0.163	158.0	0.00080
26	120	60.4	0.237	0.300	0.163	158.0	0.00080
83	105	49.7	0.255	0.300	0.163	0.33	0.00121
106	100	46.2	0.261	0.300	0.163	−0.16	0.00062
41	96	61.1	0.459	0.300	0.163	1.48	0.00283
41	96	61.3	0.413	0.300	0.163	1.48	0.00253
92	97	59.3	0.258	0.300	0.163	−2.36	0.00076
70	62	62.6	0.520	0.472	0.399	2.22	0.00290
38	109	64.3	0.204	0.472	0.399	−1.69	0.00158
103	72	56.1	0.278	0.472	0.399	−1.18	0.00155
69	52	41.7	0.449	0.472	0.399	0.14	0.00152
73	67	49.9	0.431	0.472	0.399	−16.0	0.00176
23	58	57.3	0.422	0.472	0.399	0.40	0.00231
81	17	54.3	0.456	0.472	0.399	5.85	0.00201
99	51	60.6	0.546	0.472	0.399	0.80	0.00269
87	116	45.8	0.352	0.472	0.399	−0.72	0.00111
99	51	58.9	0.593	0.472	0.399	0.80	0.00292

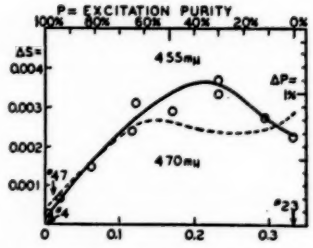

FIG. 8. Standard deviations of purity matching for dominant wave-length 455 mμ (PGN, solid curve and circles); and 470 mμ (DLM, broken curve).

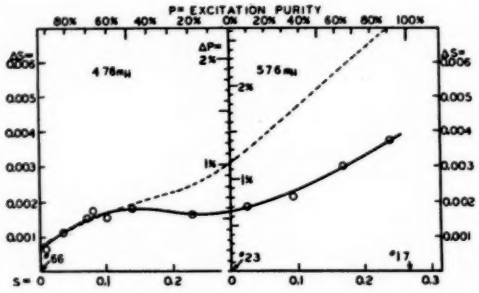

FIG. 9. Standard deviations of purity matching for dominant wave-lengths 476 and 576 mμ (PGN, solid curve and circles; DLM, broken curve).

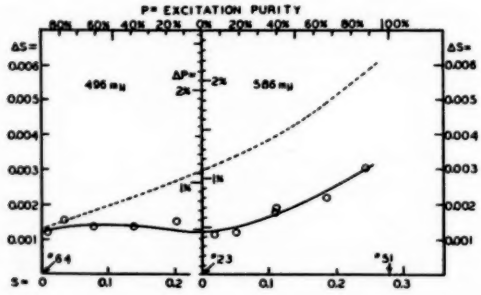

FIG. 10. Standard deviations of purity for dominant wave-lengths 496 and 586 mμ (PGN, circles and solid curve; DLM, broken curve).

color, for constant luminance of approximately 15 millilamberts, are proportional to the corresponding standard deviations of color matching by the same observer. Fluctuations of the criterion of just noticeability will, of course, alter the constant of proportionality, but this factor (approximately three) is constant throughout any series of observations of the kind specified in which the criterion of just noticeability has been proved to be constant. Therefore, the

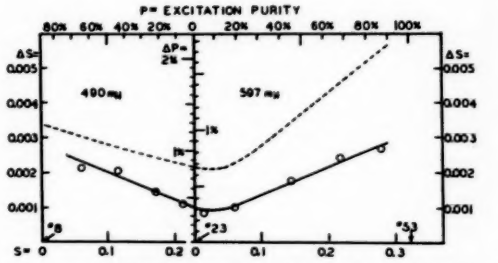

FIG. 11. Standard deviations of purity for dominant wave-lengths 490 and 597 mμ (PGN, circles and solid curve; DLM, broken curve).

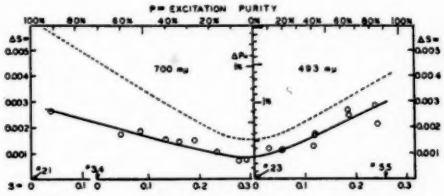

FIG. 12. Standard deviations of purity for dominant wave-lengths 493 and 700 mμ (PGN, circles and solid curve; DLM, broken curve).

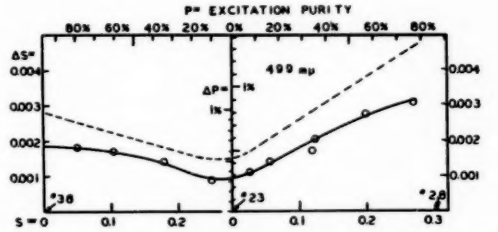

FIG. 13. Standard deviations of purity for dominant wave-length 499 mμ and complementary (PGN, circles and solid curve; DLM, broken curve).

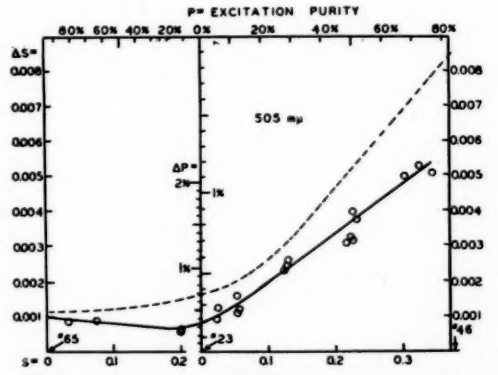

FIG. 14. Standard deviations of purity for dominant wave-length 505 mμ and complementary (PGN, circles and solid curve; DLM, broken curve).

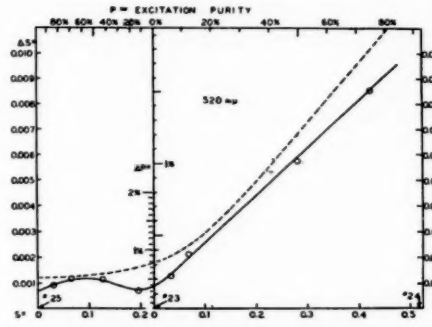

FIG. 15. Standard deviations of purity for dominant wave-length 520 mμ and complementary (PGN, circles and solid curve; DLM, broken curve).

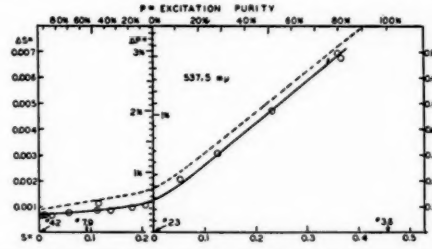

FIG. 16. Standard deviations of purity for dominant wave-length 537.5 mμ and complementary (PGN, circles and solid curve; DLM, broken curve).

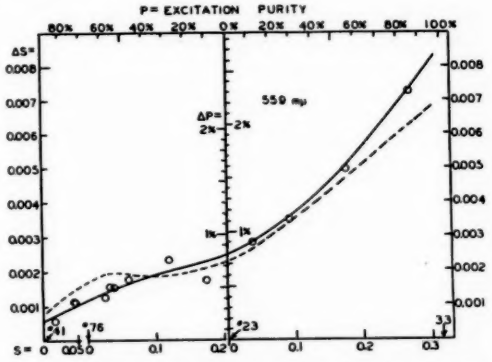

FIG. 17. Standard deviations of purity for dominant wave-length 559 mμ and complementary (PGN, circles and solid curve; DLM, broken curve).

standard deviation of color matching is considered to be a satisfactory measure of the noticeability of color differences, equivalent in significance to the just noticeable difference and more consistent in magnitude.

Tables II and III and the circled points and solid curves in Figs. 8 to 47 represent the results

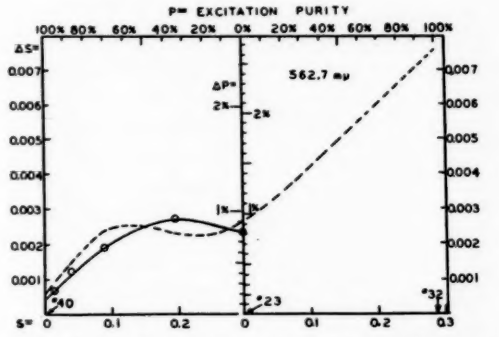

FIG. 18. Standard deviations of purity for dominant wave-length 562.7 mμ and complementary (PGN, circles and solid curve; DLM, broken curve).

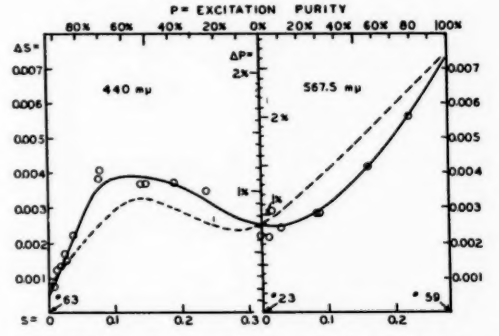

FIG. 19. Standard deviations of purity for dominant wave-lengths 440 and 567.5 mμ (PGN, circles and solid curve; DLM, broken curve).

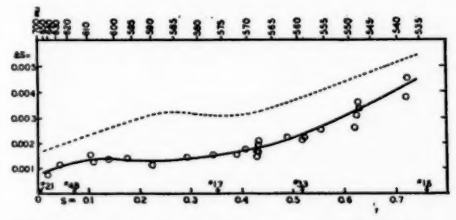

FIG. 20. Standard deviations of chromaticity along spectrum locus from 535 to 700 mμ (PGN, circles and solid curve; DLM, broken curve).

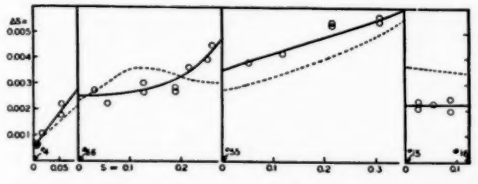

FIG. 21. Standard deviations of chromaticity along lines near spectrum locus from 400 to 535 mμ (PGN, circles and solid curves; DLM, broken curve).

derived from the observations of a single observer. Mr. Perley G. Nutting, Jr., whose interest and patience is acknowledged here with gratitude and admiration, has made nearly 25,000 settings for color match, and practically all of his results are represented in the tables and curves. Figures 8 to 19 represent the standard deviations of matching the purities of the indicated chromaticities, when purity alone was variable and subject to error. The dominant wave-lengths are indicated on the figures. Figure 20 represents the standard deviations of chromaticity matching when the chromaticity varied along a straight line very close to the spectrum locus from 533

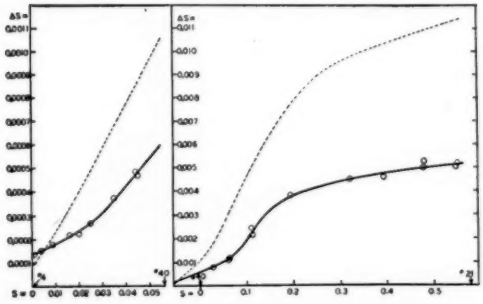

FIG. 22. Standard deviations of chromaticity along the straight line connecting points representing 440 and 700 mμ (PGN, circles and solid curve; DLM, broken curve). Note enlarged scale of portions of curve shown at left.

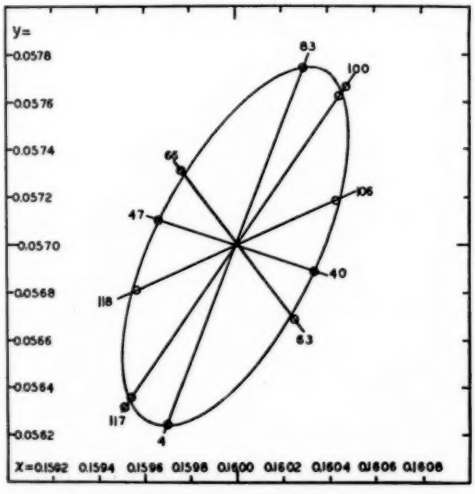

FIG. 23. Standard deviations of chromaticity from point ($x=0.160$, $y=0.057$), observer: PGN.

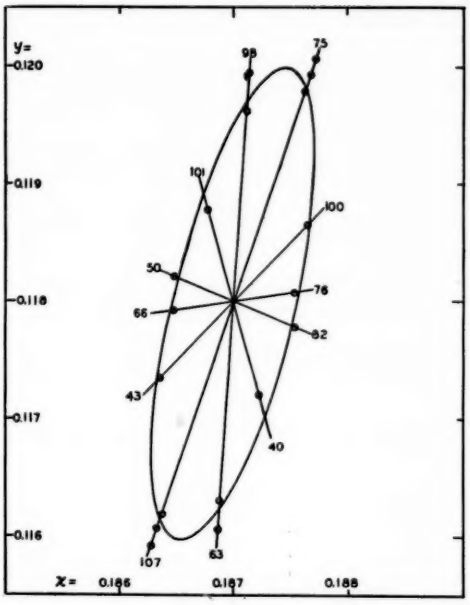

FIGS. 24 TO 47. Standard deviations of chromaticity from indicated standards, observer: PGN.

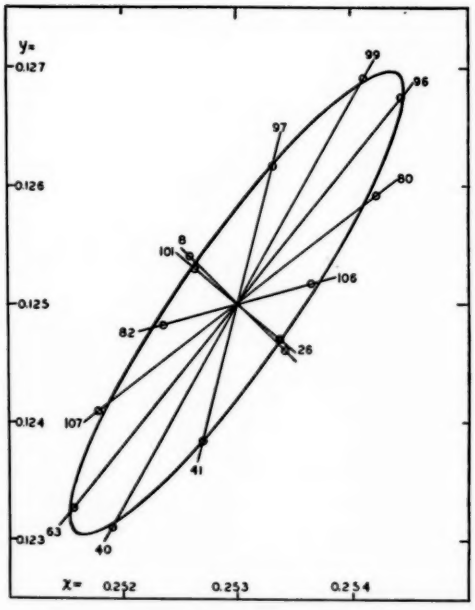

FIG. 25.

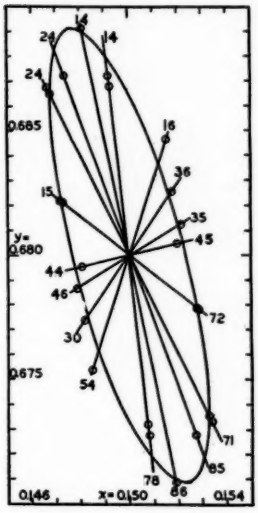

FIG. 26.

mμ to 700 mμ. Figure 21 represents the standard deviations of matching the chromaticity along straight lines close to the spectrum locus from 440 mμ to 533 mμ. Figure 22 represents the standard deviations of matching the chromaticities along the straight line from the spectrum locus at 440 mμ to the spectrum locus at 700 mμ. This last curve corresponds to the noticeability of complementary wave-length differences for highly saturated purples.

The broken curves in Figs. 8 to 22 represent the results for similar observations by the author. The discrepancies between the results for these two observers are significantly large, and appear to be correlated with position and direction of the deviations in the chromaticity diagram. Both observers have normal color vision according to all of the usual tests. The magnitude and character of the discrepancies shown in Figs. 8 to 22 are comparable with those reported by Wright.[5]

The ellipses shown in Figs. 23 to 47 represent the noticeability of chromaticity variations in all directions from the chromaticities indicated at the centers of the ellipses. The observations represented by each ellipse were obtained by selecting from five to eight pairs of filters, each pair of which could be used in the instrument to synthesize a chromaticity very closely approximating that represented by the center of the ellipse. The data represented in Figs. 23 to 47 are summarized in Table III. In every case, a filter was available which would alone produce the chromaticity indicated by the center of the ellipse. The angle to which the prisms of the

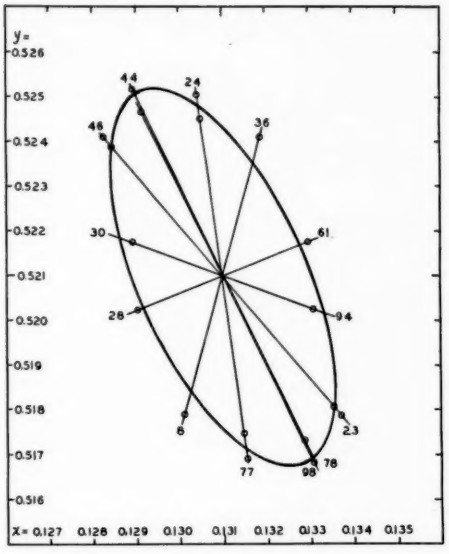

FIG. 27.

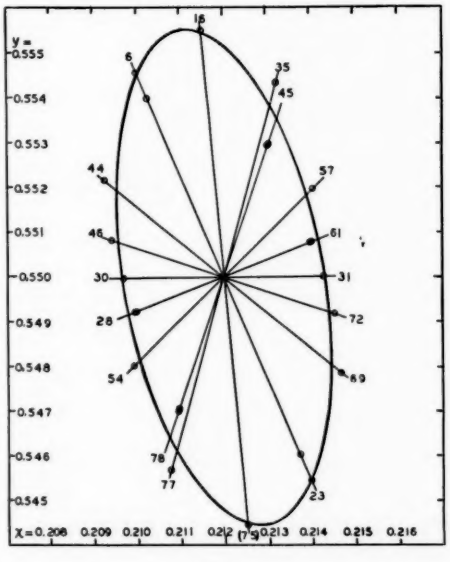

FIG. 28.

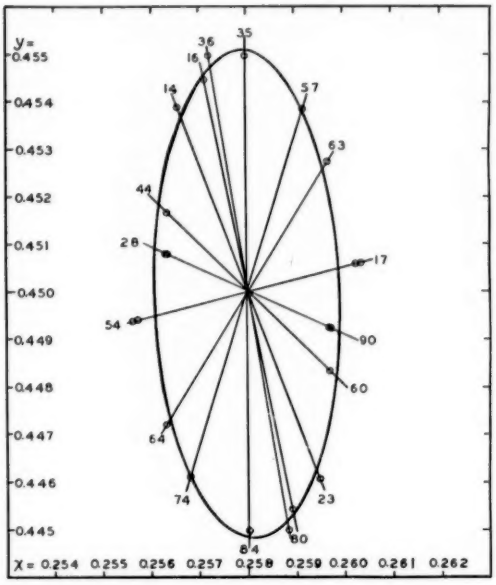

FIG. 29.

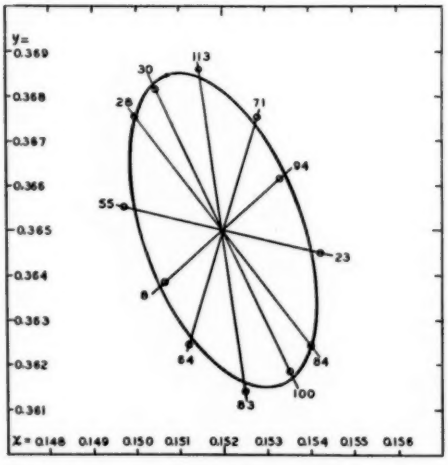

FIG. 30.

instrument should be set in order to synthesize this standard chromaticity with each pair of filters was both calculated and confirmed by observation of the resultant mixture in comparison with the light transmitted by the single filter. With one of the prisms set at this angle, so as to synthesize the desired chromaticity, the other prism was rotated by the observer until a satisfactory match was obtained. The standard deviation of fifty observations was determined. This deviation was represented by two opposite radii from the center point towards the points representing the chromaticities of the two filters used for the synthesis. Each pair of filters used for the synthesis of the standard color resulted in the establishment of another diameter of the ellipse. The complete ellipse is drawn through the points at the ends of these diameters. Several different coordinate scales are employed in

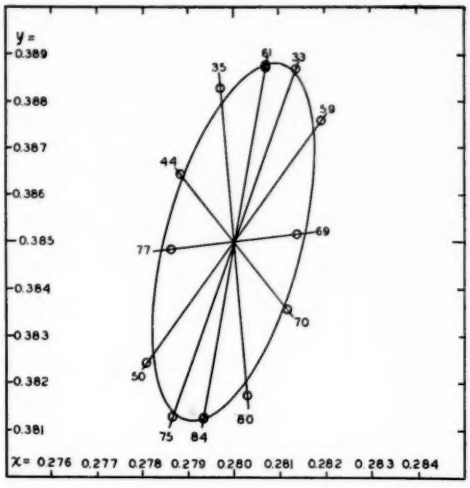

FIG. 31.

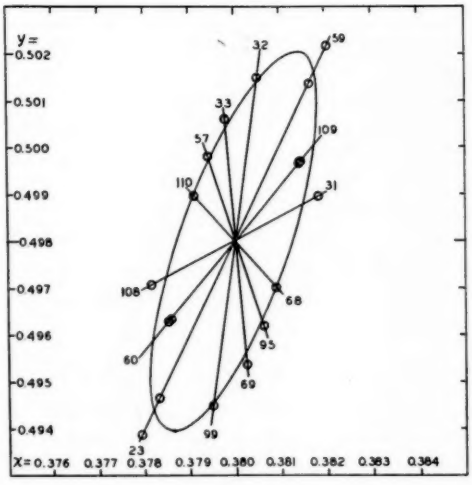

FIG. 32.

Figs. 23 to 47 in order to represent the ellipses with an accuracy comparable to that of the observations. All of these ellipses are represented to the same scale on the composite diagram in Fig. 48. In this figure, every ellipse is drawn ten times its correct size with relation to the coordinate scale of the chromaticity diagram. The centers of the ellipses are placed at their proper locations in the chromaticity diagram.

Sufficient ellipses are shown in Fig. 48 to make possible the estimation of the shape and size of the ellipse around the point representing any chromaticity ordinarily encountered in art or commerce. From such an ellipse the noticeability of a color difference in any direction can be deduced. For instance, the ordinates of the curves shown in Figs. 8 to 22 could be determined from a sufficiently complete series of ellipses. Such a series of ellipses would therefore represent all the information contained in all the curves for the noticeabilities of purity and dominant wave-length change. In addition, these

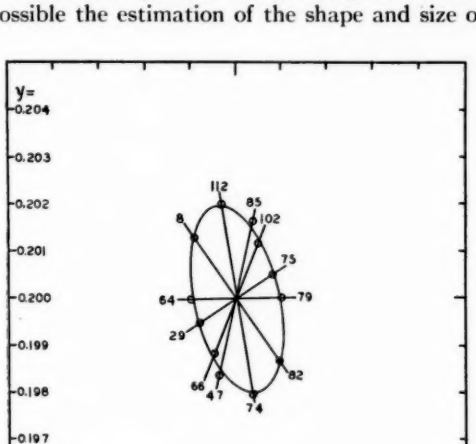

FIG. 33.

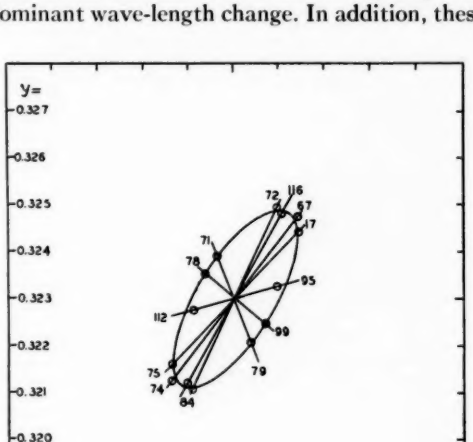

FIG. 35.

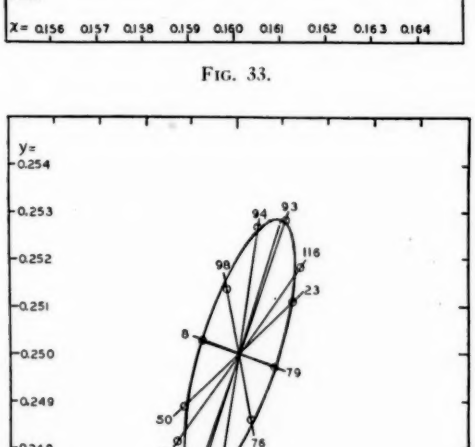

FIG. 34.

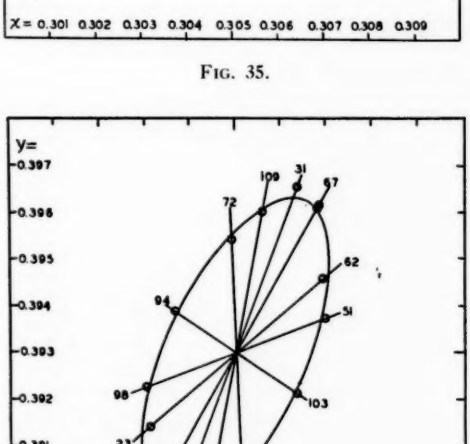

FIG. 36.

ellipses represent the noticeabilities of all conceivable combinations of purity and dominant wave-length differences.

Figure 49 represents in terms of wave-length the standard deviations of color matching for spectral colors, at constant luminance. This curve was derived from Figs. 20 and 21, together with the information contained in Fig. 48, which permits the estimation of noticeabilities of color differences in other directions, and for other chromaticities than those actually observed. Undue emphasis should not be placed on this curve, since it is based on extrapolations of observed data. This curve facilitates comparison of the present results with previous results for wave-length discrimination. Such data represent a limiting special case of color discrimination. The curve in Fig. 49 cannot be expected to be as reliable as the best results secured with apparatus and methods designed specifically for the investigation of wave-length discrimination in the spectrum. Conversely, the data for

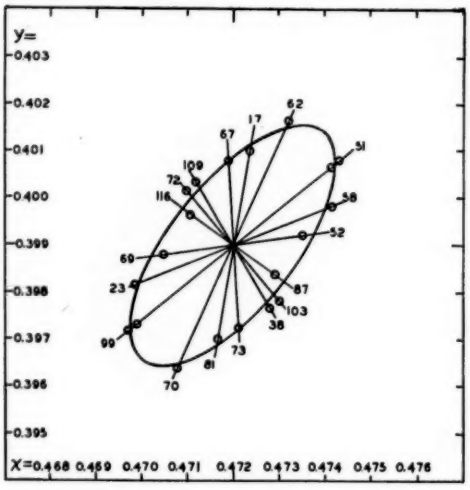

FIG. 37.

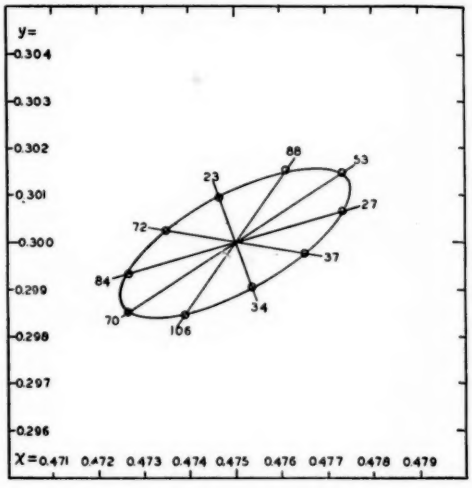

FIG. 39.

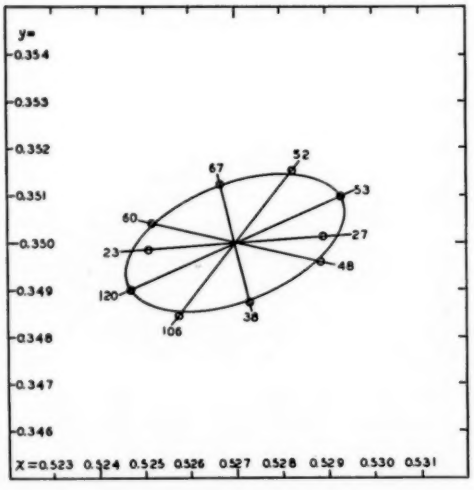

FIG. 38.

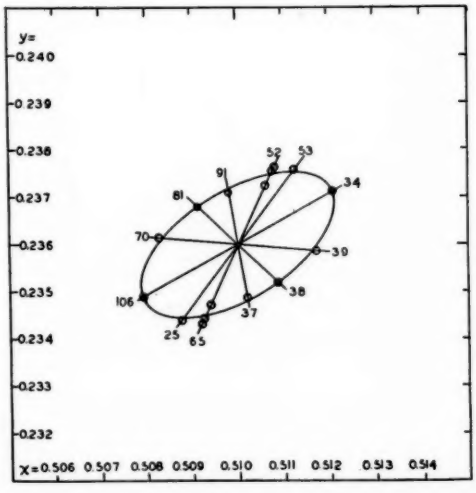

FIG. 40.

discrimination of colors of less than spectral purity, represented in Figs. 8 to 47, inclusive, secured with an instrument designed specifically for their investigation, should be more reliable than similar results obtained with apparatus primarily designed for investigations of color matching and discrimination in the pure spectrum. The curve in Fig. 49 is essentially in agreement with the results of König and Dieterici[10] and of Wright and Pitt.[12] The portion of the curve from 550 mμ to 700 mμ, which shows no evidence of a secondary minimum near 630 mμ frequently reported,[13–16] is derived directly,

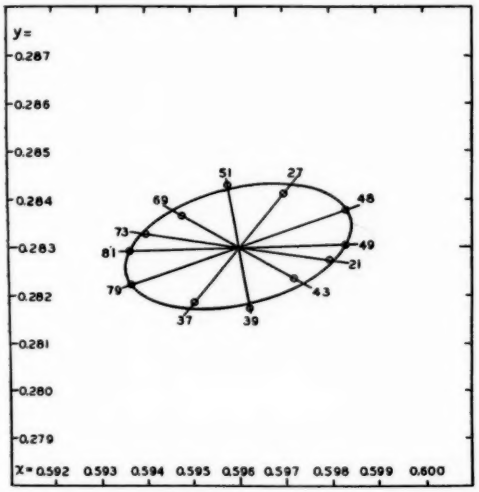

FIG. 41.

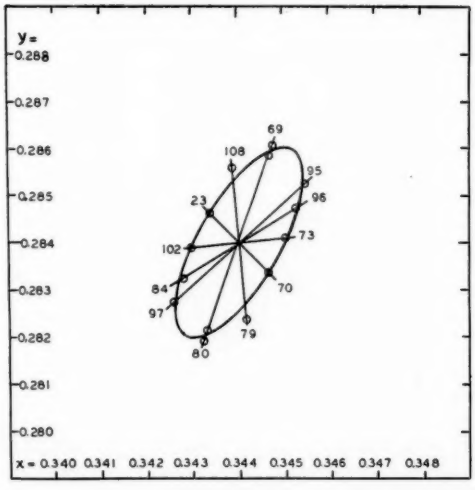

FIG. 42.

[12] W. D. Wright and F. H. G. Pitt, "Hue discrimination in normal colour-vision," Proc. Phys. Soc. **46**, 459–468 (1934).

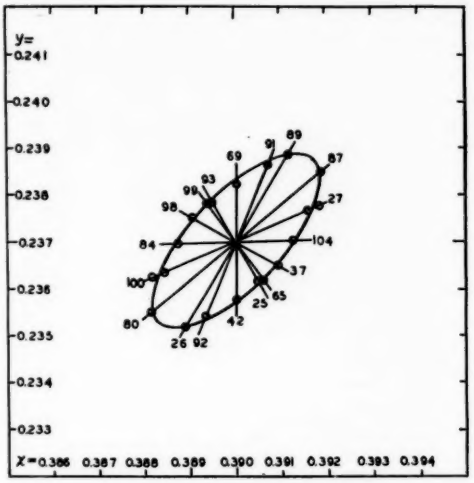

FIG. 43.

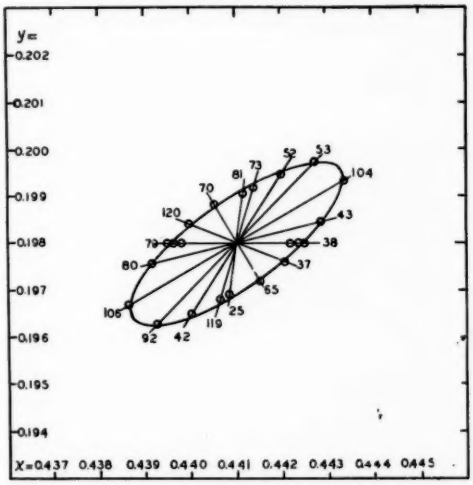

FIG. 44.

[13] O. Steindler, "Die Farbenempfindlichkeit des normalen und farbenblinden Auges," Sitzungsber. Akad. Wiss. Wien, Math.-Naturw. Kl., Abt. 2a, **115**, 39 (1906).

[14] L. A. Jones, "The fundamental scale for pure hue and retinal sensibility to hue differences," J. Opt. Soc. Am. **1**, 63–77 (1917).

[15] H. Laurens and W. F. Hamilton, "The sensibility of the eye to differences in wave-length," Am. J. Physiol. **65**, 547 (1923).

[16] E. P. T. Tyndall, "Chromaticity sensibility to wavelength difference as a function of purity," J. Opt. Soc. Am. **23**, 15–24 (1933).

without extrapolation, from the observed data represented in Fig. 20. The portion of the curve most dependent on extrapolation falls between 430 mμ and 470 mμ. For this reason, very little significance can be attached to the absence of the secondary minimum near 440 mμ reported by all previous investigators. Figure 50, representing the standard deviation of determination of complementary wave-lengths for highly saturated purples, has been derived directly from Fig. 22 and should be quite reliable.

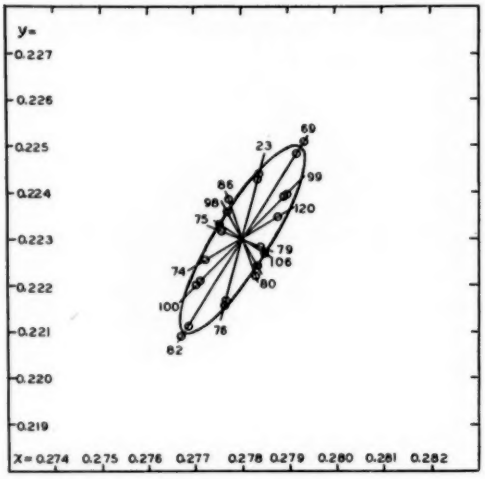

FIG. 45.

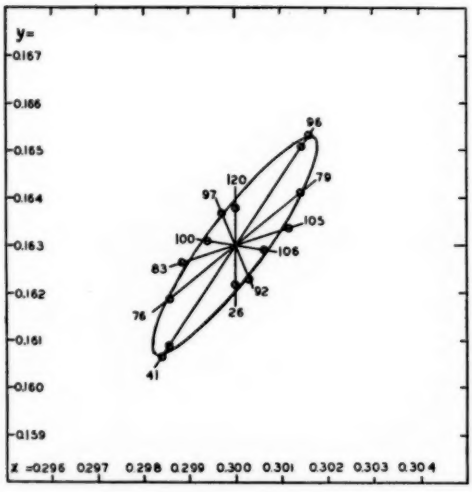

FIG. 46.

The standard deviations Δs encountered in matching a neutral color very similar to Illuminant *C* are indicated in Fig. 35, and are tabulated in the second column of Table IV. The corresponding values of excitation purity p_e were computed by dividing the values of Δs by the distance from the neutral point to the spectrum locus for each wave-length. Colorimetric purity p_c was computed by multiplying the excitation purity by the values of a given in Table I of reference 17. The logarithms of these values of colorimetric purity are compared in Table V with similar data for eight other observers. In Table V, values of log $[p_c(570\ \text{m}\mu)/p_c(\lambda)]$ are given for these nine observers. The values of IGP and FGB were computed from the values of p_c given in Table I of reference 4. The values for FLW, WJM, and LCM were computed from the values of p_c for light-adapted eyes, given in Table V of reference 18. The data for FHGP and WDW were computed by subtracting the values for 570 mμ from the values of the logarithms given in reference 19. The values for JHN were

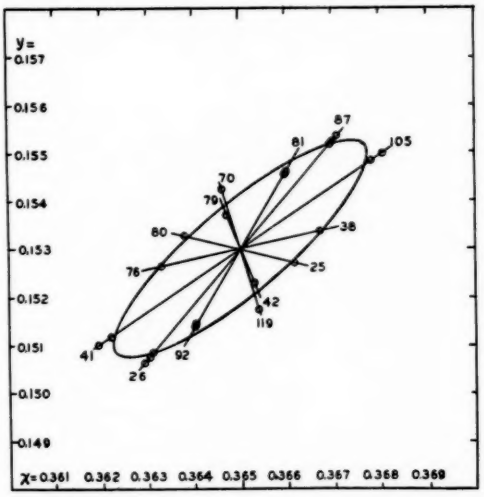

FIG. 47.

[17] D. L. MacAdam, "Photometric relationships between complementary colors," J. Opt. Soc. Am. **28**, 103–111 (1938).

[18] L. C. Martin, F. L. Warburton and W. J. Morgan, "Determination of the sensitiveness of the eye to differences in the saturation of colours," Med. Research Council, Special Report Series, No. 188 (H. M. Stationery Office, London, 1933).

[19] W. D. Wright and F. H. G. Pitt, "The saturation discrimination of two trichromats," Proc. Phys. Soc. **49**, 329–331 (1937).

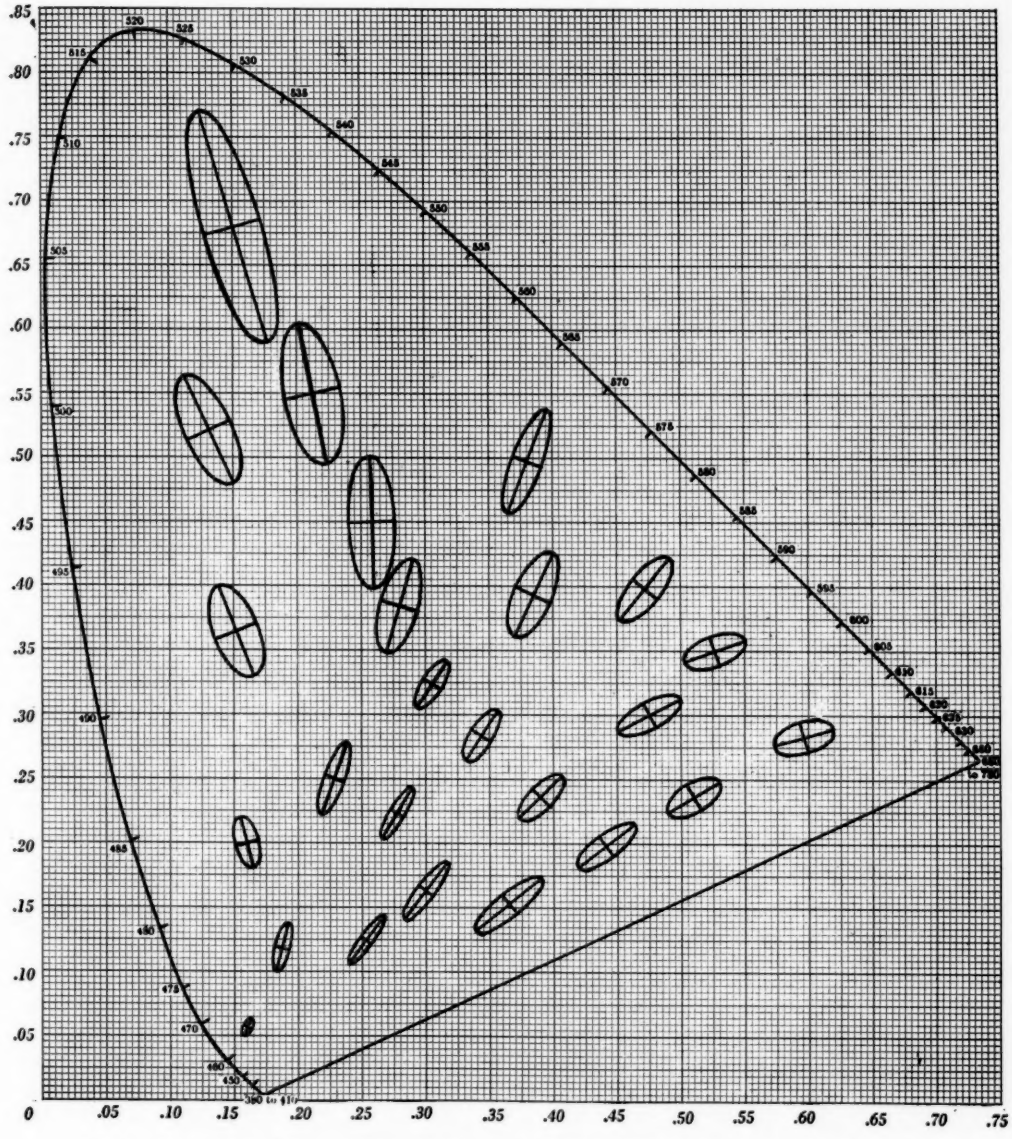

FIG. 48. Standard deviations of chromaticity from indicated standards, represented ten times actual scale on I.C.I. 1931 standard chromaticity diagram, observer: PGN.

similarly computed from those given in reference 20.

The values for PGN, computed from Table IV, are quite similar to those for the other eight observers, and to the average values, which correspond to the geometric means of the thresholds of colorimetric purity. Table IV indicates that the tremendous variation of the threshold values of colorimetric purity through the spectrum is to a great extent an artifact resulting from the use of the scale of colorimetric purity. The ellipse in Fig. 35 is considered a more satis-

[20] J. H. Nelson, "The colour vision characteristics of a trichromat," Part 2, Proc. Phys. Soc. **49**, 332–337 (1937).

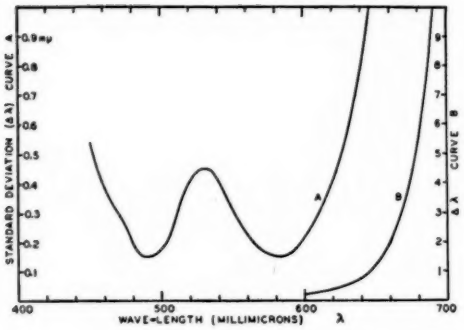

FIG. 49. Standard deviations of wave-length matching in spectrum, derived by extrapolations from Figs. 20, 21, 48.

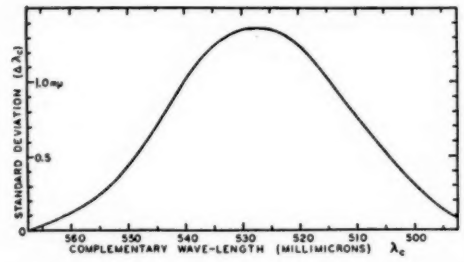

FIG. 50. Standard deviations of complementary wave-length matching for highly saturated non-spectral colors (purples).

factory representation of the data than the customary curves showing the variation of log p_c as a function of wave-length. This is one of many clear examples of the advantages secured by the use of the chromaticity diagram as the basis for the representation of color discrimination.[21] The probability of accidental misrepresentation or misinterpretation of data is less when the results are represented on a basis resulting in simple, regular figures than when they are represented by curves exhibiting marked changes of slope, and several inflections.

The representation of the noticeabilities of color differences by loci around each point in the chromaticity diagram has been suggested by several authors, including Martin, Warburton, and Morgan,[20] Judd,[22] and Silberstein,[23] but very few data of this kind have been available. The solution of the general problem of the noticeability of color difference is represented most clearly in this way. The noticeabilities of color differences involving simultaneous luminance and chromaticity variations are expected to define ellipsoids around the points representing every color in the color solid. Such ellipsoids will be required for the complete representation of color differences. The ellipses shown in Fig. 48 may be regarded as the cross sections of the ellipsoids, corresponding to constant luminance.

The development of a more elegant manner of specifying the noticeabilities of color differences than the system of ellipses suggested by Fig. 48 requires an application of the principles of differential geometry.[23] Such an analysis of the results represented in Tables II and III and Figs. 8 to 48 is now in preparation. A preliminary investigation[24] demonstrated that results of the

TABLE IV. First step from white.

Wave-length	Δs	p_c(%)	p_c(%)	$-\log p_c$
400	0.00205	0.59	0.0089	4.05
440	0.00209	0.62	0.0211	3.68
450	0.00218	0.65	0.0364	3.44
460	0.00219	0.66	0.047	3.33
470	0.00221	0.69	0.126	2.90
480	0.00182	0.64	0.269	2.57
490	0.00104	0.40	0.37	2.43
500	0.00086	0.234	0.40	2.40
510	0.00092	0.178	0.42	2.37
520	0.00096	0.171	0.45	2.34
530	0.00107	0.211	0.54	2.27
540	0.00116	0.265	0.63	2.20
550	0.00135	0.365	0.80	2.10
560	0.00172	0.55	1.03	1.99
565	0.00200	0.70	1.30	1.88
570	0.00223	0.82	1.41	1.85
575	0.00208	0.79	1.30	1.89
580	0.00172	0.65	1.00	2.00
585	0.00145	0.53	0.76	2.12
590	0.00126	0.435	0.58	2.24
600	0.00107	0.328	0.39	2.41
610	0.00099	0.274	0.29	2.54
620	0.00096	0.248	0.242	2.62
630	0.00095	0.233	0.215	2.67
640	0.00094	0.225	0.200	2.70
650	0.00094	0.221	0.191	2.72
660	0.00093	0.218	0.186	2.73
670	0.00093	0.216	0.183	2.74
680	0.00093	0.215	0.181	2.74
700	0.00093	0.214	0.179	2.75

[21] T. Smith, "The colour triangle and colour discrimination," *Discussion on Vision* (Physical Society, London, 1932), pp. 212–226.

[22] D. B. Judd, "Estimation of chromaticity differences and nearest color temperature on the standard 1931 I.C.I. colorimetric coordinate system," J. Opt. Soc. Am. **26** 421–426 (1936).

[23] L. Silberstein, "Investigations on the intrinsic properties of the color domain," J. Opt. Soc. Am. **28**, 63–85 (1938).

[24] D. L. MacAdam, "Projective transformations of color-mixture diagrams," J. Opt. Soc. Am. **32**, 2–6 (1942).

TABLE V. Comparisons of first steps from white for nine observers. log $[p_c(570\ m\mu)/p_c(\lambda)]$.

Wave-length	IGP	FGB	FLW	WJM	Observers LCM	FHGP	WDW	JHN	PGN	Aver-age
400 mμ	1.75	1.54							2.20	1.83
440	1.66	1.16	1.93		1.81				1.83	1.67
450	1.57								1.59	1.58
460	1.40	1.01	1.49	1.10	1.61				1.48	1.34
470	1.14	0.99				1.22	0.90		1.05	1.06
480	0.97	0.97	0.93	0.49	0.95	1.00	0.74	0.65	0.72	0.82
490	0.84	0.89	0.79	0.55	0.96	0.85	0.64	0.60	0.58	0.75
500	0.71	0.76	0.71	0.40		0.71	0.57	0.56	0.55	0.62
510	0.60	0.63	0.61	0.37	0.98	0.59	0.51	0.52	0.52	0.59
520	0.49	0.52	0.56	0.38	0.81	0.50	0.46	0.48	0.49	0.52
530	0.39	0.47	0.54	0.22	0.65	0.43	0.40	0.44	0.42	0.44
540	0.31	0.46	0.43	0.20	0.37	0.38	0.34	0.37	0.35	0.35
550	0.28	0.42				0.31	0.25	0.30	0.25	0.30
560	0.18	0.13				0.18	0.14	0.17	0.14	0.16
565	0.06	0.01	0.13	−0.18*	0.05				0.03	0.06*
570	0.00	0.00	0.00	0.00	0.00	0.00	0.00	0.00	0.00	0.00
575	0.03	0.22							0.04	0.09
580	0.36	0.32		0.44	0.39	0.37	0.18	0.28	0.15	0.31
585	0.46	0.39	0.26						0.27	0.34
590	0.52	0.46				0.54	0.44	0.45	0.39	0.46
600	0.63	0.58	0.50	0.39	0.77	0.63	0.63	0.55	0.56	0.58
610	0.72	0.70				0.70	0.77	0.67	0.69	0.70
620	0.82	0.78	0.71	0.44	1.05	0.74	0.85	0.76	0.77	0.77
630	0.90	0.80				0.79	0.93	0.85	0.82	0.84
640	0.98	0.82	0.78	0.55	1.12	0.81	0.99	0.96	0.85	0.87
650	1.03	0.84	0.85	0.52	1.11	0.85	1.04	1.00	0.87	0.90
660	1.06	0.85						1.06	0.88	0.96
670	1.08	0.85						1.14	0.89	0.98
680	1.08	0.86	0.92	0.85	1.29			1.18	0.89	1.01
700								1.27	0.90	1.08
Mean deviation from average	0.06	0.10	0.08	0.22	0.20	0.05	0.07	0.07	0.07	

* The value shown for WJM at 565 mμ, −0.18, is go greatly at variance with the values for all other observers that it has been omitted in computing the tabulated average. Better agreements with the averages could be secured by adding 0.24 to all of the values tabulated for WJM, and by subtracting 0.20 from all of the values tabulated for LCM. The data for these two observers would then appear to differ seriously from those of the other observers only at the wave-lengths 570 mμ and 580 mμ. If the adjustments described were made, the mean deviations from the average values would be reduced to 0.09 for both WJM and LCM.

kinds represented in Figs. 8 to 22 cannot be represented adequately by equal distances in any projective transformation of the standard 1931 I.C.I. diagram. This fact eliminates the possibility that such a transformation of the standard chromaticity diagram can constitute a uniform chromaticity-scale diagram[3] adequately representing the present data. The more general representations[23, 25, 26] which remain as possibilities for the construction of a truly uniform chromaticity-scale diagram have very complicated geometrical characteristics. The standard I.C.I. chromaticity diagram seems preferable for practical use, even though the system of ellipses shown in Fig. 48 is required as supplementary data. The standard chromaticity diagram appears as convenient as possible for the representation of color differences,[21] in the same manner that plane maps of large portions of the surface of the earth are most convenient, regardless of the distortions of distances introduced by such representations.

ACKNOWLEDGMENTS

The author gratefully acknowledges the interest and assistance of Dr. Loyd A. Jones and Mr. Earl M. Lowry of these Laboratories, who suggested this investigation, made available the special equipment employed, and contributed essential ideas and advice at all stages of the

[25] R. H. Sinden, "A further search for the ideal color system," I. "A new mechanico-graphical method," J. Opt. Soc. Am. **27**, 124–131 (1937); II. "A reconsideration of the Helmholtz line element," J. Opt. Soc. Am. **28**, 339–347 (1938).

[26] W. Peddie, "The general applicability of Fechner's law in colour sensation," Nature **124**, 791–792 (1929); "Colour vision and chromaticity scales," Nature **146**, 717–718 (1940).

work. The highly satisfactory performance of the instrument is due in large measure to Mr. Ralph E. McAdam who was responsible for the mechanical details of its design, and to Mr. Max Zill who constructed the instrument with great care and skill. It is a pleasure to acknowledge again the essential contributions of Mr. Perley G. Nutting, Jr., whose critical interest in the ideas involved in this research was much greater and more helpful than is implied by the fact that he was the principal observer. Many persons have made more or less extensive series of observations, all of which contributed to the development of the method finally adopted and to the understanding of the complex problems involved.

MAY, 1942 J. O. S. A. VOLUME 32

Calculation of Illumination from Triangular Sources

DOMINA EBERLE SPENCER
Massachusetts Institute of Technology, Cambridge, Massachusetts

(Received January 4, 1942)

1. INTRODUCTION

ALTHOUGH actual light sources with triangular boundaries occur but infrequently in practice, an important class of problems can be solved by the methods introduced in this paper. A knowledge of formulae for the triangular source allows the computer to calculate the luminous flux density, at any point on any surface, produced by a source having rectilinear outlines. Any such source can be decomposed into triangles and the flux densities produced by the individual triangles can be computed.

A special case of frequent occurrence is the rectangular window, only part of which is effective in illuminating a given surface. The plane of a tilted surface such as a drafting board will ordinarily cut the rectangular window into two parts, only one of which is useful in illuminating the board. Either the shape of this illuminating source is itself triangular or it may be decomposed into two, three, or four triangles. The problem is an important one in illuminating engineering and it is strange that no adequate solution has hitherto been available.

The paper presents a derivation of general equations for the flux density from triangular windows. A set of nomographs for the convenient solution of these equations is then given and an illustrative example is worked out.

2. CHOICE OF THE COORDINATE SYSTEM

The use of the flux-density vector **D** is convenient in this work.[1] A Cartesian coordinate system is selected with the point P (Fig. 1) as origin. The flux densities on three mutually perpendicular planes through P are called D_x, D_y, and D_z and are considered as components of the vector **D**.

The flux density at P on a tilted surface having the normal vector N is obtained by vector addi-

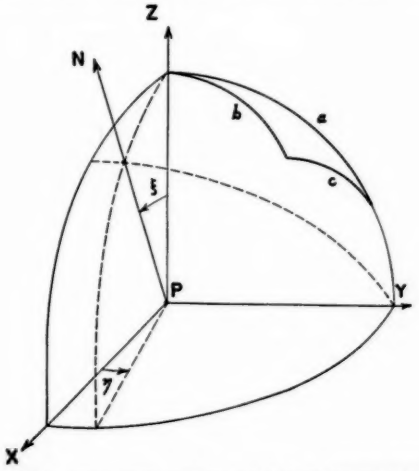

FIG. 1. The coordinate system and the spherical triangle.

[1] See, for example, A. Gershun, "The light field," translated by Moon and Timoshenko, J. Math. Phys. **18**, 51 (1939).

tion. Let ξ and η be the spherical coordinates determining the orientation of N with respect to the Cartesian system. Then the flux density on the surface whose normal is N is

$$D_N = D_x \sin\xi\cos\eta + D_y \sin\xi\sin\eta + D_z\cos\xi. \quad (1)$$

The Cartesian system can always be chosen in such a way that the z axis passes through one vertex of the triangular source (Fig. 1). The triangular lightcone cuts from the unit sphere a spherical triangle having the sides a, b, c and the angles A, B, C. Corresponding letters refer to opposite elements of the triangle, which is standard practice. It is convenient to orient the coordinate system so that one side of the triangular source lies in the yz plane and so that $B \leqq \pi/2$. An additional restriction is advisable to simplify the construction of the nomographs; namely, $a \leqq \pi/2$, $b \leqq \pi/2$, $c \leqq \pi/2$. These assumptions cause no reduction in generality.

3. FLUX-DENSITY EQUATIONS

If the helios H at P is constant[2] for all rays of the lightcone, the flux density on any plane is

$$D = (H/\pi)\sigma'', \quad (2)$$

where σ'' is the area of the figure obtained by orthogonal projection of the spherical triangle ABC onto the illuminated plane. The method of calculating flux density utilized here is ordinarily called the *unit-sphere method* or the *solid-angle method*.

The plane, determined by P of Fig. 1 and the side c of the spherical triangle, intersects the xz plane at an angle α and the xy plane at an angle β. These angles are readily determined by considering right spherical triangles. Formulae can then be written by use of Eq. (2) and by the projection of various sectors (area of sector $= \frac{1}{2}$ vertex angle) onto the proper planes. In this way the following equations are obtained:

$$\begin{aligned} \sigma_x'' &= \tfrac{1}{2}(a - b\cos C - c\cos B), \\ \sigma_y'' &= \tfrac{1}{2}(b\sin C - c\cos\alpha), \\ \sigma_z'' &= \frac{c}{2}\cos\beta. \end{aligned} \quad (3)$$

[2] The notation conforms with that of Parry Moon, "A system of photometric concepts," J. Opt. Soc. Am. to be published.

For triangle ABC,

$$\begin{aligned} \cos A &= \frac{\cos a - \cos b\cos c}{\sin b\sin c}, \\ \cos B &= \frac{\cos b - \cos a\cos c}{\sin a\sin c}, \\ \cos C &= \frac{\cos c - \cos a\cos b}{\sin a\sin b}, \\ \frac{\sin A}{\sin a} &= \frac{\sin B}{\sin b}. \end{aligned} \quad (4)$$

From the right triangles containing α and β,

$$\begin{aligned} \cos\alpha &= \cos a\sin B, \\ \cos\beta &= \sin A\sin b = \sin a\sin B. \end{aligned} \quad (5)$$

Thus,

$$\begin{aligned} \sigma_x'' &= \tfrac{1}{2}(a - b\cos C - \cos B), \\ \sigma_y'' &= \tfrac{1}{2}(b\sin C - c\cos a\sin B), \\ \sigma_z'' &= \frac{c}{2}\sin a\sin B. \end{aligned} \quad (6)$$

If we let

$$S = (\sin^2 a - \cos^2 b - \cos^2 c + 2\cos a\cos b\cos c)^{\frac{1}{2}},$$

then

$$\begin{aligned} \sin B &= \frac{S}{\sin a\sin c}, \\ \sin C &= \frac{S}{\sin a\sin b}. \end{aligned} \quad (7)$$

A combination of the foregoing equations results in a set of formulae for D_x, D_y, and D_z in terms of a, b, c, and H:

$$\begin{aligned} D_x &= \frac{H}{2\pi}\left[a - b\frac{\cos c - \cos a\cos b}{\sin a\sin b} - c\frac{\cos b - \cos a\cos c}{\sin a\sin c}\right], \\ D_y &= \frac{HS}{2\pi\sin a}\left[\frac{b}{\sin b} - \frac{c\cos a}{\sin c}\right], \\ D_z &= \frac{HSc}{2\pi\sin c}. \end{aligned} \quad (8)$$

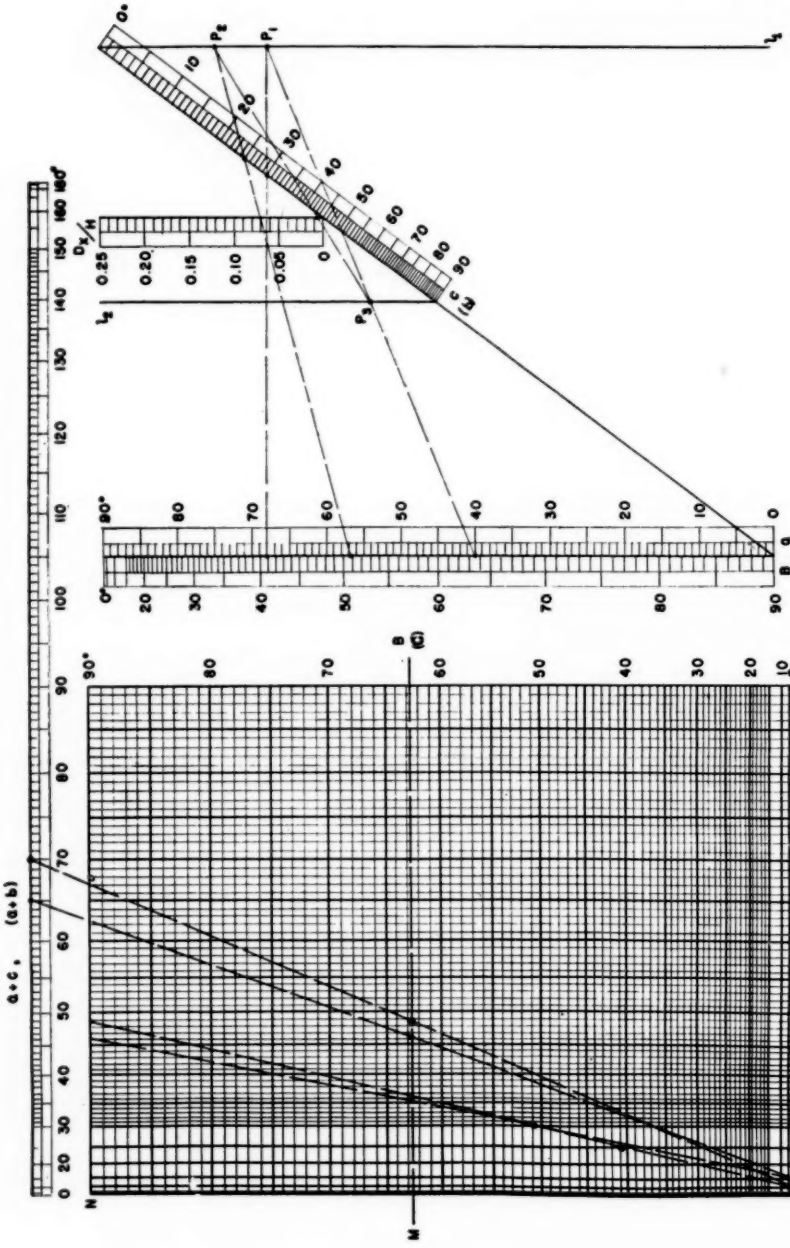

CHART I. Determination of B and C,

$$\cos B = \frac{\cos b - \cos a \cos c}{\sin a \sin c}, \quad \cos C = \frac{\cos c - \cos a \cos b}{\sin a \sin b}.$$

Example: Given $a = 40°$, $b = 25°$, $c = 30°$. Then $a + c = 70°$, $|a - c| = 10°$. Result is $\mathbf{B = 40.9°}$. Also, $a + b = 65°$, $|a - b| = 15°$, so $\mathbf{C = 50.8°}$.

CHART II. Determination of the flux density D_x,

$$D_x = (H/2\pi)(a - b \cos C - c \cos B).$$

Example: Given $a = 40°$, $b = 25°$, $c = 30°$, $B = 40.9°$, $C = 50.8°$. Result $\mathbf{D_x/H = 0.0042}$.

4. SPECIAL CASES

In lighting practice right triangles occur frequently. If the source is of such form that the spherical triangle ABC has one or more right angles, Eq. (8) simplifies as follows:

B = π/2. Then $\cos b = \cos a \cos c$, $S = \sin a \sin c$, and

$$D_x = \frac{H}{2\pi}\left[a - b\frac{\cos c - \cos a \cos b}{\sin a \sin b}\right] = \frac{H}{2\pi}[a - b \tan a \operatorname{ctn} b],$$

$$D_y = \frac{H}{2\pi}\left[\frac{b \sin c}{\sin b} - c \cos a\right] = \frac{H}{2\pi}\left[\frac{b \sin c \cos c - c \sin b \cos b}{\sin b \cos c}\right], \tag{8a}$$

$$D_z = \frac{Hc}{2\pi} \sin a.$$

C = π/2. Then $\cos c = \cos a \cos b$, $S = \sin a \sin b$, and

$$D_x = \frac{H}{2\pi}\left[a - c\frac{\sin a \cos b}{\sin c}\right] = \frac{H}{2\pi}[a - c \tan a \operatorname{ctn} c],$$

$$D_y = \frac{H}{2\pi}\left[b - c\frac{\cos a \sin b}{\sin c}\right] = \frac{H}{2\pi}[b - c \tan b \operatorname{ctn} c], \tag{8b}$$

$$D_z = \frac{Hc \sin a \sin b}{2\pi \sin c}.$$

a = b = π/2. Then $c = C$, $A = B = \pi/2$,

$$D_x = \frac{H}{4}(1 - \cos c), \quad D_y = \frac{H}{4} \sin c, \quad D_z = \frac{Hc}{2\pi}. \tag{8c}$$

The case of $A = \pi/2$, $B = \pi/2$, is handled most easily by changing the axes so that angle A becomes angle B. Equations (8a) are then employed.

5. THE NOMOGRAPHIC CHARTS

Equations (8) can be used directly in the calculation of flux density. Computations can be greatly simplified, however, by the use of nomographs based on the following set of equations:

$$\cos B = \frac{\cos b - \cos a \cos c}{\sin a \sin c},$$

$$\cos C = \frac{\cos c - \cos a \cos b}{\sin a \sin b},$$

$$D_x = \frac{H}{2\pi}(a - b \cos C - c \cos B), \tag{9}$$

$$D_y = \frac{H}{2\pi}(b \sin C - c \cos a \sin B),$$

$$D_z = \frac{Hc}{2\pi} \sin a \sin B.$$

A set of four nomographic charts has been prepared by which the three flux-density components can be calculated when a, b, c are given. The construction of the charts involves nothing more abstruse than the properties of similar triangles. The procedure in using the charts is indicated by the dashed lines drawn on them, which are for a triangular source with $a = 40°$, $b = 25°$, $c = 30°$.

Chart I. To find B

Draw line from $|a - c|$ on lower scale to $(a + c)$ on top scale. Obtain intersection of this line with horizontal line M.

Project this point vertically to obtain a point on line N.

Connect point on line N with $|a - c|$ on lower edge of chart.

The intersection of this second line with vertical line b gives B (read on horizontal scale at right of chart).

To find C, repeat the foregoing operations but use the chart labels in parentheses.

Chart II. To find D_x/H

Draw line (B, c) intersecting l_1 in P_1.

Draw line (C, b) intersecting l_1 in P_2.

Draw line (P_1, a) intersecting l_2 in P_3.

Connect P_2 and P_3. The intersection of this line with the D_x/H scale gives the result.

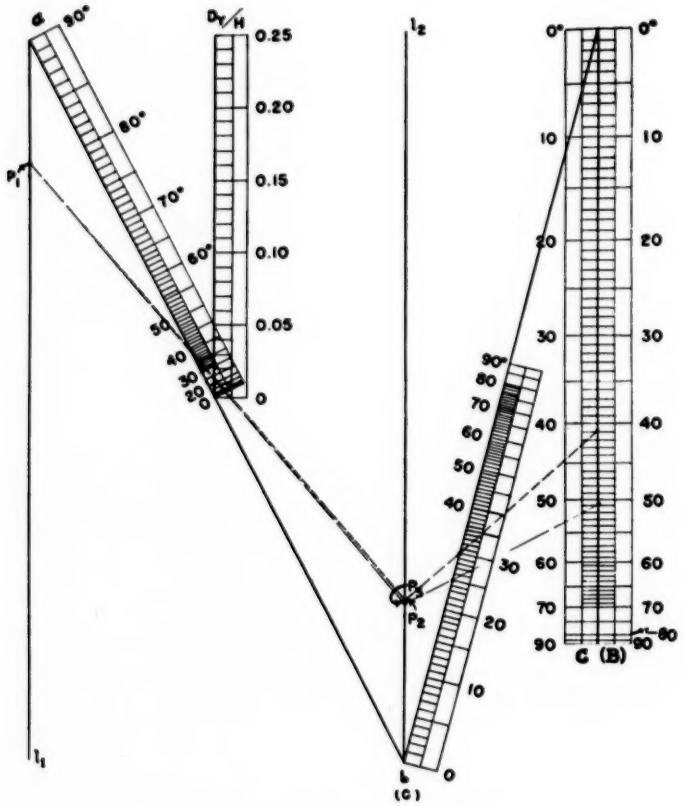

CHART III. Determination of the flux density D_y,

$$D_y = (H/2\pi)(b \sin C - c \cos a \sin B).$$

Example: Given $a = 40°$, $b = 25°$, $c = 30°$, $B = 40.9°$, $C = 50.8°$. Result $D_y/H = 0.0120$.

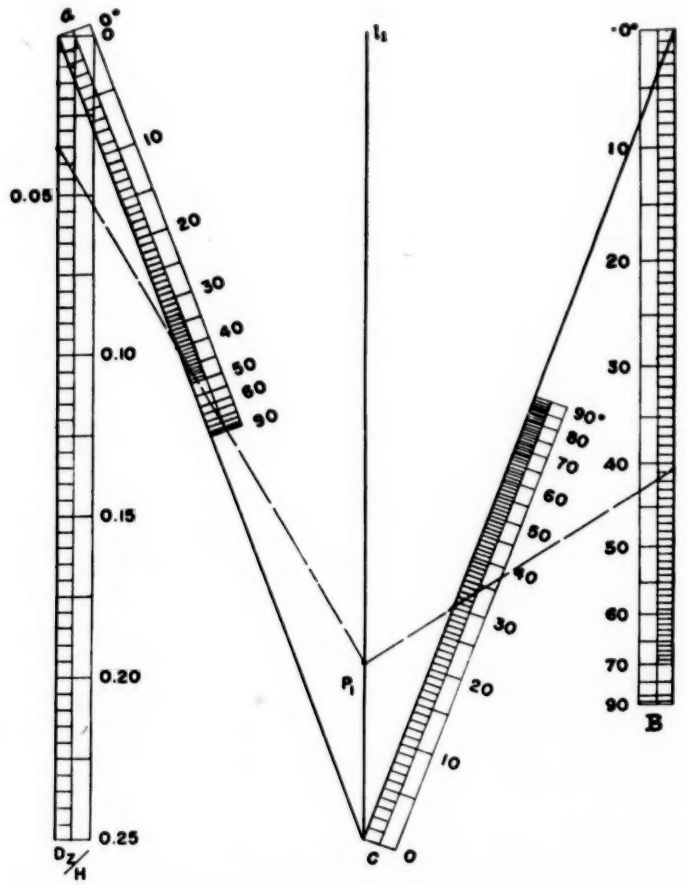

CHART IV. Determination of the flux density D_z,

$$D_z = (Hc/2\pi) \sin a \sin B.$$

Example: Given $c = 30°$, $a = 40°$, $B = 40.9°$. Result $D_z/H = 0.0351$.

Chart III. To find D_y/H

Draw line (B, c) intersecting l_2 in P_2.
Draw line (b, C) intersecting l_2 in P_3.
Draw line (P_2, a) intersecting l_1 in P_1.
Intersection of (P_1, P_3) with D_y/H axis gives value of D_y/H.

Chart IV. To find D_z/H

Draw line (B, c) intersecting l_1 in P_1.
Intersection of (P_1, a) with D_z/H axis gives value of D_z/H.

The most important charts are Nos. II, III, and IV. The first chart merely provides a simple means of solving the spherical triangles that enter the problem and the reader may, if he desires, substitute for it any of the customary methods such as direct computation, use of other types of nomographs, or stereographic projection. The assumption has been made throughout that a, b, and c are given. This is not a restriction, however, for the solution of the spherical triangle under other conditions is carried through in a similar manner. Use of the charts makes the problem of the triangular light source but little more laborious than the well-established case of the rectangular source so that any problem involving either can now be carried through in a reasonable length of time.

6. AN APPLICATION

The most important application of the formulae and charts is to the calculation of illumination, from rectangular windows, on a tilted surface such as a drafting board. In particular, suppose that the plane of the drafting board is perpendicular to the plane of the source, and that the point P at which the flux density is to be calculated is at a distance l from the source.

The source may consist of a portion of the wall, which is illuminated to give a helios H, or it may be a rectangular or triangular window. In either case the helios is assumed to be constant along every ray reaching P. Let the orthogonal projection of P on the source be P'. From P' lines are drawn to the vertices of the light source, dividing it into four triangles (Fig. 2). The normal N to the tilted surface (see Fig. 1) has $\xi=\pi/2$ when the z axis is chosen along $P'P$. Then Eq. (1) becomes

$$D_N=\sum_{i=1}^{4}(D_{xi}\cos\eta_i+D_{yi}\sin\eta_i). \tag{10}$$

If the lines drawn on the window to the corners are designated by the lengths m, n and p, then

$$\begin{aligned} m^2&=f^2+s^2+2fs\cos\theta,\\ n^2&=h^2+f^2+s^2+2f(s\cos\theta-h\sin\theta),\\ p^2&=(w-s)^2+f^2+h^2\\ &\qquad -2f[(w-s)\cos\theta+h\sin\theta]. \end{aligned} \tag{11}$$

The various angles can now be expressed in terms of the known lengths and the known angle θ.

For triangle (1), Fig. 2, the y axis of Fig. 1 is taken along the side m. Then

$$\begin{aligned} a_1&=\tan^{-1}(m/l)\\ &=\tan^{-1}\left\{\frac{1}{l}[f^2+s^2+2fs\cos\theta]^{\frac{1}{2}}\right\},\\ b_1&=\tan^{-1}(f/l),\\ c_1&=\cos^{-1}\left[\frac{2l^2+f^2+m^2-s^2}{2[(l^2+f^2)(l^2+m^2)]^{\frac{1}{2}}}\right]\\ &=\cos^{-1}\left[\frac{l^2+f^2+fs\cos\theta}{[(l^2+f^2)(l^2+f^2+s^2+2fs\cos\theta)]^{\frac{1}{2}}}\right]. \end{aligned} \tag{12}$$

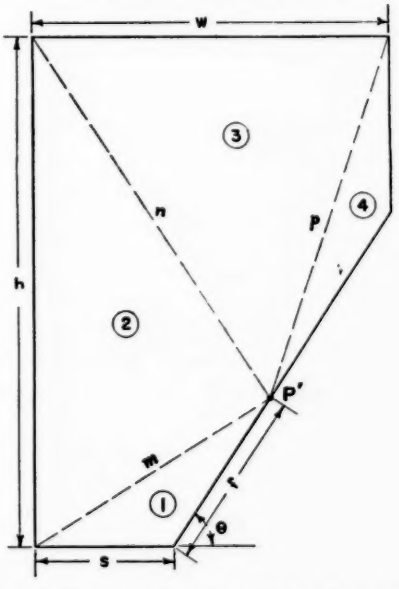

FIG. 2. Surface source illuminating a slanting surface.

The angle η is

$$\eta=\pi-C_1,$$

where C_1 is the angle between sides m and f of triangle (1). Angle C_1 can be obtained from Chart I or sin C_1 and cos C_1 can be found by use of the formulae,

$$\cos C_1=\frac{m^2+f^2-s^2}{2mf}=\frac{f+s\cos\theta}{(f^2+s^2+2fs\cos\theta)^{\frac{1}{2}}},$$
$$\sin C_1=\frac{s}{m}\sin\theta=\frac{s\sin\theta}{(f^2+s^2+2fs\cos\theta)^{\frac{1}{2}}}. \tag{13}$$

The resulting flux density at P is

$$D_{N1}=-D_{x1}\cos C_1+D_{y1}\sin C_1.$$

For triangle (2), the y axis may be taken again along m. Then

$$a_2=\tan^{-1}(m/l)=\tan^{-1}\left\{\frac{1}{l}[f^2+s^2+2fs\cos\theta]^{\frac{1}{2}}\right\},$$
$$b_2=\tan^{-1}(n/l)=\tan^{-1}\left\{\frac{1}{l}[h^2+s^2+f^2+2f(s\cos\theta-h\sin\theta)]^{\frac{1}{2}}\right\}, \tag{14}$$
$$c_2=\cos^{-1}\left[\frac{2l^2+m^2+n^2-h^2}{2[(l^2+m^2)(l^2+n^2)]^{\frac{1}{2}}}\right],$$
$$\eta_2=C_1.$$

Thus,

$$D_{N2}=D_{x2}\cos C_1+D_{y2}\sin C_1.$$

For triangles (3), the y axis may be taken along p, and

$$a_3=\tan^{-1}(p/l),$$
$$b_3=\tan^{-1}(n/l),$$
$$c_3=\cos^{-1}\left[\frac{2l^2+p^2+n^2-w^2}{2[(l^2+n^2)(l^2+p^2)]^{\frac{1}{2}}}\right], \tag{15}$$
$$\eta_3=C_4.$$

The angle C_4 is obtainable from Chart I or by use of the formula,

$$\cos C_4=\frac{[(w-s)^2+p^2+f^2-h^2]\cos\theta+2(w-s)[h\sin\theta-f]}{2p[(w-s)-f\cos\theta]}.$$

TABLE I. Illumination on a sloping surface.

$\theta=60°$, $\cos\theta=0.500$, $\sin\theta=0.866$.
$w=4.0$, $s=3.0$,
$h=2.0$, $l=1.0$, $f=0.2$ (meters).

Triangle	a	b	c	D_x/H	D_y/H
1	72.15°	11.31°	66.25°	0.002	0.015
2	72.15	74.47	32.33	0.027	0.087
3	63.85	74.47	79.48	0.115	0.111
4	63.85	60.95	4.43	0.000	0.002

$\cos C_1=0.547$, $\sin C_1=0.837$,
$\cos C_4=0.997$, $\sin C_4=0.0658$,
$\mathbf{D_{N/H}=0.221.}$

The flux density at P, produced by triangle (3) is therefore

$$D_{N3}=D_{x3}\cos C_4+D_{y3}\cos C_4.$$

In triangle (4), the y axis is again taken along p and

$$a_4=\tan^{-1}(p/l),$$
$$b_4=\tan^{-1}\left[\frac{1}{l}\left(\frac{w-s}{\cos\theta}-f\right)\right],$$
$$c_4=\cos^{-1}\left\{\frac{2l^2+p^2+\left[\frac{w-s}{\cos\theta}-f\right]^2-[h-(w-s)\tan\theta]^2}{2\left[(l^2+p^2)\left[l^2+\left(\frac{w-s}{\cos\theta}-f\right)^2\right]\right]^{\frac{1}{2}}}\right\}. \tag{16}$$

Also,

$$\eta_4=\pi-C_4,$$
$$D_{N4}=-D_{x4}\cos C_4+D_{y4}\sin C_4.$$

As in Eq. (1), the actual flux density at P on the tilted surface is the sum of the contributions from the four triangles, or

$$D_N=(D_{x2}-D_{x1})\cos C_1+(D_{x3}-D_{x4})\cos C_4+(D_{y2}+D_{y1})\sin C_1+(D_{y3}+D_{y4})\sin C_4. \tag{17}$$

7. NUMERICAL EXAMPLE AND SPECIAL CASES

Let $\theta=60°$, $w=4.0$, $s=3.0$, $h=2.0$, $l=1.0$, $f=0.2$, all dimensions being in meters. Then, by Eq. (11),

$$m^2=9.6400,\quad m=3.1048,$$
$$n^2=12.947,\quad n=3.5982,$$
$$p^2=4.1472,\quad p=2.0365.$$

Substitution of these values into the various equations gives the results shown in Table I. The flux density at P on the sloping surface, per unit helios of the source, is

$$\mathbf{D}_{N/H}=\mathbf{0.221}.$$

The foregoing analysis applies to the most complicated case usually encountered. Degenerate cases, where the source is broken up into one, two, or three triangles, are easily handled in the same way. These special cases are as follows:

(A) *Three triangles* (*Nos. 1, 2, 3*). Right boundary of source limited entirely by the plane of the illuminated surface. Then $C_4=0$, $D_{x4}=D_{y4}=0$, and Eq. (17) reduces to

$$D_N=D_{x3}+(D_{x2}-D_{x1})\cos C_1 + (D_{y2}+D_{y1})\sin C_1. \quad (17a)$$

(B) *Three Triangles* (*Nos. 2, 3, 4*). P' at lower right corner of source. Then $f=0$ and $m=s$, $n=(h^2+s^2)^{\frac{1}{2}}$, $C_1=\theta$. $D_{x1}=D_{y1}=0$.

$$D_N=D_{x2}\cos\theta+(D_{x3}-D_{x4})\cos C_4 + D_{y2}\sin\theta+(D_{y3}+D_{y4})\sin C_4. \quad (17b)$$

(C) *Two triangles* (*Nos. 2, 3*). Right boundary of source limited by the plane of the illuminated surface, and P' at the lower right corner of source. Then $f=0$, $C_1=\theta$, $C_4=0$, $D_{x1}=D_{y1}=D_{x4}=D_{y4}=0$.

$$D_N=D_{x3}+D_{x2}\cos\theta+D_{y2}\sin\theta. \quad (17c)$$

(D) *One triangle* (*No. 3*), P' at one corner. Then $f=0$, $s=0$, $C_4=0$, $D_{x1}=D_{y1}=D_{x2}=D_{y2}=D_{x4}=D_{y4}=0$. Equation (17) becomes

$$D_N=D_{x3}. \quad (17d)$$

ACKNOWLEDGMENTS

The writer wishes to thank Professor Parry Moon for his aid and encouragement in the formulation of this paper. Thanks are also due to Mr. D. P. Adams for his suggestions leading to a convenient arrangement of the nomographs.

Newly Organized Optical Society of Chicago

PERSONS in the Chicago area interested in optics have recently organized the Optical Society of Chicago, with an initial membership of about fifty. Meetings are being held on the second Tuesday of each month. At the meeting of April 7, "Gunsight Design" was discussed by Mr. Edward Bickel.

Anyone interested in further information about the new organization should write to PROFESSOR GEORGE S. MONK, *Ryerson Physical Laboratory, University of Chicago*, who was active in the foundation of the Society; to MR. EDWARD BICKEL of the *Simpson Optical Manufacturing Company, Chicago*, who is Chairman of the Program Committee; or to DR. J. C. COPELAND of the *Riggs Optical Company, Chicago*.

Phototropic Dyes

E. I. STEARNS*
Calco Chemical Division, American Cyanamid Company, Bound Brook, New Jersey
(Received January 29, 1942)

An analysis of 162 commercial dyestuffs in solution shows in the case of 10 percent of these a phototropic effect which is spectrophotometrically measurable.

INTRODUCTION

PHOTOTROPISM is defined in the dictionary as the reversible change in color of a substance when exposed to light. As a result of this phenomenon different spectrophotometric curves are obtained in the case of dyes which exhibit this property, depending on whether or not the sample has been exposed to light a short time previous to the time of measurement.

Although phototropism has been well known in the dyestuff industry for a number of years, particularly as regards cellulose acetate dyes,[1-3] and although cognizance is taken of this phenomenon in the case of some visual testing[4] where dark storage is advised before visual examination of samples, very little spectrophotometric data has been published illustrating it on

* Research Department, Calco Chemical Division, American Cyanamid Company, Bound Brook, New Jersey.

[1] C. E. Mullin, *Acetate Silk and Its Dyes* (D. VanNostrand, 1927), p. 123.
[2] W. H. Peacock, "The practical art of color matching," Rayon Text. Monthly **21**, 762 (1940).
[3] E. Greenhalgh, "The Dyeing of Artificial Silk," Dyer and Calico Printer **55**, 146 (1926).
[4] *American Association of Textile Chemists and Colorists, 1941 Yearbook* (Howes Publishing Company), p. 216.

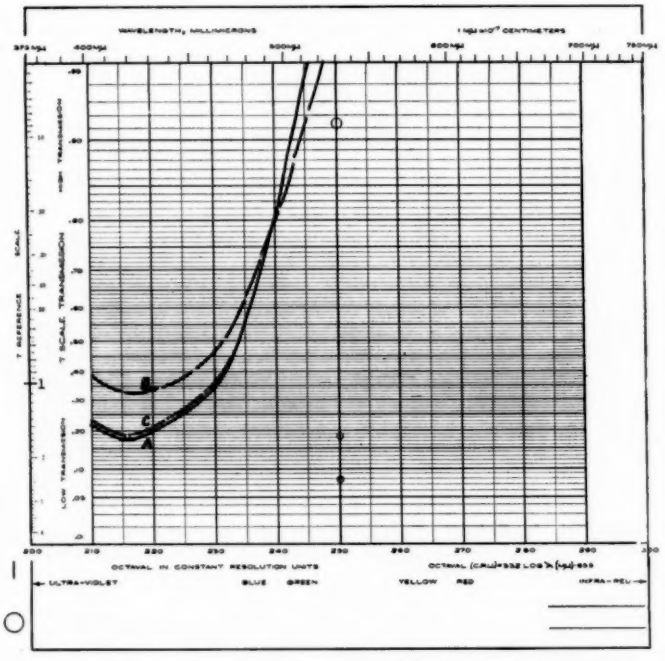

FIG. 1. Phototropic effect, Calconese yellow JT, 10 mg/l in acetone. (A) Before irradiation: (B) After 1-minute exposure to 50-watt lamp: (C) After 2-minute dark storage.

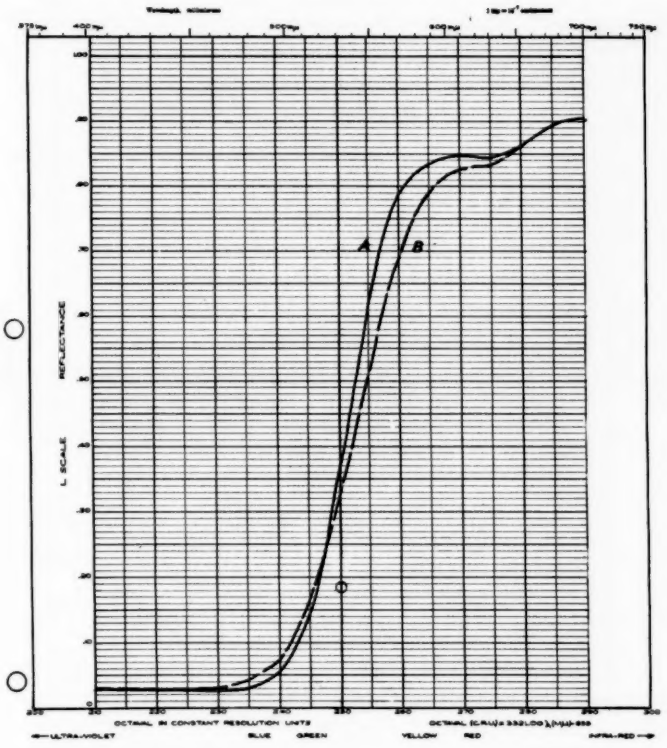

FIG. 2. Phototropic effect, Calconese yellow JT, 1 percent dyeing on cellulose acetate cloth. (A) Before irradiation: (B) After 2-minute exposure to 100-watt lamp. Sample returns to curve (A) after dark storage.

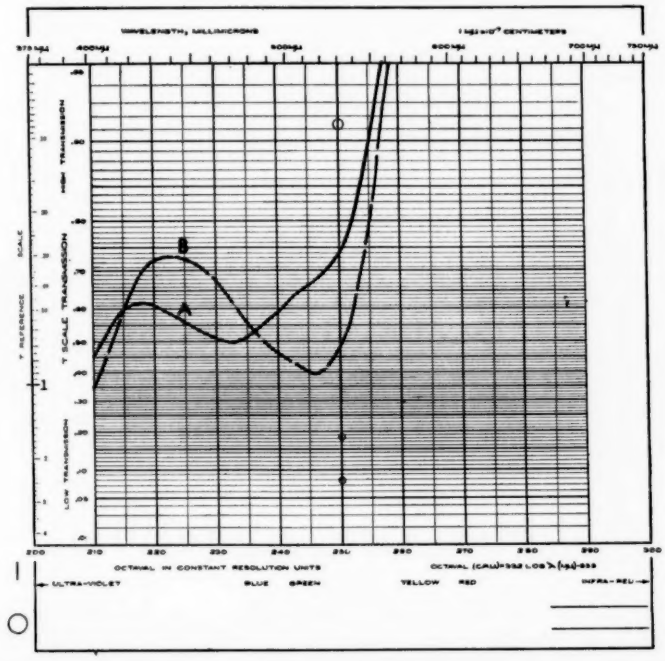

FIG. 3. Phototropic effect, Calcosol printing orange, 12 mg/l in pyridine. (A) Exposed for 1 minute to 50-watt lamp: (B) After three days' dark storage. Sample corresponds to curve (B) if given dark storage before measurement.

a quantitative basis,[5] and we have been unable to find a general statement regarding its frequency of occurrence.

EXPERIMENTAL

In a review of irradiation effect on 162 dyes in solution, the importance of this effect was found to be as follows: In 147 cases the effect was negligible and in 15 cases the effect was significant. By significant is meant that a 50-watt lamp at a 2-inch distance for 1 minute from a one-centimeter cell containing a dye solution and having a transmission of about 30 percent at the wave-length of the absorption maximum of the dye, causes an effect if the solution is measured within two minutes. An effect is defined as an extinction coefficient change of 1 percent at any wave-length.

Phototropism is not a commonly observed property of dyed fibers, because if a dye is subject to this effect it is not ordinarily recommended and may not even be marketed.

RESULTS

Figure 1 shows the phototropic effect of Calconese yellow JT in an acetone solution as measured at a concentration of ten milligrams per liter, in a one-centimeter cell. This dye has a very rapid recovery, the effect being largely reversed in two minutes. Its structural formula is given following Table I. This dye also shows an irradiation effect when dyed on cellulose acetate as shown by Fig. 2.

Figure 3 shows the phototropic effect of Calcoloid orange RD dissolved in pyridine. This has a very slow recovery, and about three days' dark storage is required for the curve to return to the original shape at room temperature. Its formula is referred to in Table I.

Phototropism is not a factor in the measurement of samples in a spectrophotometer, provided the samples are properly conditioned before measurement, because the light intensity is so low. It should be a factor in colorimetric measurements if the sample is subjected to an intense illumination.

Some other instances of phototropism are listed in Table I.

TABLE I.

Name	Medium	Rowe's C.I. No.
Calco oil yellow AAB	Toluene	15
Calco oil yellow AAB	Cellulose acetate	15
Calco oil yellow T	Toluene	17
Calco oil yellow T	Pyridine	17
Calconese yellow JT	Acetone	(1)*
Calconese yellow JT	Cellulose acetate	(1)*
Calcocid milling yellow O	Wool	640
Calcosol yellow G	Cotton	1118
Calcodur yellow 4GL	Nylon	346
Chrysophenine	Water	365
Calcomine yellow	Water	622
Calcomine orange 5RS	Water	621
Calcoloid orange RD	Pyridine	1217
Calcosol pink FF	Toluene	(2)*
Calcosol pink FF	Pyridine	(2)*

* Structural formulas not available in Rowe's Colour Index.

(1)

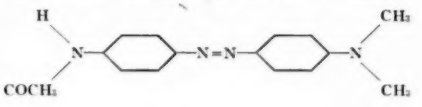

(2)

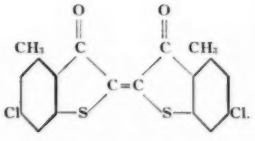

[5] Robert Livingston, "The reversible bleaching of chlorophyll," J. Phys. Chem. **45**, 1312 (1941).

Long Optical Paths of Large Aperture

JOHN U. WHITE
Esso Laboratories, Standard Oil Development Company, Linden, New Jersey
(Received January 20, 1942)

THE measurement of the vapor phase spectra of compounds having high boiling points presents an experimental problem that may be solved either by heating the absorption cells or by making them very long. In the infra-red region radiation from the hot gases in heated cells decreases the accuracy of absorption measurements. If only a small amount of sample is available, the only possibility is to use an optical system in which the radiation goes back and forth through the same volume a large number of times. Several designs for such systems have been published recently[1,2] but none of them permits the use of large angular apertures at points off the optic axis. In this paper an absorption cell is described in which the light traverses a small volume a large and arbitrarily variable number of times, and in which the angular aperture of the mirrors is not occulted either on or off the optical axis. The design gives very high light transmission and can be used for observing spectra that are very weak, or that belong to high boiling point compounds or to compounds obtainable only in very low concentrations. It can be used for any liquids or gases that do not injure the mirror surfaces, with which they are directly in contact.

The essential parts of the equipment are three spherical, concave mirrors that all have the same radius of curvature. These are set up as shown in Fig. 1 with two mirrors A and A' close together at one end of the absorption cell, and the third mirror B at the other end. The centers of curvature of A and A' are on the front surface of B, and the center of curvature of B is halfway between A and A'. This arrangement establishes a system of conjugate foci on the reflecting surfaces of the mirrors, by which all the light leaving any point on A is brought to a focus by B at the corresponding point on A', and all the light leaving this point on A' is focused back again to the original point on A. Similarly, all the light leaving any point on B and going to either A or A' is focused back to a new point on B that is somewhat offset to one side of the original one.

Figure 1 illustrates the way these properties are used to obtain very long optical paths. Light enters through a slit close to one end of B, whence it goes to A, from there to B, then to A', back to B, to A, and so on, back and forth between B and A' or A alternately. The positions of successive images can all be located by the rule that object and image points near the center of curvature of a spherical mirror always lie on a straight line whose midpoint falls on the center of curvature. Thus mirror A forms an image 1 of the entrance slit on the surface of B as far from A's center of curvature as the entrance slit is from it. Then, since the center of curvature of mirror B, shown by a circle, is halfway between A and A', B forms an image of A on A'. In the same way, mirror A' forms on B a second image 2 of the slit, whose position is determined by the distance between 1 and the center of curvature of A'. Mirror B forms an image of A' on A, and A forms another image 3 of the slit on B, which is again returned to A, and so on. Each successive image of the slit on B is offset to one side or the other of the preceding one until finally the last one falls beyond the end of B. The different images fall in order at the points marked 1, 2, 3, and 4 in Fig. 1. The large angular aperture obtainable off the optic axis is easily explained. Since all the light in the first image of the slit that is formed on B is focused on A', and since all the light falling on A' is returned to the second image on B, and so on, no light is lost off the edges of the mirrors.

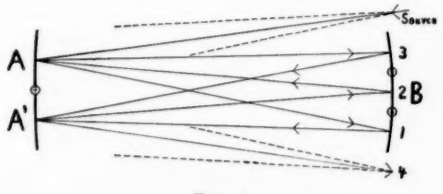

FIG. 1.

[1] H. D. Smith and J. K. Marshall, J. Opt. Soc. Am. **30**, 338 (1940).
[2] H. R. Kratz and J. E. Mack, Phys. Rev. **57**, 1059A (1940).

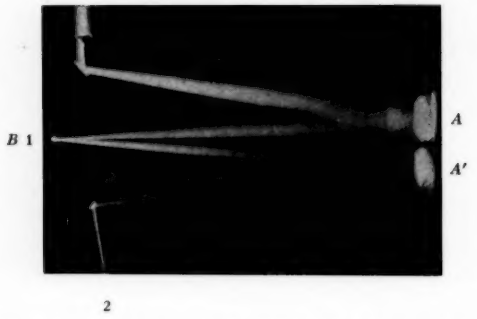

FIG. 2. Smoke photograph of optical path 2.5 meters long.

The only way intensity can be lost is by absorption or scattering on the reflecting surfaces.

The optical adjustments of this system are not critical; most of the tests and photographs described here were made manually without screw adjustments. The most important adjustment is the separation of the centers of curvature of the mirrors A and A'. This determines the number of times the light goes through the cell and the uniformity of the separation of the images formed on B. If A and A' are adjusted symmetrically about B and its center of curvature, each image on B is separated from the ones nearest to it by the distance between the centers of curvature of A and A'. The ratio of the length of B to this separation determines the number of times the light passes through the cell. This may be either four times for one image on B, eight times for three images, twelve for five, sixteen for seven, etc. Intermediate numbers are not possible. If A and A' are not symmetrically adjusted horizontally, the images on B occur in pairs rather than uniformly spaced. If A or A' is out of adjustment in the vertical rather than the horizontal angle, alternate images are raised or lowered above the others. In neither case is there any loss of intensity or troublesome cumulative effect of the error. If B is out of adjustment either horizontally or vertically, the first image of A does not fall exactly on A', and some light is lost around its edges. However, after one reflection there is no further loss, because that part of the light which did fall on A' is reflected back and forth between the same points on A and A'.

This method of obtaining long optical paths in restricted volumes has many advantages over those of a system using a spherical mirror and a truncated prism or a spherical mirror and a pair of flat mirrors:

I. The full angular aperture of the condensing mirrors is maintained to the extremities of the final image. The length of the image is limited by the size of the mirrors or by astigmatism and coma. The resulting increase in the intensity of the image off the axis can be partially obtained in the other two designs of absorption cell by using concave cylindrical mirrors instead of plane mirrors or by grinding convex cylindrical surfaces on the 45° faces of the truncated prism. In each case such cylindrical surfaces should have radii of curvature 1.414 times the radius of curvature of the spherical concave mirror, and both should have their axes in a plane perpendicular to the slit. Such an arrangement would form an astigmatic image of the concave mirror on itself, and hence greatly reduce the amount of light lost beyond the edges of that mirror. However, the lens defects are cumulative in this arrangement and should be quite serious.

II. The number of traversals of the absorption cell can be changed by a simple adjustment of mirrors A and A' from 4, to 8, or 12, or any reasonable multiple of 4. As neither the position nor the direction of the emergent beam is changed by this, no readjustment need be made in the rest of the optical system.

III. None of the adjustments is difficult to make. The tolerances on all but the horizontal angles of A and A' are usually large, because the principal errors introduced by small inaccuracies are neither troublesome nor cumulative.

IV. Losses of light on the mirror surfaces are kept to the absolute minimum. There are only two reflections, both at normal incidence, for each round trip of the light through the tube. Dust, pinholes, and spots on mirrors A and A' have a less serious effect than ordinarily, because the light from any point on one of these mirrors always goes back to the same point. If there is a hole in one of them, the light falling on the hole is lost, but on the second reflection from that mirror no more light is lost.

V. Except for the entrance and exit windows, there is no transmission of the light through glass or other optical material, with the consequent

reflection losses. For the same reason there are no extraneous images formed by multiple reflections.

VI. The separation between the images on B can ordinarily be made large enough to permit the source and final image to be completely outside the absorption cell. Small, plane mirrors are placed near the ends of mirror B to accomplish this.

VII. The space inside the absorption cell is used efficiently. The volume of a large aperture cell designed to give a ten-meter absorption path with sixteen traversals is only 10 liters.

VIII. The image formed by the mirror system after 12 traversals is quite sharp. It shows slight astigmatism, but except for this the individual turns of a common, coiled filament light bulb can be resolved.

IX. The principal disadvantages of this device are that the three concave mirrors must be specially made to have the same focal length and that, like all equipment in which multiple reflections are used from the same mirror, there is bound to be a certain amount of light scattered into the emergent beam without going through the cell the proper number of times.

Figures 2, 3, and 4 show the paths of the light beams for different arrangements of the mirrors. They were obtained by blowing smoke between the mirrors and photographing the light scattered from the optical path. Illumination was supplied by an a.c. carbon arc with an orange filter in front of it. Without the filter scattering and reflection losses attenuated the beam so fast that only the shortest optical paths could be photographed, and even with it the exposures were all less than fifteen minutes. The mirrors shown in the photographs have radii of curvature of 62.5 cm, are 8×11 cm and 5.5×15 cm, and can be set up in a vacuum-tight absorption cell of 10-liters volume. The order in which the different images of the slit were formed is shown in each case by the numbers beside them, although the decrease in intensity of the beams can be used as an equally good indication. Figure 2 shows the simplest possible case with one reflection each from A and A'. The full aperture of the mirrors is used, and two flat mirrors are inserted near B to bring the entrant and emergent images outside the body of the absorption cell. These auxiliary mirrors would ordinarily be incorporated in any design using this system. Figure 3 shows the next longer arrangement that gives a five-meter path with eight traversals of the cell. In this photograph the aperture of the entering light beam is cut down to a narrow pencil of rays. Figure 4 shows the case of twelve traversals with the formation of five intermediate images of the slit to give an optical path of 7.5 meters. The aperture of the light beam is here limited by the condensing lens, and the variations in intensity across the beam are due to changes in the arc during the exposure.

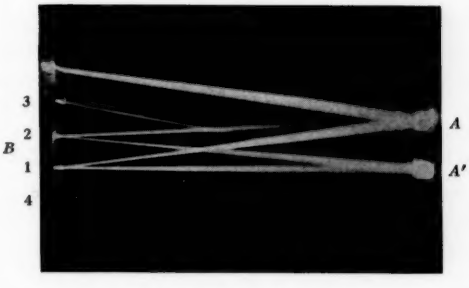

FIG. 3. Smoke photograph of optical path 5 meters long.

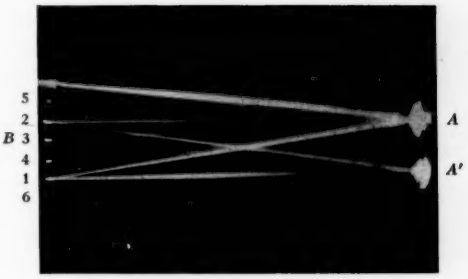

FIG. 4. Smoke photograph of optical path 7.5 meters long.

The results of preliminary tests of this cell have been most satisfactory. Using the mirrors with 62.5-cm radii of curvature, it was possible to set up the equipment on the top of a table so that the emergent beam had traversed the cell 90 times, corresponding to an optical path 56 meters long. Under these conditions the intensity of the beam was a great deal less than it had been on entering the system. The intensity of the image formed after 12 traversals was measured with a General Electric light meter and compared to that of the image formed after the first reflection. On the

optic axis of the system it was 30 percent as great, and at a point 1 cm from the axis it was 20 percent. These losses are not considered serious in view of the relatively poor condition of the mirrors at the time the measurements were made. The increase of reflectivity with wave-length makes this cell quite satisfactory in the infra-red. At a wave-length of 3 microns it transmitted through a ten-meter path 70 percent as much light as a simple cell that gave only a 90-cm path.

In conclusion the author wishes to express his thanks to Dr. W. J. Sweeney of the Esso Laboratories for his encouragement and backing in developing and building this absorption cell.

MAY, 1942 J. O. S. A. VOLUME 32

Resolving Power as a Function of Intensity

B. P. RAMSAY, E. L. CLEVELAND,* AND W. A. BOWEN, JR.
Department of Physics, University of Kentucky, Lexington, Kentucky

(Received January 2, 1942)

I. OBSERVATIONS WITH A MICROSCOPE

ON the basis of a calculation due to Airy, the Rayleigh criterion gives the limit of resolution for the microscope as

$$X = 0.5\, F\lambda/d, \tag{1}$$

where X is the minimum separable distance between two neighboring disk objects, λ is the wave-length of light, F is the focal length of the microscope objective, and d is the diameter of the aperture. Experiments with virus bodies, the size of which was below the limit of resolution according to the above formula, led Merling-Eisenberg to make the following statement: "It has been observed that reduction of intensity shows details that would not be visible in some cases and not resolvable in other cases if the formula was strictly right." [1] In another paper he makes the further observation that ". . . it becomes clear that the effect of increased resolution by means of reduced intensity is not within the content of the present formula of resolution." [2] From his experiments he draws the conclusion that the formula for the limit of resolution needs to be altered to include intensity I in the following manner:

$$X = Ik\lambda/A = IkF\lambda/d, \tag{2}$$

where A is the numerical aperture.[3] Since the Rayleigh objective resolving power is the reciprocal of the limit of resolution, it must be inversely proportional to intensity if (2) is valid. This conclusion is a matter of more than pedantic interest, for it has led to the development of techniques for resolving virus bodies which are "sub-microscopical" according to the Airy formula. Details of the internal structure of bacterial cells have been clearly resolved; and bacteria have been observed visually and photographically before, during, and after lysis.[4]

There are three respects in which this notable work needs to be extended. In the first place, it is directly applicable only to objective resolving power.[5] However, the persuasion that spectroscopic and objective resolution are comparable phenomena suggests that they are likely to be related similarly to intensity. But this cannot be assumed without adequate arguments. Secondly, the measurements upon which (2) is based have been in large measure visual rather than photographic. The reason for this has been the extreme smallness of the particles in which Merling-Eisenberg has been interested. His experiments

---

* Now an instructor at the Pennsylvania State College, State College, Pennsylvania.

[1] K. B. Merling-Eisenberg, Nature **139**, 416 (1937).

[2] K. B. Merling-Eisenberg, J. Quekett Microscopical Club **1**, 324–332 (1937).

[3] K. B. Merling-Eisenberg, J. Quekett Microscopical Club **1**, 311–323 (1937).

[4] K. B. Merling-Eisenberg, J. Exper. Pathology **19**, 338–342 (1938).

[5] As here used, objective resolving power refers to the ability of an optical instrument to distinguish between two objects radiating the same wave-length, while spectroscopic resolving power refers to the ability to distinguish between two spectral lines from the same source.

with various viruses, lipoids, and bodies of known size have shown that it is impossible to record photographically the extreme limits of the increased resolution that has been obtained. Finally, it may be mentioned that Merling-Eisenberg has not made it clear whether the relation between resolving power and intensity is an exact inverse proportionality, as implied by (2), or whether it is merely an inverse function.

II. OBSERVATIONS WITH A MICROPHOTOMETER

(a) Spectroscopic Resolution

In an attempt to study the matter impersonally, photographs have been made and studied with a microphotometer. In the case of spectroscopic resolution, the procedure consisted of taking a series of exposures of the just resolved D lines of sodium. The intensity was varied in convenient steps from each exposure to the next. For the purpose, a transmission replica grating was used on a spectrometer. A single movement slit was the variable stop for controlling the degree of resolution of the D lines. The variable stop was adjusted until the D lines were just resolved visually in the focal plane of the spectrometer telescope. The telescope was then replaced by the spectrometer camera. A number of preliminary photographs were taken to determine the optimum time of exposure, and the intensity variation allowable for utilization of the full length of the straight portion of the $D-\log E$ sensitometric curve. For convenience and accuracy in timing exposures, a shutter was adapted to the camera. Fourteen exposures were taken on each plate. The intensity of successive exposures was decreased in five-percent steps from an arbitrary maximum by means of two Nicol prisms which were placed between the sodium vapor lamp, which was used as the source, and the collimator slit.

Eastman spectroscopic plates, type 103-G, were used. The plates were developed in Eastman D-19 developer at 65°F, in tray, for a time of four minutes. Great pains were taken to keep all photographic factors, except intensity, constant for all exposures on any one plate. A Hilger microphotometer, H.451, was used in obtaining the results presented below.

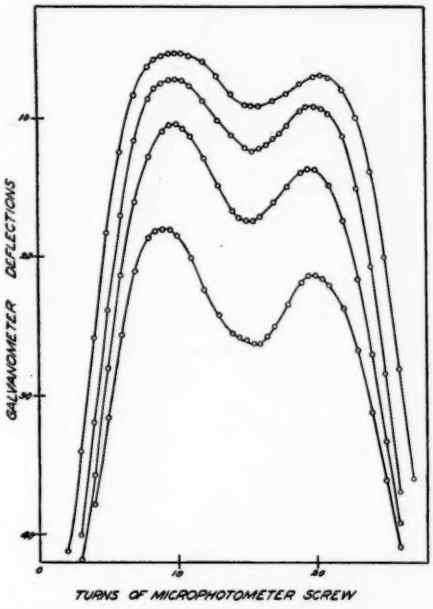

FIG. 1. Microphotometer deflection patterns for the D lines of the sodium spectrum. The relative intensities of the four patterns are 1.00, 0.85, 0.70, and 0.55, respectively.

(b) Objective Resolution

For the microphotometric study of objective resolution, the procedure was similar to that employed in the spectroscopic case. The D lines of sodium were replaced by two close slit sources of monochromatic light. Light from a mercury vapor lamp passed through a Wrattan filter, 77A, and illuminated two transparent slits in an opaque screen. These slit sources of green light were placed in the focal plane of a collimator having a focal length of 50 cm. Each slit was fairly uniform in width, and the parallelism of the two slits was found to be close. The average widths were 0.188 mm and 0.195 mm, respectively. The variable stop, telescope, and camera were used as in the spectroscopic case. As before, five-percent reductions in intensity for successive exposures were employed, and fourteen exposures were taken on each plate.

(c) Results of Experiments

In Fig. 1 the microphotometer deflection patterns for four of a set of fourteen exposures are shown. While the other ten might have been

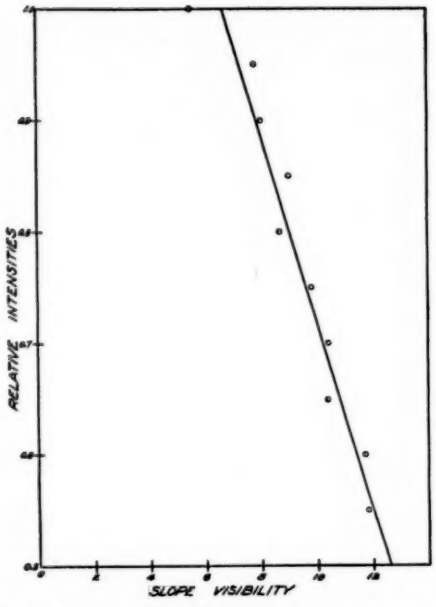

FIG. 2. Graph in which slope-visibility is plotted against intensity to show that under the conditions of observation the resolution of the lines shown in Fig. 1 is an inverse function of intensity.

shown, nothing would have been gained by crowding the large number of curves on a single figure. The relative intensities of the curves shown were 1.00, 0.85, 0.70, and 0.55, respectively. These curves show clearly that resolution as indicated by microphotometer deflections is affected by variations in intensity. It appears, in fact, that greater discrimination is obtained with lines of lesser intensity.

To show graphically the effect of intensity on the resolution of the lines, a deflection slope-visibility SV was plotted (Fig. 2) against the relative intensity for each exposure. Here SV is defined by

$$SV=(d''-d')/a'+(d''-d''')/a'', \qquad (3)$$

where d' and d''' are the deflections corresponding to the maxima of intensity, d'' is the deflection corresponding to the central minimum, a' is the distance in microphotometer turns between the positions of d' and d'', and a'' is the distance between the positions of d'' and d'''. Thus SV is proportional to the average slopes of the deflection pattern when the slopes are taken over the interval from maximum to central minimum. It is assumed that SV is a measure of discrimination as indicated by the microphotometer deflections. The straight line relation in Fig. 3 shows that the discrimination measured in this way is inversely proportional to the intensity over the range of values shown.

The data for objective resolution were obtained and treated in the same manner. The results were so similar as to make it unnecessary to show additional curves for this case.

(d) Significance of the Experiments

The conclusion which may be drawn from these observations is that experimental conditions may be found under which discrimination varies inversely with intensity. In regard to the general problem, it is impossible to be more specific than to say that discrimination is a function of intensity. It has been mentioned that preliminary experiments were employed to determine what intensity variation corresponded to the straight portion of the $D-\log E$ curve, and that the microphotometer observations which have been described were made within this range. Similar observations made when this restriction was not maintained showed that discrimination is not simply inversely proportional to the intensity. It may even increase with intensity, or in certain regions be independent of it. Thus if resolving power is to be a measure of discrimination obtainable, it, too, must be a function of intensity.[6]

III. THE RESOLVING POWER OF AN OPTICAL SYSTEM

For each optical device, or system of optical devices, there is a characteristic intensity function I which may be written as the product

$$I=I'\Psi, \qquad (4)$$

where Ψ is the distribution function which describes the pattern produced by unit intensity,

[6] The desirability of distinguishing between resolving power and resolution has been presented previously (cf. reference 9). Problems of the latter type are concerned with discrimination in those cases in which there are either more than two components to be resolved or the two components are unequal in relative intensity. It is assumed that the present argument need not be confused by the introduction of considerations of the latter sort here.

and I' is a factor which expresses the maximum of the intensity distribution in terms of the quantities upon which it depends. A change in intensity of the source is described simply as a change in the numerical value of I'. Thus the intensity distribution is the same for all values of I'. The dependence of resolving power cannot be explained as resulting from a change in the distribution I; for this does not occur. The explanation rests upon the fact that resolving power depends upon the observing mechanism, or the process of observation. This is the significant fact which has been emphasized by the experiments of Merling-Eisenberg.

There are two properties of an observing mechanism which may contribute to the dependence of resolving power on intensity. The first of these is the distortion introduced by the process of observation. A $D-\log E$ sensitometric curve represents the chief distortion introduced by a photographic process, although there are secondary factors such as graininess, the Eberhard effect, and spreading of the equiluminous lines.[7] Distortions occur in observations with other mechanisms, too—such as a thermocouple with galvanometer, or a photoelectric cell with galvanometer. In such cases, it is possible to infer from the use of a calibrating curve what the true intensity distribution must have been. A perfectly calibrated intensity distribution is therefore independent of the absolute value of the intensity. Indeed, a test of a method of calibration is whether it gives calibrated curves whose half-intensity widths and shapes are independent of the absolute intensities employed. Nevertheless, any method of calibration is an approximation, and it is not likely to be equally sensitive to all intensity values. Since a calibration cannot actually improve the discrimination, the discrimination is poor where the sensitivity of the calibration is poor. It is a consequence of this that resolving power of the calibrated curves is a function of intensity.

A second property of an observing mechanism which may contribute to the dependence of resolving on intensity was considered by Merling-Eisenberg to be the essential element for the explanation of the experiments in which he was interested. It is the threshold of observability, a minimum energy below which detection is impossible. This effect also might be considered a distortion; but by considering it separately, it may be noted that resolving power may be a function of intensity even when the response of the observing mechanism is linearly related to the intensity stimulus. Resolving power is sure to be independent of intensity only when the response is directly proportional to the stimulus.

To discuss the case algebraically, let B represent the magnitude of the threshold energy. Further, let Y be the maximum of the observable intensity which corresponds to the source intensity I'. Then,

$$Y=I'-B. \tag{5}$$

The consequences of a relation of this kind are illustrated by Fig. 3, where intensity curves of the form $I=I'(\sin^2\alpha)/\alpha^2$ have been plotted. Since the threshold B cuts off a strip of the I distribution at the bottom, the observed half-width is less than the half I width. Corresponding statements are true if the widths are measured at any other relative positions. The effect may be increased either by decreasing I', or by increasing B. Either of these processes alone would justify Eq. (2) if the I distribution were represented by an isosceles triangle. Although this is never the case, it is possible that for some distributions the deviations from a triangular distribution are not experimentally significant over the ranges of intensity employed. However, Merling-Eisenberg finds a combination of these effects responsible for the explanation of his experiments. He shows curves for the Airy distribution which is appropriate for the microscope. For these, he has calculated the radius of

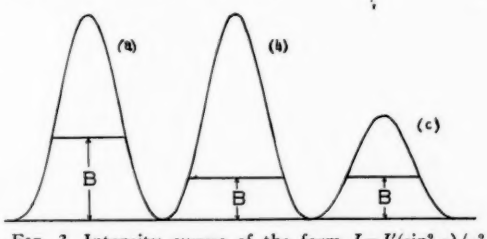

FIG. 3. Intensity curves of the form $I=I'(\sin^2\alpha)/\alpha^2$, showing thresholds, B. Comparison of curves (a) and (b) shows that the width of the line is effectively decreased by raising the threshold level; comparison of curves (b) and (c) shows that the width of the line may be effectively decreased by diminishing I', the absolute intensity of the line.

[7] F. E. Ross, *The Physics of the Developed Photographic Image* (D. Van Nostrand Company, 1924), Chapter 4.

the diffraction disks at a constant threshold level. The manner in which the diameter of the observed disk varies with I' would not obey Eq. (2) if the threshold for the eye were constant, as assumed. Actually, the threshold for the eye is known to decrease with intensity, except for very low values.[2] If one could rely on the validity of Eq. (2), it would be possible to calculate the manner in which the threshold for the eye varies with intensity. It should be pointed out, however, that the entire argument about the width of the observed disks may have a fallacious implication concerning the dependence of resolving power on intensity; for resolving power is more a matter of contrast than of actual width of the observed disks.

IV. THE EPOCH-SLOPE FORMULA

In several previous papers, certain deficiencies in the Rayleigh definitions of spectroscopic and objective resolving power have been noted.[8–11] It is unnecessary to review these here, for the merits of the epoch-slope resolving power P have already been advanced. The defining equation for the epoch-slope resolving power is

$$P=(\alpha/Y)(\Delta I/\Delta\alpha). \tag{6}$$

In this relation, α is called the epoch function.[8] It is proportional to the order of interference in multiple beam devices. The intensity-epoch slope, $\Delta I/\Delta\alpha$, describes the dependence of resolving power upon the width and form of the characteristic intensity distribution of an optical system. It shows also that a criterion of resolution is the necessary specification of the interval over which the intensity-epoch slope is to be taken.[9] The inverse factor Y must have the dimensions of intensity in order that P may be a dimensionless quantity, but it may be used also to describe the functional dependence of resolving power on intensity.[10]

It is neither desirable nor necessary to limit the concept of resolving power to a description of the properties of an isolated optical device, such as a prism, a grating, or an etalon.[11] Resolving power is a property of the entire system, including the source and the observing mechanism. In the epoch-slope formula, the wave-length of the source is included in the epoch function α. This may be simply illustrated by the case of a grating for which

$$\alpha=\pi d/\lambda, \tag{7}$$

where d is the path difference of rays from adjacent elements of the grating, and λ is the wave-length. The effect of the optical instruments on resolving power is contained in the product $\alpha(\Delta I/\Delta\alpha)$. The effect of the intensity of the source on resolving power is contained in the function Y which describes the manner in which the observing mechanism responds to this intensity. Equation (5) gives a simple example of the Y function.

In conclusion, it may be noted that the epoch-slope formula is capable of greater subtlety than is ordinarily required. For instance, defects in the optical surfaces and materials may cause the characteristic intensity function to be quite different from that of an ideal instrument. A case in which absorption significantly affects the I function has been considered in detail.[8] In many cases, however, the magnitude of these effects may not be known; or even if they are, it may be desirable to neglect them because of their smallness. Likewise, the exact form of the function Y may be unknown. In comparing the suitability of two different instruments for a given purpose, it is unnecessary to know the Y function if the observing mechanism is the same in the two cases. When this is so, the ratio P_1/P_2 of the resolving powers is independent of Y. Actually, the comparison of optical instruments used under identical conditions for the same purpose is the end which formulas for resolving power usually serve. It is probable that it was never anticipated that a formula for the Rayleigh resolving power, such as Eq. (1), would be called upon to describe the effectiveness of a given instrument under various conditions of observation.

There are other things to be said, for much that has been learned about problems of resolution from many laboratories has not been related to the theory of optical instruments. And in addition, a detailed consideration of objective resolving power from the method of approach employed here should prove interesting.

[8] B. P. Ramsay, O. T. Koppius, and E. L. Cleveland, J. Opt. Soc. Am. **30**, 439–444 (1940).
[9] B. P. Ramsay, E. L. Cleveland, and O. T. Koppius, J. Opt. Soc. Am. **31**, 26–33 (1941).
[10] B. P. Ramsay, O. T. Koppius, and E. L. Cleveland, J. Opt. Soc. Am. **31**, 202–208 (1941).
[11] B. P. Ramsay, E. L. Cleveland, and O. T. Koppius, J. Opt. Soc. Am. **31**, 296–300 (1941).

Colors of Furniture

PARRY MOON
Massachusetts Institute of Technology, Cambridge, Massachusetts
(Received January 19, 1942)

1. RESULTS

THIS paper completes a survey of the light-reflecting properties of 602 materials used in rooms. Previous reports[1] have listed data on materials used for ceiling, floor, and walls, while the present contribution considers furniture. It is hoped that the trichromatic coefficients will help in obtaining pleasing color arrangements in rooms and that the reflection factors will be valuable in the predetermination of lighting.

Figures 1 to 8 show representative spectrophotometric curves. From these curves were computed the values listed in Table I. The methods of test and computation were the same as described previously.[2] The first column of Table I gives a designating number which agrees with the number on the right margin of the curve sheets. The second column gives the specification of the material, while the third column refers to the manufacturer. (See Table II, also Table II of the paper on acoustical materials.)

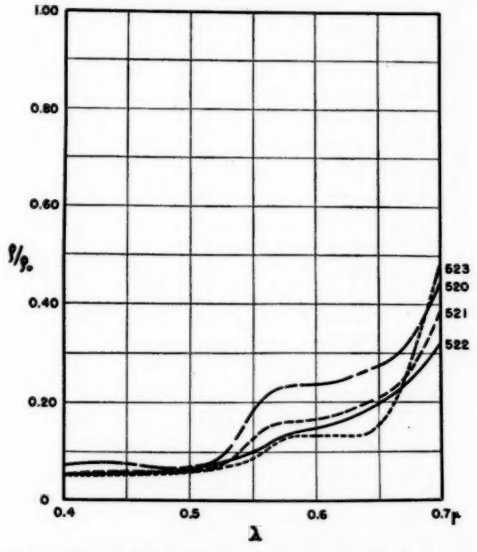

FIG. 1. Spectrophotometric curves for wood desk tops. Birch and maple samples stained a reddish brown.

Materials 520 to 523, inclusive, are standard desk tops for schools. They are of hard wood which has been stained a reddish brown. Many wood desks for offices have similar reflecting properties. Modern steel desks, however, ordinarily have linoleum tops. A popular color has been dark green (Nos. 528, 529), but recently there has been considerable agitation for the use of lighter colors. Nos. 525, 526, and 527 represent the recent "light, highly reflecting" desk tops which are advocated by manufacturers and by illuminating engineers.[3]

Steel desks, steel filing cabinets, and other office furniture are made in a variety of finishes.

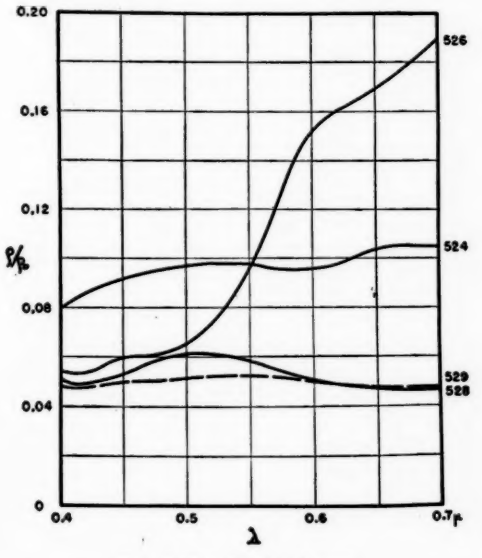

FIG. 2. Linoleum desk tops.

[1] Parry Moon, "Optical reflection factors of acoustical materials," J. Opt. Soc. Am. **31**, 317 (1941); "Colors of ceramic tiles," J. Opt. Soc. Am. **31**, 482 (1941); "Wall materials and lighting," J. Opt. Soc. Am. **31**, 723 (1941); "Reflection factors of floor materials," J. Opt. Soc. Am. **32**, 238 (1942); "Optical reflection factors of some materials used in schoolrooms," J. Opt. Soc. Am. **32**, 243 (1942).

[2] It is a pleasure to thank Mr. J. Margolskee for his help in this investigation, also the National Youth Administration, the M.I.T. Color Measurements Laboratory, and the furniture manufacturers.

[3] J. C. Forbes, "Lighter-colored desk tops," Mag. of Light, No. 1, p. 24 (1941).

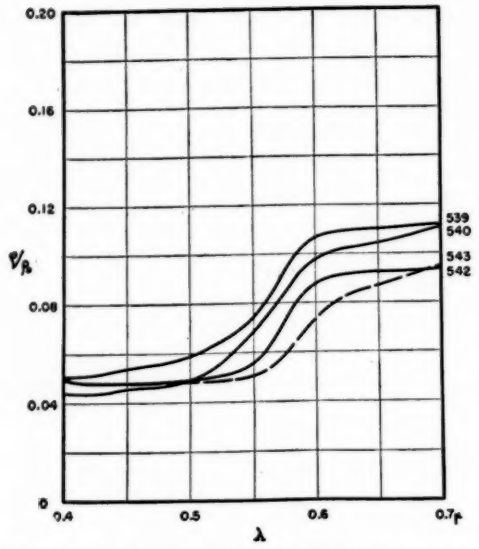

FIG. 3. Steel desks and filing cabinets finished to represent walnut and mahogany.

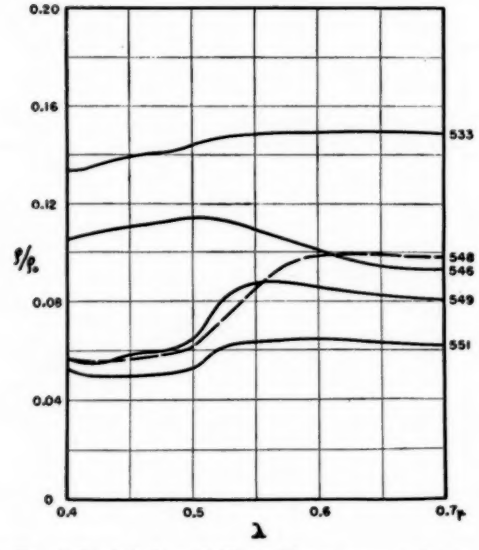

FIG. 4. Steel desks and filing cabinets, green and gray.

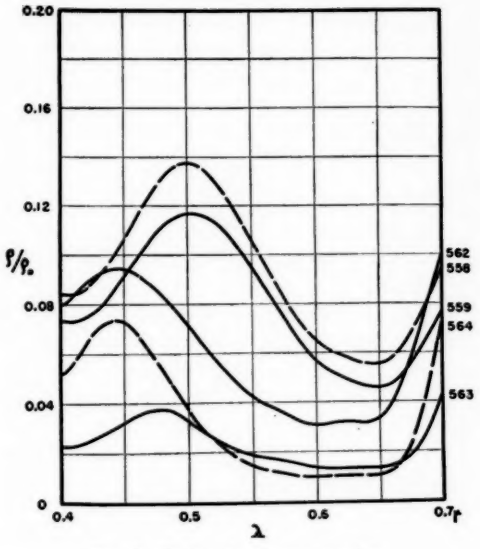

FIG. 5. Cloth upholstery materials.

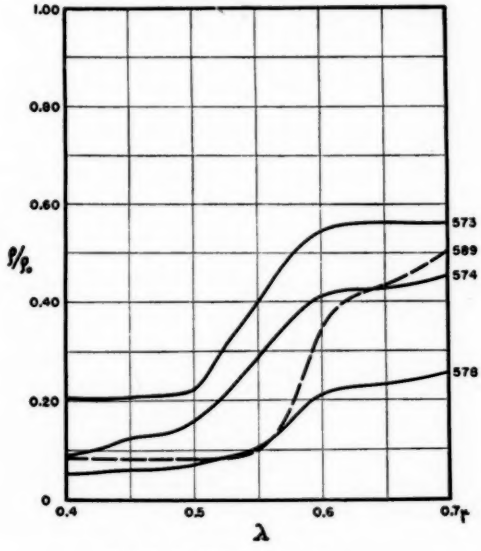

FIG. 6. Artificial leather; brown.

The highest reflection factors of any samples tested are obtained with a metallic gray finish (Nos. 530, 531, 532) and even this finish gives hardly more than 20 percent reflection. The popular green color (No. 547 to 551) has a much lower reflection factor, ranging from 6 to 9 percent. The imitation walnut and mahogany finishes are likewise very low in reflection factor and seem surprisingly alike for the various manufacturers.

2. FURNITURE AND LIGHTING

The principal reason that the illuminating engineer must consider the reflection factors of

furniture is that such reflection factors usually determine contrasts in the field of view. Investigations of the most diverse kind show that a human being sees best and visual fatigue is reduced to a minimum when the entire field of view is of approximately the same luminosity as that to which the fovea is adapted.[4] This effect is not very noticeable at low levels of illumination but becomes very marked at the high illuminations now coming into use.[5] Thus it is important that furniture should not be too dark nor too light, compared with the object on which the attention is focused. If this object is a piece of white paper with $\rho=0.80$, then ideal visual conditions[6] are obtained only if $\rho \geqq 0.40$ for other objects that are equally illuminated.

Consider first the conditions in a school room, with a pupil reading a book printed on white paper and with equal illumination on the paper and on the desk. Luminosity ratios will then be as follows:

No.	Material	ρ	L_A/L_D
520	Wood desk top	0.192	4.2
521	Wood desk top	0.140	5.7
522	Wood desk top	0.120	6.7
523	Wood desk top	0.106	7.6
537	Steel side of desk	0.0805	9.9

where L_A = adapting luminosity (for $\rho=0.80$),

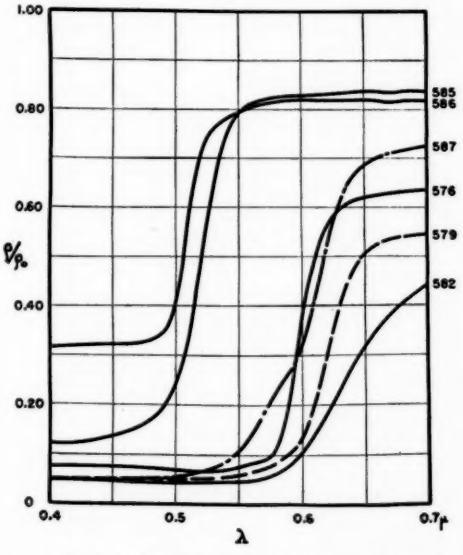

FIG. 7. Artificial leather; yellow, orange, and red.

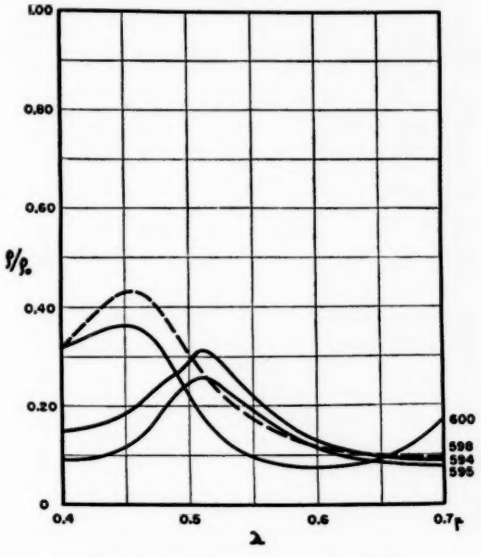

FIG. 8. Artificial leather; green and blue.

L_D = luminosity of desk. These ratios are much too high for ideal seeing conditions.

Conditions are even worse for office desks:

No.	Material	ρ	L_A/L_D
525	"Light materials"	0.125	6.4
526		0.117	6.8
527		0.100	8.0
528	"Dark materials"	0.0535	15.0
529		0.0503	15.9

There seems to be little reason for the use of such low reflection factors for desk tops. Certainly, other materials are available. Floor linoleums are obtainable with reflection factors of over 0.50. A few possibilities are listed in Table III. Another

[4] R. J. Lythgoe, "The measurement of visual acuity," Med. Research Council, Spec. Rep. **173**, 85 (1932). J. Steinhardt, "Intensity discrimination in the human eye," J. Gen. Physiology **20**, 185 (1936). M. Luckiesh and F. Moss, "Brightness contrasts in seeing," Trans. I.E.S. **34**, 571 (1939). H. L. Logan, "Specification points of brightness," Trans. I.E.S. **34**, 881 (1939). A. S. Mengel and G. W. Clark, "The effect of the peripheral field on visual comfort," M.I.T. Thesis (1941).

[5] Ward Harrison, "Indirect luminaires—efficient and inefficient," Trans. I.E.S. **34**, 255 (1939).

[6] Paper on wall materials, reference 1.

TABLE I. Reflection factors and trichromatic coefficients

No.	Name	Mfgr.	Approx. color	A			C		
				x	y	ρ	x	y	ρ
	Wood desk tops								
520	Color 47	37	Brown	0.5331	0.4136	0.192	0.4257	0.3818	0.171
521	Color 42	37	Brown	0.5280	0.4100	0.140	0.4128	0.3732	0.126
522	Maple, L-48 finish	33	Brown	0.5267	0.4053	0.120	0.4084	0.3681	0.109
523	Birch plywood, L-48 finish	33	Brown	0.5255	0.4050	0.106	0.4051	0.3654	0.0958
	Linoleum desk tops								
524	No. 1707 gray	39	Dk. gray	0.4509	0.4103	0.0952	0.3141	0.3235	0.0952
525	Brown No. 20SB	1, 38	Brown	0.5171	0.4016	0.125	0.3898	0.3561	0.117
526	Std. brown	40	Brown	0.5241	0.4061	0.117	0.4029	0.3623	0.106
527	No. 1701 brown	39	Brown	0.5209	0.4001	0.100	0.3960	0.3528	0.0912
528	Green No. 022SB	1, 38	Dk. green	0.4378	0.4244	0.0535	0.2991	0.3266	0.0550
529	No. 1705 green	39	Dk. green	0.4435	0.4124	0.0503	0.3086	0.3225	0.0505
	Enameled steel								
530	No. 640	34	Gray	0.4536	0.4139	0.221	0.3150	0.3248	0.221
531	No. 4362 gray	38	Gray	0.4502	0.4122	0.218	0.3122	0.3219	0.218
532	Seal gray	36	Gray	0.4465	0.4110	0.217	0.3104	0.3224	0.219
533	No. 650	34	Gray	0.4595	0.4151	0.145	0.3157	0.3239	0.145
534	No. 5	34	Brown	0.4916	0.4227	0.141	0.3685	0.3679	0.134
535	Metropolitan 2	34	Brown	0.5206	0.4152	0.138	0.4020	0.3752	0.126
536	No. 517 brown	38	Dk. brown	0.4884	0.4128	0.0862	0.3560	0.3457	0.0822
537	Desk	37	Dk. brown	0.4860	0.4096	0.0805	0.3491	0.3365	0.0771
538	No. 101 walnut	40	Dk. brown	0.5083	0.4093	0.0866	0.3764	0.3510	0.0805
539	No. 102 walnut	39	Dk. brown	0.5053	0.4100	0.0861	0.3747	0.3507	0.0801
540	Walnut	38	Dk. brown	0.5098	0.4086	0.0784	0.3840	0.3560	0.0724
541	No. 5 walnut	36	Dk. brown	0.5033	0.4011	0.0779	0.3701	0.3424	0.0735
542	No. 110 mahogany	40	Dk. red	0.5072	0.4018	0.0688	0.3704	0.3364	0.0638
543	No. 93 mahogany	39	Dk. red	0.5010	0.3974	0.0604	0.3565	0.3252	0.0566
544	No. 5 mahogany	36	Dk. red	0.4929	0.3925	0.0584	0.3499	0.3210	0.0556
545	Mahogany	38	Dk. red	0.4983	0.3953	0.0577	0.3523	0.3218	0.0541
546	No. 55 bluegreen	39	Dk. green	0.4347	0.4113	0.103	0.2994	0.3160	0.105
547	No. 3 green	36	Dk. green	0.4592	0.4319	0.0977	0.3366	0.3611	0.0960
548	Olive F	34	Dk. green	0.4892	0.4204	0.0871	0.3601	0.3567	0.0832
549	No. 112 O. G.	40	Dk. green	0.4724	0.4306	0.0824	0.3408	0.3583	0.0809
550	No. 46 green	39	Dk. green	0.4716	0.4279	0.0783	0.3419	0.3569	0.0766
551	Olive green	38	Dk. green	0.4656	0.4208	0.0615	0.3310	0.3416	0.0605
	Upholstery materials, cloth								
552	Arabesque, wheat 8784	35	Brown	0.5211	0.4070	0.158	0.4000	0.3759	0.145
553	Earl, medallion gold 1559	35	Tan	0.5434	0.4057	0.105	0.4371	0.3977	0.0935
554	Mosaic, bagdad rose 25	35	Red	0.5425	0.3603	0.0794	0.3927	0.2940	0.0686
555	Corinth, rose 6731	35	Red	0.5529	0.3614	0.0781	0.4095	0.3044	0.0662
556	Crochette, copper rust 8984	35	Red	0.5813	0.3638	0.0769	0.4636	0.3351	0.0632
557	Danbury, desert beige 367	35	Dk. pink	0.5116	0.3942	0.118	0.3749	0.3406	0.109
558	Empress, turquoise 40	35	Green	0.3810	0.4269	0.0878	0.2589	0.3204	0.0968
559	Cortona, turquoise 221	35	Green	0.3805	0.4303	0.0771	0.2597	0.3251	0.0851
560	Breton, ferngreen 248	35	Green	0.4510	0.4403	0.0760	0.3269	0.3892	0.0775
561	Gros Point, acadia blue 333	35	Blue	0.4094	0.4055	0.0755	0.2724	0.3020	0.0802
562	Moresque, twilight blue 55	35	Blue	0.3652	0.3620	0.0401	0.2311	0.2310	0.0445
563	Molano, blue 9273	35	Dk. blue	0.3732	0.3832	0.0179	0.2368	0.2676	0.0200
564	Serenade, royal blue 9708	35	Dk. blue	0.3005	0.2872	0.0149	0.1908	0.1577	0.0183
	Upholstery materials, artificial leather								
565	Moleather 1001	2	White	0.4525	0.4100	0.880	0.3160	0.3236	0.875
566	Alhambra, white 64	35	White	0.4514	0.4102	0.786	0.3148	0.3240	0.788
567	Moleather 1029	2	Ivory	0.4661	0.4165	0.775	0.3341	0.3425	0.760
568	Canfield, ivory 7500	35	Ivory	0.4710	0.4189	0.727	0.3417	0.3500	0.711
569	Grenadier, old white 6817	35	Lt. gray	0.4630	0.4117	0.575	0.3281	0.3322	0.567
570	Alhambra, dove gray 6811	35	Gray	0.4512	0.4056	0.271	0.3126	0.3160	0.270
571	Alhambra, sand 5020	35	Tan	0.4868	0.4146	0.486	0.3584	0.3536	0.464
572	Moleather 1019	2	Buff	0.4843	0.4205	0.463	0.3590	0.3631	0.445
573	Fabrikoid No. 1107F	11	Tan	0.5140	0.4159	0.440	0.4148	0.3658	0.404
574	Alhambra, moka beige 7089	35	Lt. brown	0.5235	0.4176	0.324	0.4167	0.3903	0.295
575	Canfield, beige 5943	35	Tan	0.4902	0.4129	0.311	0.3616	0.3539	0.296
576	Canfield, ember red 7069	35	Red	0.6130	0.3460	0.215	0.5104	0.3212	0.163
577	Fabrikoid No. 2021	11	Brown	0.5252	0.4108	0.152	0.4143	0.3753	0.137
578	Canfield, harness tan 6810	35	Brown	0.5411	0.3995	0.150	0.4288	0.3684	0.133
579	Grenadier, holly red 5555	35	Red	0.6065	0.3454	0.130	0.4895	0.3194	0.101
580	Alhambra, rust 5116	35	Brown	0.5652	0.3708	0.116	0.4380	0.3353	0.0988
581	Canfield, autumn brown 82	35	Brown	0.5210	0.3997	0.111	0.3954	0.3524	0.101
582	Fabrikoid No. 5025	11	Dk. red	0.5866	0.3514	0.0903	0.4567	0.3134	0.0720
583	Moleather 1015	2	Dk. brown	0.4964	0.4070	0.0738	0.3663	0.3458	0.0696
584	Alhambra, apricot 7051	35	Pink	0.5147	0.3996	0.453	0.3844	0.3465	0.413
585	Canfield, jonquil 7248	35	Lt. yellow	0.4913	0.4386	0.757	0.3815	0.4035	0.725
586	Canfield, canary 3223	35	Yellow	0.5180	0.4459	0.728	0.4350	0.4489	0.674
587	Canfield, orange 5113	35	Orange	0.6071	0.3656	0.241	0.5236	0.3635	0.188
588	Moleather 1020	2	Orange	0.5960	0.3734	0.231	0.5113	0.3640	0.183
589	Alhambra, burnt orange 7539	35	Orange	0.5773	0.3724	0.210	0.4781	0.3270	0.159
590	Grenadier, aztec rust 6805	35	Dk. orange	0.5852	0.3749	0.171	0.4886	0.3566	0.138
591	Canfield, chartreuse 6010	35	Y. green	0.4690	0.4640	0.432	0.3681	0.4360	0.429
592	Grenadier, palmgreen 7563	35	Y. green	0.4429	0.4447	0.222	0.3241	0.3753	0.226
593	Canfield, sage green 7545	35	Green	0.3999	0.4372	0.200	0.2781	0.3405	0.214
594	Alhambra, aqua 4900	35	Green	0.3738	0.4463	0.182	0.2589	0.3444	0.201
595	Grenadier, tropic green 6808	35	Green	0.3873	0.4597	0.156	0.2729	0.3784	0.171
596	Moleather 1010	2	Dk. green	0.4145	0.4351	0.0653	0.2908	0.3439	0.0678
597	Canfield, rose mauve 7047	35	Orchid	0.5181	0.3839	0.225	0.3775	0.3167	0.202
598	Alhambra, thistle blue 7541	35	Blue	0.3344	0.3552	0.156	0.2170	0.2179	0.180
599	Grenadier, grapetone 7046	35	Purple	0.5170	0.3730	0.147	0.3656	0.2982	0.132
600	Grenadier, capri blue 7542	35	Blue	0.3281	0.3142	0.100	0.2070	0.1811	0.116
601	Moleather 1011	2	Dk. blue	0.3964	0.3803	0.0622	0.2585	0.2597	0.0666
602	Grenadier, midnight blue 5033	35	Dk. blue	0.3926	0.3734	0.0510	0.2537	0.2527	0.0549

TABLE II. Manufacturers. (For other manufacturers, see Table II of paper on acoustical materials.)

No.	Name
33	American Seating Co.
34	Art Metal Construction Co.
35	L. C. Chase and Co.
36	Globe-Wernicke Co.
37	Heywood-Wakefield Co.
38	Metal Office Furniture Co.
39	Security Steel Equipment Corp.
40	Shaw-Walker Co.

TABLE III.

No.	Material	ρ	L_A/L_D
205	Micarta 856	0.723	1.1
280	Linoleum, ivory	0.563	1.4
193	Prima vera, natural	0.447	1.8
305	Linoleum, light gray	0.434	1.8
393	Rubber, gray	0.318	2.5
195	White oak, natural	0.281	2.8
281	Linoleum, gray	0.273	2.9
388	Cork	0.233	3.4

way of improving visual conditions is to cover the entire desk with heavy white paper. This reduces L_A/L_D to unity and the covering can be replaced easily whenever it gets soiled.

Another peculiarity is the excessively low reflection factors of enameled steel furniture. That light colors are feasible in enameled steel and that they tend to produce a bright and cheerful effect is attested by any modern kitchen. Yet the office continues to use the reflection factors of 0.06 and 0.08 which were popular in the 1890's.

3. SURVEY OF REFLECTION FACTORS

A summary of the results obtained on the 602 samples is shown in Table IV. The representative values of reflection factor in the last column of the table give a rough idea of what is being used today. Evidently the manufacturers have made a sincere effort to provide highly reflecting ceiling materials and wall materials. In nearly all types of ceiling and wall materials, including venetian blinds and window shades, whites can be obtained with reflection factors of over 70 percent.

Ivory, cream, yellow, and pink materials also have high reflection factors though not as high as one might suppose. Tinted surfaces that look *almost* as light as white (in the absence of direct comparison) may have reflection factors of 0.40 or 0.50. Thus the common practice of always using something that is *not* pure white may result in a surprising loss of light.

Floor materials are seen to be much darker than wall materials on the average, though highly reflecting floor tiles and linoleums can be obtained. Carpets are found to reflect much less light than any other form of floor covering.

One of the surprising results of the investigation is the extraordinarily low reflection factor of furniture. Desk tops, both in schools and offices, should be almost as light as white paper in order to get optimum seeing conditions and reduce eyestrain. Yet actual desk tops are darker than floors. Steel filing cabinets and other office equipment are also made as dark and gloomy as possible. It would seem that the furniture manufacturers are overlooking a real opportunity if they do not improve the reflection factor of their products.

4. CONCLUSIONS

This paper presents final data on an investigation of the reflection factors and trichromatic coefficients of 602 materials used in interiors. The

TABLE IV. Representative values of reflection factor.

Location	Material	Reflection factor Max.	Min.	Representative
Ceiling	Acoustical materials	0.816	0.265	0.50
	Paints	0.901	0.0922	0.60
Walls	Acoustical materials	0.816	0.265	0.50
	Wood veneers	0.447	0.0955	0.14
	Wall boards	0.893	0.0492	0.20
	Wall linoleums, etc.	0.770	0.147	0.50
	Wall tiles, asphalt	0.780	0.0452	0.30
	ceramic	0.875	0.0526	0.50
	Chalkboards, light	0.906	0.540	0.60
	dark	0.133	0.0627	0.08
	Paints	0.901	0.0922	0.60
	Venetian blinds	0.819	0.229	0.60
	Window shades	0.758	0.0621	0.30
Floor	Floor tiles, asphalt	0.595	0.0396	0.10
	ceramic	0.715	0.0853	0.20
	rubber	0.537	0.195	0.30
	Linoleums	0.629	0.0417	0.15
	Oak flooring	0.288	0.131	0.20
	Cork, natural	0.233	0.114	0.18
	Carpets	0.119	0.0143	0.05
Furniture	Desk tops, wood	0.192	0.106	0.14
	linoleum, light	0.125	0.100	0.11
	linoleum, dark	0.0952	0.0503	0.06
	Enameled steel	0.221	0.0577	0.08
	Upholstery, cloth	0.158	0.0149	0.05
	coated fabric (artificial leather)	0.880	0.0510	0.20
	Woods, natural finish	0.447	0.0955	0.14

highest reflection factor was 0.901 (a white paint) while the lowest were 0.0149 for an upholstery fabric and 0.0143 for a carpet. The darkest floor tile was a black asphalt tile with a reflection factor of 0.0396, and the darkest linoleum was black with a reflection factor of 0.0417.

A large variety of attractive colors and high reflection factors is available for ceilings and walls. A few highly reflecting materials are obtainable for floors, though it is felt that most floor materials are too dark. Furniture is much too dark, being even worse than floor materials in that respect.

The newly developed integral-equation method allows a quantitative evaluation of room lighting and leads to the following conclusions:

(a) The ceiling and walls of a room should be pure white, not ivory, cream, or yellow. This use of maximum reflection factor gives the most economical lighting system for a given illumination, as well as the best diffusion of light. Harsh shadows and glaring contrasts tend to disappear.

(b) Venetian blinds and window shades should be white and should cover the windows when the artificial lighting system is in use.

(c) Floors should have sufficiently high reflection factors so that they do not contrast unpleasantly with the remainder of the room. Values of $\rho = 0.50$ can actually be used without undue cleaning trouble.

(d) Present desk tops are much too dark for good visual conditions. Reflection factors of at least 0.40 should be used instead of the usual values of 0.06 to 0.14.

(e) Steel filing cabinets, desks, etc. should be produced in lighter, more cheerful colors. Obviously, imitation walnut and mahogany should be consigned to limbo.

Illuminating Engineering Nomenclature and Photometric Standards

Approval by American Standards Association of New I.E.S. Report on Nomenclature and Photometric Standards Received

"ILLUMINATING Engineering Nomenclature and Photometric Standards," which was first published in the September, 1941, issue of *Illuminating Engineering*, was approved on February 27, 1942, as American Standard Z7.1-1942 by the American Standards Association. Prepared by the Committee on Nomenclature and Standards of the Illuminating Engineering Society, this new report will supersede the previous I.E.S. nomenclature and photometric standards report, which became American Standard Z7 in 1932.

Reprints of this report are now available through the Illuminating Engineering Society, 51 Madison Avenue, New York, N. Y. Single copies are 25¢. Quantity prices upon request.

The Photographic Reciprocity-Law Failure and the Ionic Conductivity of the Silver Halides*

J. H. WEBB
Kodak Research Laboratories, Eastman Kodak Company, Rochester, New York

(Received January 9, 1942)

A method is given for determining from reciprocity-law failure measurements at different temperatures the value of the energy exponent ϵ in the equation for ionic conductivity of silver bromide

$$N_i = Ae^{-\epsilon/kT} \text{ ions/sec.} \quad (1)$$

According to present theory, the reciprocity-law failure at high intensities is due to the sluggishness of the secondary process of latent-image formation consisting of migration of Ag^+ ions to the specks. The free electrons produced in the grains by exposure can move practically instantaneously and independently of temperature. However, if the Ag^+ ions cannot move up to the specks at a sufficient rate to keep them discharged, an inefficiency is introduced. This inefficiency may be said to depend upon the number of free electrons produced in the grain per second, N_e, compared with the number of free Ag^+ ions, N_i, available for ionic conduction. The number of free electrons produced can be controlled by the light intensity, I, whereas the number of conducting Ag^+ ions can be controlled by temperature in accordance with Eq. (1). By choosing points on the reciprocity curves made at different temperatures such that the change of efficiency arising from a change of intensity I_1 to I_2 is equal to the change of efficiency arising from a change of temperature T_1 to T_2, the relation is shown to hold

$$\log I_2/I_1 = \frac{0.434\epsilon}{k}\left(\frac{1}{T_1} - \frac{1}{T_2}\right). \quad (2)$$

Substitution of experimental values in this equation for I_1, I_2, and T_1, T_2 gives a value of $\epsilon = 0.69$. Direct measurement of the ionic conductivity at different temperatures on a single crystal of AgBr gives the value of $\epsilon = 0.66$. The close agreement between the ϵ values obtained by photographic means and by direct measurement affords quantitative evidence that the high intensity reciprocity-law failure is due to the ionic conductivity effect alone.

INTRODUCTION

ACCORDING to present theory,[1] the formation of the photographic latent image depends upon two properties of the silver halides: photoconductance and ionic conductivity. On exposure to light, photoconducting electrons are released in the grains of the emulsion, and these electrons are free to move about within the grain just as the conduction electrons move in a metal. In order that a latent-image speck may begin to form, it is required that one of these free electrons become trapped at some point on the surface of the grain. This can occur at any point in the grain where there is an energy level lying below the conduction band of the silver bromide crystal. It has been shown[2] that specks of silver sulfide are formed on the surface of the grains during the process of emulsion manufacture, and it is believed that these impurity specks function as the initial traps for electrons set free by light. At points where electrons are trapped, local electric fields are set up. Under the influence of these fields, Ag^+ ions migrate to the specks where they neutralize the electrons to form silver atoms. When a silver speck has grown large enough in this way to act as a nucleus in development, it constitutes a latent-image speck.

The migration of Ag^+ ions in latent-image formation as outlined above may be termed an ionic current. Ionic conductivity of the silver halides has been studied extensively[3] in macroscopic specimens of these materials under externally applied electric fields. From such measurements, it has been found that the ionic conductivity of these materials arises from the movement of the Ag^+ ions alone and that the negative halide ions play no part. This conductivity has been explained[4] as follows: In a

* Communication No. 837 from the Kodak Research Laboratories.

[1] R. W. Gurney and N. F. Mott, Proc. Roy. Soc. **164**, 151 (1938).

[2] S. E. Sheppard, Phot. J. **65**, 1 (1925).

[3] C. Tubandt in W. Wien and F. Harms, *Handbuch der Exper. Physik* (Akademie Verlag, Leipzig, 1932) Vol. 2.

[4] J. Frenkel, Zeits. f. Physik **35**, 652 (1926). W. Jost, J. Chem. Phys. **1**, 466 (1933).

perfect crystal lattice of silver bromide at the absolute zero of temperature, every lattice point is occupied by either a Ag^+ or a Br^- ion. At any higher temperature, however, there is a certain probability that ions of both types will be dislodged from their normal positions and pushed into interstitial positions. Energy is required to do this, and if too much energy is needed, very few ions will be thus dislocated. In a silver bromide crystal, the energy required to remove a Br^- ion to an interstitial position is so high that the event rarely happens. On the other hand, the energy required to transfer a Ag^+ ion to an interstitial position is small enough so that at ordinary temperatures, this happens very frequently. As a consequence, at all ordinary temperatures, a silver bromide crystal contains a large number of Ag^+ ions displaced from their regular lattice positions. These displaced ions may be thought of as quasi-free Ag^+ ions which give rise to ionic conductivity. Likewise, they may be considered to be the ions which migrate to the specks in the photographic grains to complete the formation of the latent image. The number of such ions and their mobility through the crystal depend upon thermal motion and therefore vary with temperature.

From measurements at different temperatures, it has been shown[5] that the ionic conductivity of the silver halides can be represented by an equation of the type

$$N_i = Ae^{-\epsilon/kT}. \tag{1}$$

In this equation, N_i represents the number of Ag^+ ions per second reaching the electrode, k is the molecular gas constant, T is the absolute temperature and ϵ is an energy term connected with the production of free Ag^+ ions and their movement through the crystal. Physically, ϵ is made up of two parts:[6]

$$\epsilon = \tfrac{1}{2}W + U,$$

where W represents the energy required to remove a Ag^+ ion from its regular lattice position to an interstitial position and U represents the energy required to move an ion from one interstitial position to another in the lattice. Since these terms are not separable by ordinary experiments, only the composite term ϵ will be used here. It may be considered to be a characteristic constant of the particular silver halide under consideration.

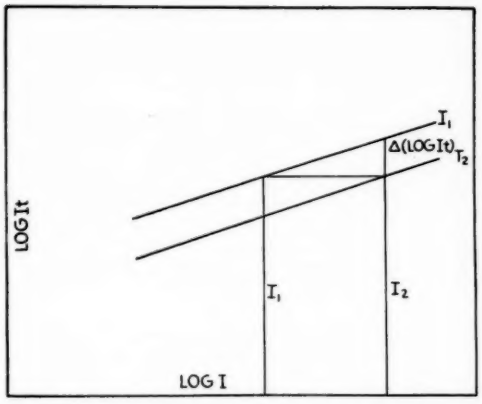

FIG. 1. Schematic representation of the high intensity ends of two reciprocity-failure curves at temperatures T_2 and T_1.

THE HIGH INTENSITY RECIPROCITY-LAW FAILURE

In accordance with the theory of latent-image formation just outlined, the failure of the photographic reciprocity law at high intensities is attributed to the sluggishness of the secondary part of latent-image formation[1,7] consisting of the migration of the Ag^+ ions to the charged specks. On exposure to light, the electrons freed in the crystal can move through the crystal practically instantaneously, and the number freed is independent of temperature. Accordingly, the electrons start to charge up the specks immediately on initiation of exposure. However, if the Ag^+ ions do not move up to the specks at a sufficiently high rate to keep them discharged, the specks acquire a negative charge which interferes with the trapping of electrons. Electrons will be repelled from the speck because of the excess negative charge and these repelled electrons retard the building of a developable speck. The inefficiency arising in this way will depend upon the number of free electrons produced per unit of time in the grain relative to the number of

[5] W. Lehfeldt, Zeits. f. Physik **85**, 717 (1933).
[6] N. F. Mott and R. W. Gurney, *Electronic Processes in Ionic Crystals* (Oxford Press, 1940), p. 42.
[7] J. H. Webb and C. H. Evans, J. Opt. Soc. Am. **28**, 249 (1938).

Ag^+ ions which can reach the speck per unit of time.

THEORETICAL FORMULATION

In Fig. 1, the high intensity ends of two reciprocity-law failure curves (constant density) made at two temperatures are shown schematically. At high intensities,* the reciprocity curves become straight lines as shown here and can be represented by the equation

$$(\log It) = C + \log I^a \qquad \text{Den.} = \text{const.} \tag{2}$$

where C and a are constants. This equation represents the amount of exposure required to produce a constant density as a function of the intensity of exposing light I. If it is assumed that the number of free electrons, N_e, produced per unit of time in the grains is proportional to the incident light intensity, i.e.,

$$N_e = bI, \tag{3}$$

Eq. (2) can be written in the form

$$(\log It) = C_1 + \log N_e^a \qquad \text{Den.} = \text{const.} \tag{4}$$

where C_1 is a constant but different from C; Eq. (4) shows how the efficiency varies with the number of free electrons, N_e, under the condition (temperature constant) that the number of Ag^+ ions, N_i, that can reach the speck per unit time is constant. The question immediately suggests itself: If the number of Ag^+ ions, N_i, which can reach the speck per unit time be changed by altering the temperature, how would this affect the efficiency? The most logical assumption appears to be to include the factor N_i in Eq. (4) as shown below:

$$(\log It) = C_2 + \log (N_e/N_i)^a \qquad \text{Den.} = \text{constant.} \tag{5}$$

In words, Eq. (5) proposes that the efficiency of the photographic process at high intensities would be changed by the same amount in the two cases:

(a) that N_i is held constant and N_e is increased α-fold or

(b) that N_e is held constant and N_i is decreased α-fold. The proposal made in Eq. (5) can be justified only by its compatibility with experimental facts, which will now be demonstrated.

By means of Eqs. (1) and (3), Eq. (5) can be written in terms of I and T,

$$(\log It) = C_3 + a \log \frac{I}{e^{-\epsilon/kT}} \qquad \text{Den.} = \text{constant}, \tag{6}$$

in which C_3 is a new constant. Now, let the change in $\log It$, i.e., $\Delta(\log It)$ be written down for the two respective conditions:

(a) the temperature T is held constant and I is changed from I_1 to I_2;

(b) the intensity I is held constant and the temperature T is changed from T_1 to T_2. The equations,

$$\Delta(\log It) = a \log (I_2/I_1), \quad T = \text{constant}, \qquad \Delta(\log It) = \frac{a\epsilon}{k}\left(\frac{1}{T_1} - \frac{1}{T_2}\right)\log e, \quad I = \text{constant}, \tag{7}$$

are obtained. If cases are considered for which $\Delta(\log It)$ is the same for a change of I or T, the right sides of Eq. (7) can be equated, and the relation obtained

$$\log \frac{I_2}{I_1} = \frac{0.434\epsilon}{k}\left(\frac{1}{T_1} - \frac{1}{T_2}\right). \tag{8}$$

Equation (8) corresponds to the case illustrated in Fig. 1 and affords a means of determining the value of ϵ in the conductivity Eq. (1). If the value of ϵ obtained by this photographic method is found to agree with the value determined by direct measurements of ionic conductivity, then the proposal made in Eq. (5) will be supported, and quantitative evidence will have been obtained that the reciprocity-law failure at high intensities is due to the ionic conductivity effect alone.

DETERMINATION OF ϵ

In Fig. 2, a series of experimental reciprocity-law failure curves for different temperatures is

* The intensity at which the curves become straight lines varies with the emulsion and temperature.

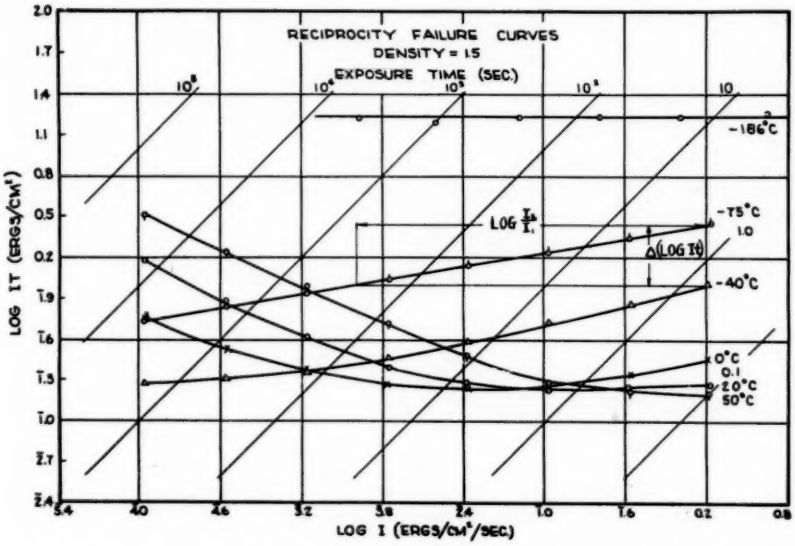

FIG. 2. Reciprocity-law failure curves at different temperatures for an actual emulsion.

shown. The curves for $-40°C$ and $-75°C$ have a long straight-line region in which Eq. (8) can be applied and a value of ϵ determined. Using the values $\log I_2/I_1(=2.6)$ corresponding to the two temperatures $T_1=198°A$ and $T_2=233°A$, as indicated on the diagram of Fig. 2, and the value for k $(=0.862\times10^{-4}$ ev) in Eq. (8), we obtain

$$\epsilon=0.68 \text{ ev}.$$

Other values of ϵ determined from a series of emulsions[8] in the same way are given in Table I. Values of ϵ for AgBr obtained by several experimenters from direct measurement of ionic conductivity are also given in Table I. It may be seen that the values of ϵ obtained by the photographic method are in good agreement with the direct measurements of ϵ. Lehfeldt's value of $\epsilon(=0.66)$ was the only one determined for a single crystal of silver bromide, the others being obtained by measurements on pressed samples. It is probable that the single crystals used by Lehfeldt correspond more nearly to the condition in the photographic grain. It is to be noted that the average of the photographic determination (0.69) agrees very closely with Lehfeldt's value (0.66). The variation of ϵ with wave-length in the photographic determinations appears to be real but is probably due to a variety of causes too complex to evaluate. Because of the greater absorption of silver bromide for the short wave-lengths, the image is confined to a thinner layer of emulsion in this case than for the longer wave-length. Therefore, different grain-size distributions are operative in the two cases. Furthermore, at long wave-lengths, the absorption of light probably takes place to a greater extent in the distorted regions of the lattice than in the regions of regular lattice structure. Either of these effects might account for small variations in the value of ϵ obtained.

The agreement between the values of ϵ ob-

TABLE I.

Emulsion	Exposing radiation	Temperature	ϵ (ev) Photographic	ϵ (ev) Direct	
I	3650	$-40°C\rightarrow-75°C$	0.63	0.66[a]	0.85[b]
	4360	"	.68	.78[c]	
	5460	"	.78		
II	4360	"	.68		
III	4360	"	.68		

[a] See reference 5.
[b] A. Joffe, Zeits. f. Physik **62**, 730 (1930).
[c] A. Smekal, Zeits. f. tech. Physik **8**, 561 (1927). Measurements by Tubandt and Lorenz, Zeits. f. physik. Chemie **87**, 513 (1914).

[8] J. H. Webb, J. Opt. Soc. Am. **25**, 4 (1935).

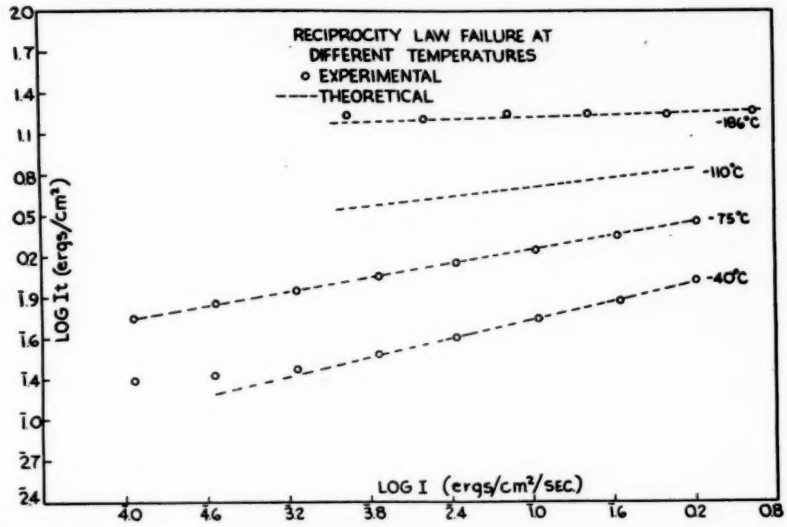

FIG. 3. Comparison between theoretical and actual slopes of a series of reciprocity-failure curves at different temperatures.

tained photographically and by direct measurement of the ionic conductivity as shown in Table I is considered as quantitative evidence that the high intensity reciprocity-law failure arises entirely from the effect of ionic conduction in latent-image formation.

CALCULATION OF THE SLOPE OF RECIPROCITY CURVES

A further calculation of interest which can be made in this connection is the slope of the reciprocity-failure curves $(\Delta(\log It)/\Delta(\log I)=a)$ as a function of the absolute temperature T. For this purpose, Eq. (8) can be written in the slightly altered form

$$\log \frac{I_2}{I_1}=\frac{0.434\epsilon}{k}\frac{T_2-T_1}{T_2T_1}.$$

If T_1 and T_2 are taken near together, then this equation can be written as

$$\log I_2-\log I_1=\Delta(\log I)=\frac{0.434\epsilon}{k}\frac{\Delta T}{T^2}. \quad (9)$$

If this equation be considered in the region for which $(\log It)$ changes linearly with T, then

$$\Delta T=K\Delta(\log It), \quad (10)$$

where K is a constant. Condition (10) is approximately true for high intensity exposures over the range $T=0°C$ to $T=-186°C$ as may be verified from Fig. 2. At temperatures below this region, it is probable that no ionic conductivity at all can occur in the time of an ordinary exposure (*circa* 1 second) and therefore, the whole effect of intensity level considered here breaks down. Substituting for ΔT in (9) from (10) the following equation is obtained:

$$\Delta(\log It)/(\Delta(\log I)=a=kT^2/(0.434\epsilon K). \quad (11)$$

Straight-line curves of slope given by (11) for different temperatures are shown in Fig. 3. The value of the constant multiplier of T^2 in (11) was determined from the $-75°C$-curve of Fig. 2. The slopes of the other curves were then obtained, using the same constant. The experimental points shown in Fig. 3 were taken from the curves of Fig. 2. It may be seen that the slopes of the theoretical curves are, in all cases, in close agreement with those obtained experimentally.

The Determination of the Concentration of Benzene and Toluene in Air by a Spectroscopic Method

PETER A. COLE
Associate Physicist, Division of Industrial Hygiene, National Institute of Health, Bethesda, Maryland
(Received April 1, 1942)

INTRODUCTION

As a result of the national war effort there has been an increased use of certain aromatic solvents such as benzene, toluene, etc. A need has arisen for a more reliable means of quantitative and qualitative analysis for the vapors of these solvents in order to make a better appraisal of the exposure of workers in industrial establishments to these toxic substances.

This investigation is a part of a research program now being carried out by the Division of Industrial Hygiene of the National Institute of Health concerned with the investigation of the toxicity of certain organic substances and the determination of extent of exposure to these materials in various war industries.

There are many methods of analysis of air for aromatic organic compounds which involve both physical and chemical[1-2] properties of these substances. Many of these methods are non-specific, involve rather detailed procedures, and possess much lower sensitivity than the method to be described. A method involving ultraviolet spectroscopic examination of alcoholic solutions of benzene and toluene has been described by Hammer[3] and Luszczak.[4] The materials are extracted from the air sample by alcohol. This method was deemed inadvisable since the maximum sensitivity was desired. Many of the usual means of analysis were similarly ruled out since a small grab sample of only 500 cc was permitted.

The ultraviolet absorption spectrum of many aromatic vapors is distinctive and its intensity can be measured under certain controlled conditions. This affords a means of analysis of air for these vapors which is sufficiently accurate both qualitatively and quantitatively in the range of toxicological importance (10 to 1000 parts per million by volume) when a 500 cc sample of air is used.

The absorption spectrum of benzene vapor has been investigated by many workers, notably Henri,[5] and more recently by Sponer, Sklar, Nordheim, and Teller,[6] and Radle and Beck.[7] Data on the absorption spectrum of toluene vapor have been reported by Savard.[8] Only one or two of the more intense bands reported by these investigators were used other than in a qualitative way. For benzene the bands appearing at 2590 and 2601A and for toluene those at 2668 and 2628A were found sufficient to make quantitative analyses for the vapor in question.

MATERIALS AND METHODS

A new and convenient sampling bulb was devised by Martin Shepherd of the National Bureau of Standards and F. H. Goldman of this

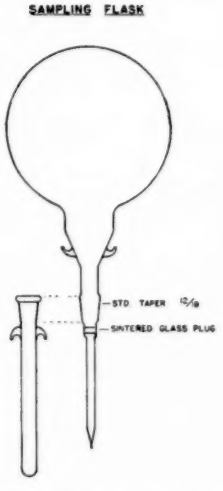

FIG. 1. Schematic diagram of bulb used for sampling solvent vapors in air.

[1] S. Nemura and Y. Kosaka, J. Soc. Chem. Ind. Japan **32**, 279 (1929); J. Harand, Monats. F. Chem. **65**, 153 (1935); K. Hradsky, Chem. Obzor. **11**, 120 (1936).
[2] W. Yant, S. Pearce, and H. Schrenk, Report of Investigations, U. S. Bureau of Mines, 3287 (1935); 3323 (1936).
[3] E. Hammer, Abhandl. Gesamtgebiet Hyg. **12**, 28 (1933).
[4] A. Luszczak, Abhandl. Gesamtgebiet Hyg. **12**, 51 (1933).
[5] V. Henri, J. de phys. et rad. **3**, 181 (1922).
[6] H. Sponer, G. Nordheim, A. L. Sklar, and E. Teller, J. Chem. Phys. **7**, 207 (1939).
[7] W. Radle and C. Beck, J. Chem. Phys. **8**, 507 (1940).
[8] J. Savard, Ann. de Chemie **11**, 287 (1929).

laboratory. Since the bulbs were to contain solvent vapors the use of stopcock greases or waxes was prohibited. In Fig. 1 is shown an illustration of the sampling bulb which will remain gas-tight indefinitely.

The bulb was prepared for use by evacuating and sealing off. The air sample was then taken by breaking the tip of the bulb, and the test tube, which was partially filled with mercury, was then placed over the end and fitted snugly in the standard taper joint (12/18). The test tube was held in place by rubber bands or light wire which could be hooked around the glass horns as shown in the figure. The bulb was supplied with a sintered glass plug to prevent the mercury from entering the flask. This plug also served to minimize loss of vapor while the bulb was being attached to the absorption apparatus.

The apparatus used to measure the ultraviolet absorption of the vapor in the air sample has been described in a previous paper.[9] Briefly, it consisted of a hydrogen discharge tube which served as a source of ultraviolet radiation, a fused quartz absorption cell, and a medium-sized quartz spectrograph. The absorption cell was fitted with the female part of the standard taper joint (12/18). Directly beyond this was a ring seal, the inner tube of which was drawn down to a small bent capillary. This enabled the apparatus to be pumped down by means of a mechanical vacuum pump while at an elevated temperature (300°C) and thus to be purged of solvent vapor. The system was then allowed to cool to room temperature. By means of the interchangeable ground joints the sample bulb was attached quickly to the absorption apparatus and the glass capillary referred to above was broken by means of the customary iron plug magnetic hammer. The volume of the absorption apparatus was determined so that bulbs of various capacities could be employed.

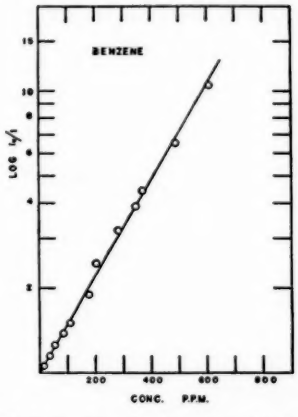

FIG. 2. Working curve for benzene. Ordinates are the ratio of intensity of background to intensity of absorption band at 2590A plotted on a logarithmic scale. Abscissae, concentration of vapor in air in parts per million by volume on a linear scale.

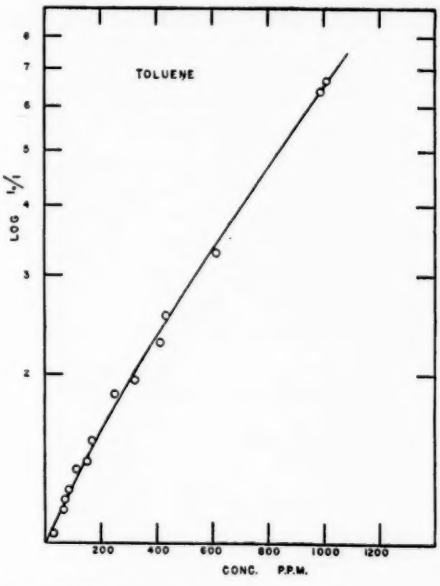

FIG. 3. Working curve for toluene. Coordinates same as Fig. 2 except for toluene band at 2668A.

Working curves relating intensity of absorption to concentration of vapor in air were obtained for benzene and toluene as follows: The concentrations of vapor were set up in a chamber similar to the one previously described.[9] They were measured interferometrically by Mr. Dronenburg of this laboratory and checked occasionally with a combustible gas indicator and by a chemical colorimetric method.[2] These working curves were also checked by introducing weighed samples into the absorption cell, the volume of which was known. Intermediate concentrations could be obtained by pumping out

[9] P. A. Cole and D. W. Armstrong, J. Opt. Soc. Am. **31**, 740 (1941).

the system to known fractions of the original pressure. This procedure was tested experimentally and is considered justified by the results of Figs. 2 and 3 (see below). In a similar manner an unknown which proved to be too high in concentration for practical purposes for the bands under observation could be reduced in pressure and amount until measurements were feasible. Exposure times were less than one minute. Calibration and reduction of the plates were accomplished by means of a step-sectored disk and a modified Bausch and Lomb densitometer.

RESULTS AND DISCUSSION

The results for benzene are shown in Fig. 2 where the ratio of the relative intensity of the background to the relative intensity of the absorption band at 2590A is plotted on a logarithmic scale against concentration in parts per million by volume on a linear scale. Similar results are shown in Fig. 3 for toluene for the band appearing at 2668A. These working curves were obtained from four different samples of benzene and six different samples of toluene whose concentration had been determined interferometrically. The additional points result from pumping out some of the samples by known amounts.

The straight line character of these working curves shows an agreement with Beer's law. The slight curvature of the toluene graph is perhaps caused by inability to obtain a correct I_0 due to overlapping bands at the higher concentrations. Several samples of air from various war industries have been analyzed for benzene and toluene. The results of these analyses are confidential.

CONCLUSION

A convenient spectroscopic method of qualitative and quantitative analysis of air samples for certain aromatic vapors is described. This method is sufficiently precise (± 10 percent) for application in the range of toxicological importance when only a 500-cc sample of air is used. The method is limited to those vapors which have discrete band spectra in the near ultraviolet region of the spectrum. A convenient sampling bulb is described which is useful for air samples containing inflammable solvents. Working curves relating intensity of absorption to concentration are shown for two important solvents, benzene and toluene.

Third Midwest Conference on Spectrochemical Analysis

A CONFERENCE on Spectrochemical Analysis was held at the University of Michigan, Ann Arbor, Michigan, on Saturday, April 11, 1942.

The following program was given:

Method of Spectrochemical Analysis of Stainless Steels. JOHN SCHUCH, *Harry W. Dietert Company, Detroit, Michigan,* AND CHARLES E. HARVEY, *Applied Research Laboratories, Glendale, California.*

Laboratory Design for Spectrographic Analysis. J. L. SAUNDERSON AND T. M. HESS, *Dow Chemical Company, Midland, Michigan.*

Ultimate Purities of Materials and Ultimate Sensitivities of Analyses by Spectrographic Means. OTTO G. KOPPIUS, *Mathieson Alkali Works, Niagara Falls, New York.*

Absorption Spectra and Structure of Dyes. WALLACE R. BRODE, *Ohio State University, Columbus, Ohio.*

Preliminary Report on the Effects of Stray Light in Photoelectric Filter Photometers. M. N. STATES AND J. C. ANDERSON, *Central Scientific Company, Chicago, Illinois.*

New Laboratory for Spectrographic Analysis in the Northwestern Technological Institute. RUSSELL A. FISHER, *Northwestern University, Evanston, Illinois.*

Problem of Slit Illumination. W. C. PIERCE, *The Technological Institute, Northwestern University, Evanston, Illinois.*

Comparison of Microphotometers. M. M. WHITE, *Ford Motor Company, Detroit, Michigan.*

A True-Area Photometric Distribution Curve

FRANK BENFORD
Research Laboratory, General Electric Company, Schenectady, New York.
(Received April 1, 1942)

THE accurate pictorial presentation of the distribution of light flux about a lamp has long been an engineering problem. If the intensities in candles are plotted in their proper directions, the area included by the distribution curve is in no sense a true picture of the quantity of light emitted. For example, an intensity of 100 candles in the zone of 5-deg. radius about the axis of the lamp represents 2.4 lumens, while an equal intensity in the zone extending 5 deg. to one side of the equator represents 54.8 lumens, or 22.9 times as much light for equal areas under the distribution curve. This distortion of areas depends upon the angle of emission, but there is a second type of distortion that depends upon the relative intensities I_θ and I_θ' of two lamps, at the same angle θ. As an example, take the case of two units that have identical distributions of light, but one is three times as intense as the other. When plotted to uniform candle scales one curve encloses not three, but nine times, the area of the other.

The "lumens' constants" that are used to compute the lumens in a zone from the known intensities in candles are found from the formula

$$Z = 2\pi \int \sin\theta d\theta.$$

The area under a photometric distribution curve may be considered as made up of elemental triangles formed by adjacent radii vectors ϱ and a section of the curve. The included area is found by performing the integration

$$A = K \int \varrho^2 d\theta.$$

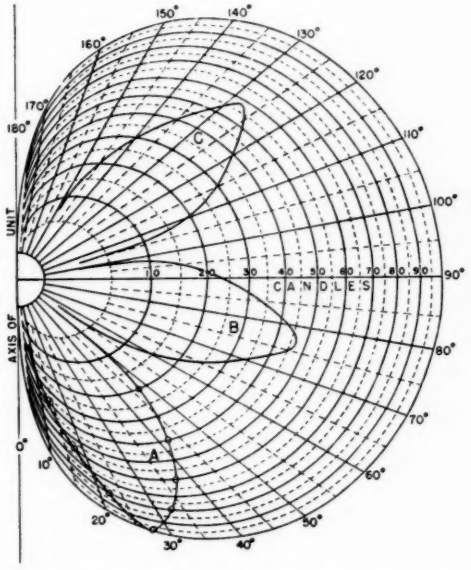

FIG. 1. These three photometric distribution curves represent identical amounts of light flux. Their areas are the same, but there is some distortion of form.

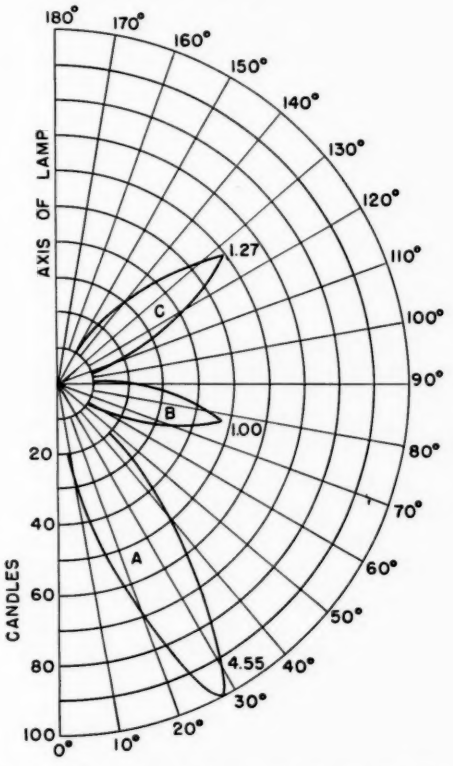

FIG. 2. These three photometric distribution curves represent the same number of lumens. There is a wide variation in areas, but no distortion of the shapes of the curves.

This is necessarily so because the area of a plane figure varies as the square of any one of its dimensions. Since we want areas directly proportional to a linear element we may put

$$\varrho = (\sin \theta)^{\frac{1}{2}};$$

then the two integrands become identical, and the area under the curve will bear a linear relation to the zone area. This eliminates the first distortion and leads to a form of plotting web illustrated in Fig. 1. The length of each radius is proportional to the square root of the sines of the angles marked around the edge of the web.

To correct the distortions of area that ordinarily exist when the candles are plotted to a uniform scale it is only necessary to plot the candles to a scale that varies as the square root of the natural numbers. In Fig. 1 the concentric curves follow this rule and two similar distribution curves will have areas strictly proportional to the total lumens emitted.

In Fig. 2 the three-candlepower distribution curves *A*, *B*, and *C* each represent the same number of lumens. (It is customary to show this type of distribution by symmetrical curves to the right and left of the axis, but in Figs. 1 and 2 only one side is shown in order to have a larger scale.) The areas of the three curves are as 4.55 to 1.00 to 1.27. In Fig. 1 the web is constructed as outlined above and the same distributions of light now give three curves of equal area. Comparison for flux can be made either visually or by means of a planimeter, and when two curves are plotted to the same scale this web gives an accurate picture of the relative outputs of two units.